CHEMICAL REVIEWS

REVIEW

pubs.acs.org/CR

Ion and Molecular Recognition by Lower Rim 1,3-Di-conjugates of Calix[4]arene as Receptors

Roymon Joseph and Chebrolu Pulla Rao*

Bioinorganic Laboratory, Department of Chemistry, Indian Institute of Technology, Bombay, Mumbai 400 076, India

CONTENTS

1. INTRODUCTION

Calixarenes are one of the macrocyclic receptors known to date besides crown ethers, cyclodextrins, cryptands, and cucurbiturils.[1−3] These are synthesized from the base-catalyzed condensation reaction of *p-tert*-butyl phenol with formaldehyde.[4] Calixarenes have several advantages over other molecular systems, such as the presence of a hydrophobic cavity, easy organic modifiability both at lower and upper rims, and it can be adorned by a flexible but well-defined binding core. These can exhibit hydrophobic as well as hydrophilic properties simultaneously from the same molecule.[5−7] The direct involvement of calixarene moiety in the complexation of metal ions is established in the literature as a result of the cation−π interaction.[7,8] It may be noted that a preorganization of the benzene ring, at least in some cases, assists the complexation between the calixarene moiety and the metal ion. The inclusion of solvent and other guest species in the cavity of the calixarene[7,9] and the participation of phenolic oxygens in the complexation are also known in the literature as evident from their crystal structures.[10] Encapsulation of guest species is helpful in performing the chemical transformations and guest exchange reactions within the cavity.[11]

Calix[*n*]arene exists in different conformations depending upon the substituent present at the lower rim as well as at the *para*-position. The size and the shape of the cavity are altered when the number of phenyl units change.[2,12] The complexation properties of a calixarene conjugate depend on its conformation as well as on the donor groups present. The conformation of a calix[4]arene conjugate can be altered by the presence of a particular ion.[13,14]

Received: December 27, 2010
Published: April 22, 2011

 © 2011 American Chemical Society

Among several calix[*n*]arenes, calix[4]arene has been used as a popular building block due to its ability to exist in cone conformation and the ease of organic functionalization both at lower as well as upper rims.[15−17] Calix[4]arene derivatives are well-known for their high selectivity and binding efficiency toward ions and molecular species provided preorganized cores are built onto the system, although these are flexible.[1,2,18,19] Because of the importance in biology, environment, and chemical processes, conjugates of calix[4]arene have been explored for their selective recognition of ions and molecules, and the extraction of various species.[14,20,21] Although there are a number of receptors including supramolecular ones in the literature, calix[4]arene-based conjugates received greater attention due to their versatility and the special features that they exhibit.[5,22,23] All of this is further supported by the properties displayed by the calix[4]arene derivatives in the area of ion and molecular recognition,[18,19,24−29] host−guest chemistry,[5] catalysis,[30] enzyme mimics,[31] interaction with biomolecules,[21,32,33] ion extraction,[34] and selective ion transport.[35] Calix[4]arenes are also known for their complex molecular architectures; for example, double calix[4]arenes and calix[4]arene-based tubes are some among these.[36]

The binding abilities of the parent calix[4]arene will be enhanced by functionalizing at its lower rim, because the resultant conjugates can provide preorganized binding cores suitable for various ions and molecular species.[18,19] Although mono-, di-, tri-, and tetra-functionalizations are possible on the calix[4]arene, especially the 1,3-disubstitution at the lower rim has become more attractive due to the presence of two phenolic-OH's (also provide extra coordination) and its ability to maintain cone-conformation by retaining two hydrogen bonds at the lower rim. However, such structures are still flexible and may change the conformation upon complex formation. Examples of 1,3-disubstituted derivatives where the free-OH's interact with different guest species are demonstrated in this Review. The calix[4]diquinone derivatives are attractive because of their redox properties. In effect, the binding efficiency of the conjugates of calix[4]arene toward various guest species depends on the ring size, nature and number of binding groups attached, conformation of the arms, and certainly the nature of the guest species. Generally, the recognition events are monitored either by spectroscopy or by visual methods or both.[18,24−26,37] Such conjugates bearing chromogenic units detect the guest species by fluorescence, absorption, and/or color changes. For this purpose, a chromophore is necessary that may be integrated into the binding core region either directly or through a spacer.

The reviews that deals with the biological applications and enzymatic models of various calix[4]arene conjugates[21,31−33] and the biochemistry aspects of sulfonato-calix[n]arenes[27] appeared recently in the literature. Some of the reviews that emphasize the synthesis and properties of various calixarene conjugates include[36] oxacalixarenes,[38] homocalixarenes,[39] and functionalization of calix[4]arenes with different donor atoms.[40] The other reviews are based on the coordination chemistry of larger calix[*n*]arenes[41] including their ion sensing aspects by spectral techniques,[19] catalytic properties of metallocalixarenes,[30] self-assembled water-soluble *p*-sulfonatocalix[4,5]arenes,[42] and thermodynamics of pyridinocalix[4]arenes with monovalent cations.[43] Ion sensing properties of fluorescent calix[4]arene derivatives with main emphasis on the photophysical aspects[18,25,26] and the detection of toxic ions[24] are reviewed recently. Therefore, the reviews already reported in the literature gave major importance to the synthesis of various calixarene conjugates, their biological applications, and ion recognition properties and were not much concerned with the 1,3-disubstituted derivatives of calix[4]arene. Because the literature is being enriched with these derivatives at a high rate, frequent reviewing would be of great advantage. A number of 1,3-diconjugates of calix[4]arene are known in the literature for their ion and molecular recognition, and the present Review deals with all of these.

The 1,3-diconjugates of calix[4]arene bearing suitable functional moieties act as receptors for biologically relevant ions and lanthanides including those of toxic ones.[18,19,24,26] The cores built on calix[4]arenes are mainly rich with N,O-binding groups and sparingly with S, suitable for interaction with cations and anions.[44] Although a number of calix[4]arene-based fluorescent probes selective for the recognition of ions and molecular species were developed, it is important to determine the mode of interaction between the host and the guest species.

Cations, anions, and amino acids are involved in a variety of biochemical functions by affecting the enzymes, coenzymes, and cofactors to determine the biological aspects.[45−47] Deficiency or excess presence of these in the biological fluids is harmful to health.[48−50] On the other hand, the heavy metal ions are well-known to be toxic by being present in the environment that enters into the ecological cycles.[51] While the development of receptors for the spherical cations is rather simpler, it however requires special synthetic skills to introduce moieties into the arms of calix[4]arenes to selectively detect anions and amino acids.[52] Both of these can be selectively sensed by introducing moieties, which can involve in hydrogen bonding as well as hydrophobic interactions with the incoming guest species, into the arms of calix[4]arenes.[53,54] So the introduction of such moieties into the arms of calix[4]arene appropriately can provide receptors suitable for the selective recognition of cations, anions, and amino acids or their side chains when present in peptides.[18,19,55] Factors responsible for the chiral recognition can also be introduced into these arms.

Therefore, this Review mainly deals with the ion and molecular recognition including the chiral recognition, extraction, and complexation aspects of various 1,3-disubstituted derivatives of calix[4]arene reported during the past 10 years. Although this Review is focused on the 1,3-disubstituted derivatives of calix[4]arene, some tetra-substituted derivatives have also been included where their 2,4-positions contain nonbinding groups such as methyl, propyl, etc.

2. FUNCTIONALIZATION AT THE 1,3-POSITIONS OF CALIX[4]ARENE

Calixarenes are functionally modified either at its lower rim or at its upper rim by different substituents. The hydroxyl groups present at the lower rim of calixarene provide excellent sites for the introduction of substituents containing donor groups, ester, ketone, or ether mainly for hard alkali and alkaline earth ions.[56] Introduction of moieties containing O, N, and S on the calixarene brings the selectivity toward transition metal ions.[7,41,57] It is also possible to incorporate preorganized binding cores onto the calixarene by attaching chelating group to facilitate ion complexation and stabilization of the same using chelate and macrocylic effects.[19] Appropriate functionalization can improve the solubility and can extend its range of applications. Because this Review deals with the ion and molecular recognition properties of 1,3-disubstituted derivative of calix[4]arene, the functionalization of these is discussed here (Scheme 1). O-Alkylation and O-acylation are the two easiest ways to introduce derivatization at the lower rim of calix[4]arene.[58] It is easy to functionalize

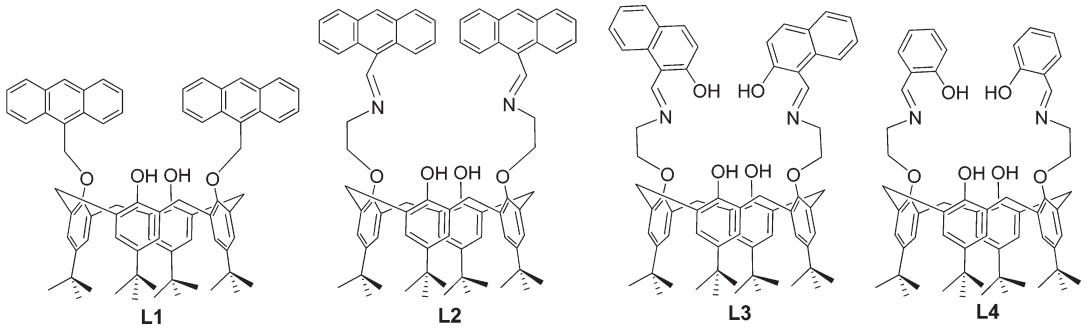

Figure 1. Schematic representation of **L1**, **L2**, **L3**, and **L4**.

Scheme 1. Some Precursors for the Synthesis of 1,3-Disubstituted Derivatives of Calix[4]arene

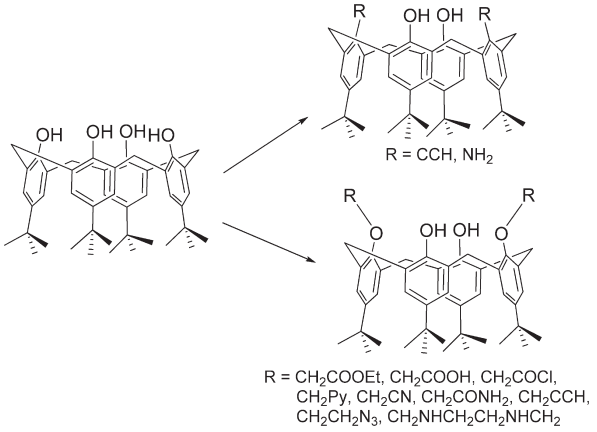

1,3-positions of the calix[4]arene by using different electrophiles.[22] For example, a reaction of *p-tert*-butyl calix[4]arene and ethyl bromoacetate in a 1:2 ratio in the presence of K_2CO_3 in dry acetone under reflux for 15 h results in 1,3-diester derivative of calix[4]arene in 78% yield. The ester derivative can be easily converted to the corresponding diacid derivative by the hydrolysis with NaOH in ethanol under reflux, followed by acidification. The reaction of the diacid derivative with $SOCl_2$ results in a highly reactive acid chloride, which, in turn, can couple with amines to result in amido-conjugates. Another important reaction for the functionalization is the O-alkylation with chloroacetonitrile followed by reduction with $LiAlH_4$ resulting in diamine conjugate.[16,17,59] It is also possible to make cyclic conjugates through derivatization affecting 1- and 3-positions of calix[4]arene using appropriate reaction conditions.[16] Sonogashira-type cross-coupling reactions on trifluoromethanesulfonate-substituted calix[4]arene compounds are also being reported in the literature.[60] Aryl ethers of calix[4]arene can be synthesized by the use of S_NAr or Ullmann reactions.[61] The free-OH groups present at the lower rim can also be converted to NH_2.[62] The calix[4]arene-based crown and azacrowns have also been synthesized by capping 1,3-arms.[63] Double calix[4]arenes can be synthesized by using alkyl spacer[64] or performing cycloaddition reactions.[65]

3. CATION RECEPTORS

3.1. Zn^{2+} Recognition

A number of 1,3-disubstituted calix[4]arene derivatives have been developed and demonstrated for their Zn^{2+} recognition as reported in the literature. Therefore, the discussions on these have been grossly divided here into two sections, one concerned with the derivatives possessing imino-phenolic moiety and the other concerned with those derivatives possessing any other binding cores. The first section has been further divided into two parts, one possessing only the imino-phenolic core and the other possessing an imino-phenolic core in conjunction with the triazole core.

3.1.1. Receptors Possessing Imino-phenolic Core. A simple *O*-methylanthracenyl derivative, **L1** (Figure 1), exhibits a low fluorescence enhancement toward some transition metal ions.[66] When an imine moiety is introduced into this to result in **L2** (Figure 1), this starts exhibiting some selectivity by showing significant fluorescence enhancement toward a few transition ions over the others in the order, $Fe^{2+} \approx Cu^{2+} \gg Zn^{2+} \gg$ other 3d ions, and hence is poorly selective. Further, when the arms were derivatized with 2-hydroxy naphthalidene moiety as in Figure 1, **L3** exhibits selectivity toward Zn^{2+} over a number of other ions studied, Ti^{4+}, VO^{2+}, Cr^{3+}, Mn^{2+}, Fe^{2+}, Co^{2+}, Ni^{2+}, Cu^{2+}, Mg^{2+}, Cd^{2+}, and Hg^{2+}, by showing a large fluorescence enhancement that is sufficient enough to detect Zn^{2+} even at $\leq$60 ppb, in methanol.[67] The fluorescence enhancement is attributable to the reversal of PET when Zn^{2+} forms a 1:1 chelate complex with **L3** using its imine and phenolic-OH moieties present on both of the arms wherein the association constant has been found to be 2.3×10^5 M^{-1} in methanol.

The structure of **L3** as determined by single crystal XRD shows an N_2O_2 core that is suitable for metal ion binding (Figure 2). The Zn^{2+} complex of **L3** has been modeled by computations at the HF/6-31G level and was found to form a tetrahedral complex (Figure 2). The structure shown in Figure 2 is convincing when one compares this to the crystallographically determined structure of the Cu^{2+} complex of the corresponding salicylidene analogue, **L4** (Figure 1), as its pyridine adduct [Cu(**L4**)(Py)] (Figure 2).[68] While the coordination core is N_2O_2 in both of the cases, the Zn^{2+} with **L3** shows a tetrahedral structure and the Cu^{2+} with **L4** shows a square pyramidal due to the presence of a pyridine in its apical position as acquired from the solvent during crystallization. Complexes of Zn^{2+}, Cu^{2+}, and Ni^{2+} of both **L3** and **L4** were isolated and characterized by analytical and spectral techniques and confirmed the formation of 1:1 complexes.[69] On going from **L1** to **L2** to **L3**, the fluorescence sensitivity as well as selectivity increase in the presence of Zn^{2+}. The structural features exhibited by the complexes of **L3** and **L4** reinforce the observation that an imino-phenol core suitable for metal ion chelation with optimal hard−soft character seems to impart selectivity.

The receptor **L5** that possesses an additional $-CH_2OH$ moiety in conjunction with the imino-phenolic core (Figure 3)

dx.doi.org/10.1021/cr1004524 |*Chem. Rev.* 2011, 111, 4658–4702

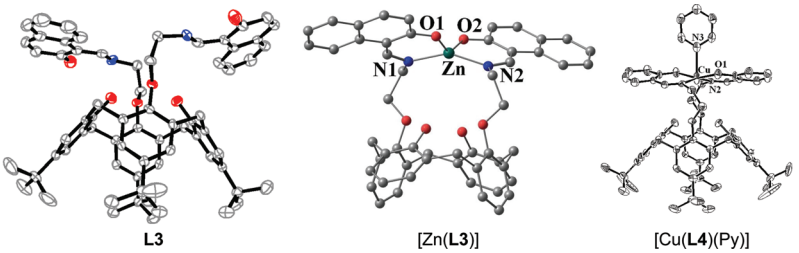

Figure 2. Single crystal X-ray structure of **L3**. Computationally optimized structure of Zn^{2+} complex of **L3**, [Zn(**L3**)] (*tert*-butyl groups were removed before optimization). Single crystal X-ray structure of [Cu(**L4**)(Py)], where "Py" is pyridine. Reprinted with permission from ref 68. Copyright 2005 Elsevier.

seems to exhibit higher sensitivity toward Zn^{2+}, although it is sensitive toward Cd^{2+}, as compared to **L3** and **L4** that lacks the $-CH_2OH$ moiety.[70] In effect, **L5** exhibits a 10-fold higher binding toward Zn^{2+} ($K_a = (2.7 \pm 0.1) \times 10^4\ M^{-1}$) as compared to Cd^{2+} ($K_a = (3.6 \times 0.6) \pm 10^3\ M^{-1}$) in methanol. The complex formed is still 1:1 with **L5** using N_2O_2 core for Zn^{2+} and N_2O_4 core for Cd^{2+} (Figure 3b,c) as obtained from the computational studies. While the geometry around Zn^{2+} is best fitted to a trigonal bipyramidal with one vacant site, that around Cd^{2+} is best fitted to a capped octahedron with one vacancy. Thus, **L5** exhibits a dual binding core, whereas **L3** and **L4** provide only a single binding core. The in situ prepared Zn^{2+} complex of **L5** selectively detects inorganic phosphate and biomolecules containing phosphate moieties such as AMP, ADP, and ATP by fluorescence quenching. The phosphate detection is attributable to the removal of Zn^{2+} from the complex by the phosphate ions. The minimum concentration of HPO_4^{2-} that can be detected by [Zn**L5**] was found to be 426 ppb. The dechelation of Zn^{2+} from [Zn**L5**] by phosphate ions has been further supported by absorption titrations. The **L5** exhibits INHIBIT logic gate properties by using Zn^{2+} and HPO_4^{2-} as inputs.

3.1.2. Imino-phenolic Core Linked through Triazole Moiety. The selectivity of Zn^{2+} toward the imino-phenolic core has been further demonstrated using **L6**, **L7**, and **L8** (Figure 4) where each arm is linked through a triazole moiety.[71] Although the involvement of the triazole moiety in the metal ion recognition has been shown[72] in case of **L9**, in case of **L6**, **L7**, and **L8** the triazole core is not involved in the binding because these possess an imino-phenolic core that is otherwise absent in **L9**. The fluorescence studies carried out with **L6**, **L7**, and **L8** exhibit increasing levels of association of the Zn^{2+} ([Zn**L8**] ≫ [Zn**L7**] > [Zn**L6**]), which is consistent with the presence of zero, one, and two $-CH_2OH$ groups in case of **L6**, **L7**, and **L8**, respectively. The receptor, **L8**, has been shown to be selective toward Zn^{2+} in methanol, acetonitrile, and also in their aqueous mixtures. The conjugates possessing bent arms are capable of forming 1:1 complex intermolecularly rather than in intramolecular fashion (Figure 5a). Such intermolecular 1:1 complex formation can be reconciled in the light of the crystal structures reported using small molecular analogues (Figure 5b). Relevant small molecular structures clearly supported[73] the formation of 4-, 5-, as well as 6-coordination about Zn^{2+}, wherein four of these coordinations were satisfied by the imino-phenolic core; the rest are either by the neighbor alcoholic-OH or by the solvent. Thus, [Zn(**L6**)], [Zn(**L7**)], and [Zn(**L8**)] exhibit 4-, 5-, and 6-coordinations, respectively, as also supported by the observed fluorescence enhancement.

On the other hand, a conjugate similar to that of **L6** but having a variation in the relative positioning of the triazole to the

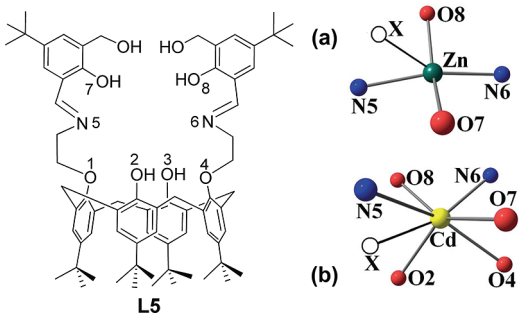

Figure 3. Schematic structure of the Zn^{2+} receptor, **L5**. Computationally obtained coordination cores of (a) Zn^{2+} in [Zn(**L5**)] and (b) Cd^{2+} in [Cd(**L5**)]. "X" indicates vacant site in the coordination sphere.[70]

salicylaldimine moiety, as that in **L10**, results in the arrangement of arms in such a way that an intramolecular 1:1 Zn^{2+} complex is formed via N_2O_2 core using both of the arms (Figure 6).[74] This has been shown by establishing the crystal structure. The structure is similar to that observed in other cases, such as [Zn(**L3**)] and [Zn(**L5**)]. The selectivity of **L10** toward Zn^{2+} continues even in the presence of blood serum and/or the albumin proteins, thus making this receptor suitable for biological applications. Although the presence of triazole core alone provides coordination to the metal ion through one of its nitrogens, when the same is present in the conjugate in conjunction with imino-phenolic core, it is the latter that dominates in terms of ion binding, and the selectivity is toward Zn^{2+}.

3.1.3. Receptors Possessing Cores Other than the Imino-phenolic Ones. The interaction of Zn^{2+} ($K_a = 1.7 \times 10^4\ M^{-1}$) and Cd^{2+} ($K_a = 5.18 \times 10^4\ M^{-1}$) by a pyrenyl appended triazole-based calix[4]arene (**L9**) was demonstrated in CH_3CN by ratiometric fluorescence enhancement of pyrene monomer versus the fluorescence quenching of pyrene excimer, although the selectivity difference between these two ions is marginal as evident from their K_a values.[72] A model for M^{n+} binding has been proposed invoking interactions through a triazole nitrogen of each arm and the two lower rim phenolic moieties as derived on the basis of NMR spectroscopy (Figure 7). Ions such as Pb^{2+}, Hg^{2+}, and Cu^{2+} exhibit fluorescence quenching of both the monomer and the excimer emissions of **L9** due to their heavy atom effects. Other metal ions did not cause any significant change in the emission spectra.

An oxyquinoline derivative of calix[4]arene (**L11**) exhibits 1:1 and 1:2 complexes when titrated with Zn^{2+} through fluorescence quenching.[75] When the two solvent molecules present in this complex were replaced by 2,9-dimethyl-4,7-diphenyl-1, 10-phenanthroline as bidentate ligand (Figure 8), it exhibits

dx.doi.org/10.1021/cr1004524 |*Chem. Rev.* 2011, 111, 4658–4702

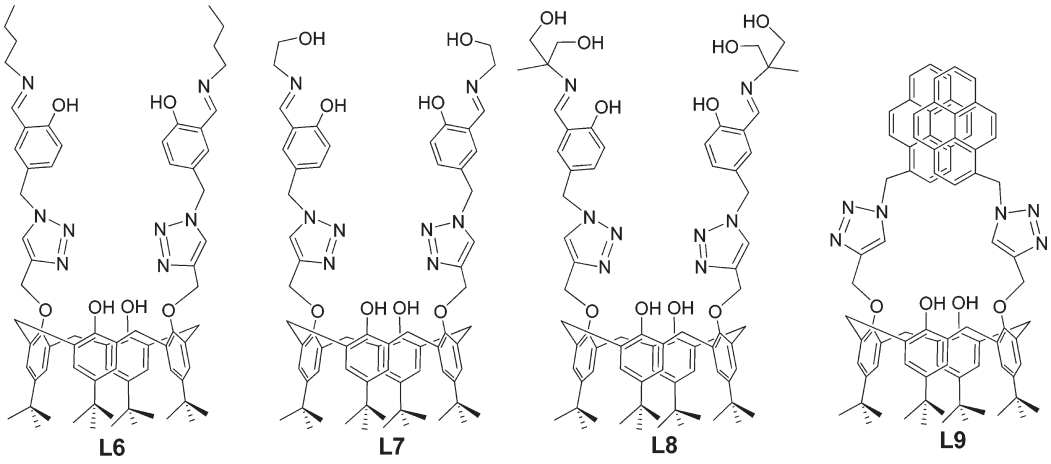

Figure 4. Schematic structures of triazole linked Schiff's base conjugates of calix[4]arene possessing different binding cores (**L6**, **L7**, and **L8**) and schematic structure of **L9**.

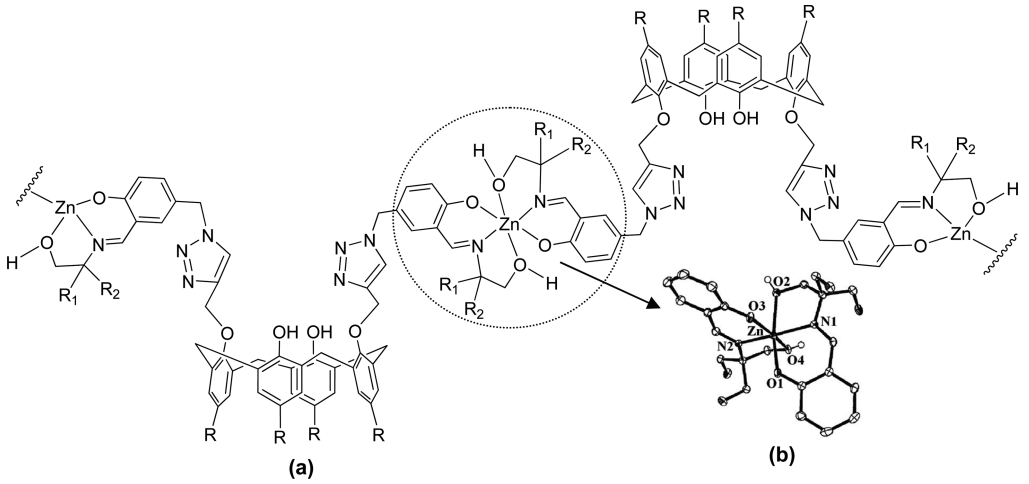

Figure 5. (a) Proposed structure of intermolecular Zn^{2+} binding in **L7** (R = *tert*-butyl, R_1, R_2 = H) and **L8** (R = *tert*-butyl, R_1 = CH_3, R_2 = CH_2OH). (b) Single crystal X-ray structure of [$Zn(saltris)_2$] that mimics the circled portion of the binding core observed in (a) {"saltris" is a Schiff's base formed from salicylaldehyde and tris(hydroxymethyl)aminomethane}. Reprinted with permission from ref 73. Copyright 2002 Wiley-VCH.

enhancement in the fluorescence as a result of the interaction of phenanthroline with Zn^{2+} followed by energy transfer. The interaction has also been proven by ^1H NMR spectroscopy.

The receptor **L12** possessing two bipyridyl cores (Figure 9) that exhibits 1:2 binding with Zn^{2+} in solution, however, resulted in an 1:1 complex when isolated, even when the reactions were carried out under 2 equiv of zinc salt.[76] Zn^{2+} is bound to only the bipyridyl core of one of the arms where the four-coordination is being filled by the bipyridyl and two chloride ions, keeping the second bipyridyl moiety of the other arm unoccupied (Figure 9).

An amide conjugate of calix[4]arene bearing a bispyridyl {$-N(Py)_2$} moiety on each of the arms (**L13**, Figure 10) exhibits two binding cores as can be noticed from its crystal structure (Figure 10a).[77] **L13** responds toward Zn^{2+} through switch-on and Ni^{2+} through switch-off fluorescence emission. The binding cores have been derived on the basis of the computational calculations. While Zn^{2+} binds through N_4 core, the Ni^{2+} exhibits an N_4O core (Figure 10b,c). However, when both of the ions are present in the medium, these bind together cooperatively by Ni^{2+} taking over the nitrogen core and Zn^{2+} taking over the oxygen core, and thus **L13** acts as a dual sensor.

When the two arms were connected together to give a cyclic amido derivative possessing N_4O_2 core, **L14** (Figure 11) forms 1:1 complex with Zn^{2+} as well as with Ni^{2+} as studied on the basis of UV−vis, fluorescence, NMR spectroscopy, and mass spectrometry.[78] On the basis of the NMR spectroscopy, it has been proposed that Zn^{2+} is tentatively located nearer to the nitrogen centers in **L14**. Even **L14** gives similar fluorescence changes in the presence of Zn^{2+} and Ni^{2+}. However, **L14** does not show dual sensing, because the cyclization of both of the arms in **L14** does not allow these two ions to bind simultaneously as a result of the binding core constraints built into **L14**. On going from imino-phenolic (**L3**, **L10**) to pyridyl-phenolic (**L13**) to simple pyridyl (**L12**), the affinity of these toward Zn^{2+} seems to be reduced and is shifted more toward other ions, including that of Ni^{2+} and Cd^{2+}. However, the presence of $-CH_2OH$ group in addition to imino-phenolic core always strengthens the Zn^{2+} affinity as shown in case of **L7** and **L8**.

dx.doi.org/10.1021/cr1004524 |*Chem. Rev.* 2011, 111, 4658–4702

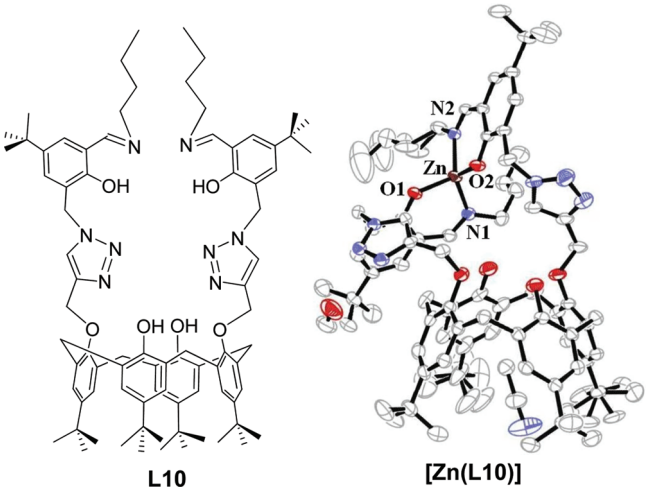

Figure 6. Schematic structure of **L10** and single crystal X-ray structure of the zinc complex of **L10**, [Zn(**L10**)]. Reprinted with permission from ref 74. Copyright 2010 The Royal Society of Chemistry.

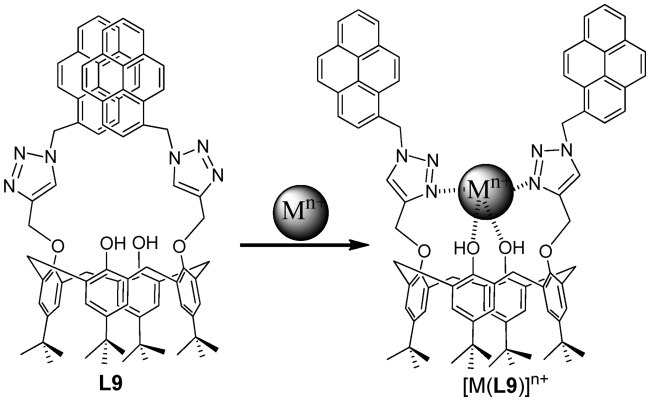

Figure 7. Schematic representation of the structure of **L9** (excimer) and its proposed M^{n+} bound complex, $[M(\mathbf{L9})]^{n+}$ (no excimer).

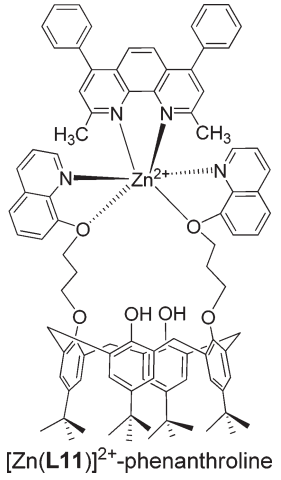

Figure 8. Proposed structure for $[Zn(\mathbf{L11})]^{2+}$ with batho-phenanthroline acting as bidentate ligand in the coordination sphere. In the absence of batho-phenanthroline ligand, two CH_3CN molecules occupy its place.

It is known from the literature that Schiff's base conjugates of calix[4]arene bearing a phenolic −OH in conjunction with imine functionality exhibit fluorescence turn-on behavior toward Zn^{2+}. The imine function alone is not selective for Zn^{2+}. However, the presence of additional −OH's increases the Zn^{2+} recognition several folds. The fluorescence enhancement exhibited by the interaction of Zn^{2+} is by blocking the PET process when it chelated through the imine and phenolate functions. The species of recognition in case of Zn^{2+} is generally tetrahedral where two phenolic-OH's and two imine nitrogens (N_2O_2) are involved in binding (Figures 2, 3a, 6). However, the coordination number seems to increase when additional −OH groups are present in the vicinity. Thus, the common binding cores observed for the Zn^{2+} complexes other than Schiff's base ones were N_2O_2 (phenolic-OH's form the calix[4]arene part), N_2 plus two chloride ions, or N_4 by the involvement of four pyridine moieties (Figures 7, 9, 10). However, the Cd^{2+} demands six or higher coordination (Figure 3b) for the recognition, and hence most of the receptors that are selective toward Zn^{2+} show some sensitivity even for Cd^{2+}. Therefore, Cd^{2+} goes closer to the lower rim oxygens to pick additional coordination, which is not the case for Zn^{2+}.

3.2. Cu^{2+} Recognition

3.2.1. Cyclic Conjugates. A 9,10-anthraquinone-substituted calix[4]arene, **L15** (Figure 12), showed selective recognition toward Cu^{2+} among 16 ions studied by exhibiting K_a of 1.80×10^2 M^{-1} in CH_3CN.[79] The interaction of Cu^{2+} with **L15** results in the formation of a new absorption band at 450 nm resulting from the internal charge transfer (ICT). This conjugate forms a stoichiometric complex and shows color change from yellow to red upon interaction with Cu^{2+}.

A 4-aminophthalimide fluorophore connected to calix[4]azacrown unit, **L16** (Figure 13), showed the highest fluorescence enhancement for Cu^{2+} and Fe^{3+}, while the same kind of enhancement was observed with Ni^{2+} and Zn^{2+} only at a higher concentration of these ions.[80] **L16** forms a 1:1 complex with all of the ions studied and exhibits K_a of 2.3×10^5 and 1.6×10^5 M^{-1}, respectively, for Fe^{3+} and Cu^{2+}, whereas these are 2.5×10^4 and 1.7×10^3 M^{-1}, respectively, for Zn^{2+} and Ni^{2+} in tetrahydrofuran. Two derivatives of 1,3-bridged calix[4]azacrowns (**L17**, **L18**) (Figure 13) exhibit selectivity toward Cu^{2+} where the stoichiometry of the complex formed was 1:1 and 1:2 ($L:M^{2+}$), respectively, for **L17** and **L18**.[81] The formation of 1:2 complex in case of **L18** may be conceivable by considering the bridging perchlorate. A cyclic naphthalimide-based calix[4]arene receptor having N_2O_2 core with two lower rim phenolic-OH groups (**L19**, Figure 13) has been studied for its ion recognition by fluorescence, absorption, and ^1H NMR spectroscopy.[82] The N_2O_2 core was used for copper binding, which is evident from the red-shift emission of **L19** mainly due to the deprotonation of the naphthalimide NH in presence of Cu^{2+}; however, Cu^{2+} reduction to Cu^+ was not reported. **L19** showed F^- selectivity over the other anions, $H_2PO_4^-$, HSO_4^-, $CH_3CO_2^-$, I^-, Br^-, and Cl^-, studied. This forms a 1:1 stoichiometric complex with F^- by showing NH···F and OH···F interactions as supported by ^1H NMR spectroscopy. The chemical shift observed at 16 ppm in the ^1H NMR spectrum corresponds to the formation of FHF with an association constant of 1.1×10^4 M^{-1} in CH_3CN as obtained from fluorescence titration studies.

Two cyclic crown derivatives possessing S_2O_6 (**L20**) and S_3O_6 (**L21**) cores exhibit selective association, respectively, with Cu^{2+} and Ag^+ ions over several alkali, alkaline earth, and transition metal ions studied by the conductometric titrations, due to the

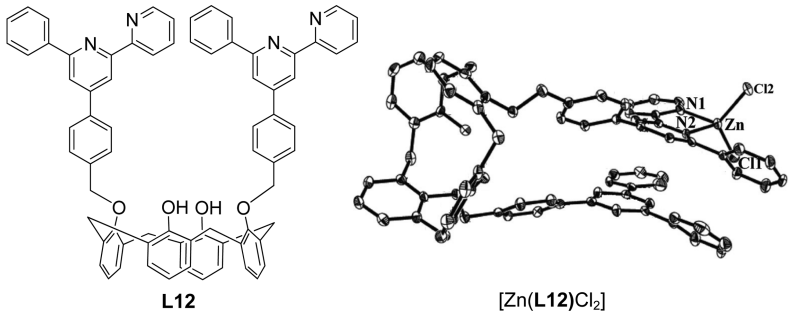

Figure 9. Schematic representation of the structure of **L12** and its zinc complex, $[Zn(\mathbf{L12})Cl_2]$. Reprinted with permission from ref 76. Copyright 2010 Elsevier.

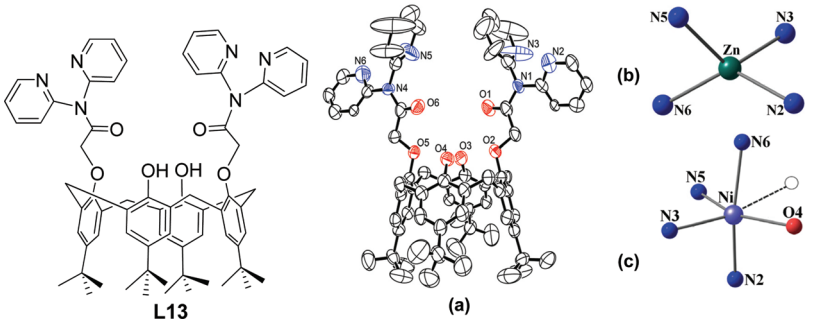

Figure 10. Schematic structure of **L13**. (a) Crystal structure of **L13** as ORTEP picture. Computationally obtained primary coordination spheres of (b) Zn^{2+}, (c) Ni^{2+} complexes of **L13**. Reprinted with permission from ref 77. Copyright 2008 Elsevier.

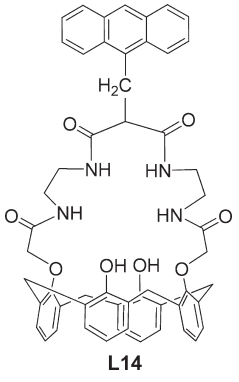

Figure 11. Schematic representation of the structure of **L14**.

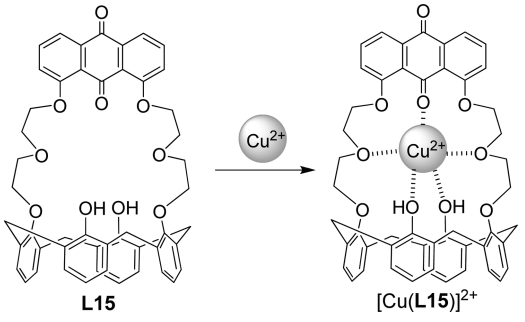

Figure 12. Schematical representation of **L15** and its Cu^{2+} complex, $[Cu(\mathbf{L15})]^{2+}$.

size and the number of ligating centers present in each of these cores (Figure 14).[83]

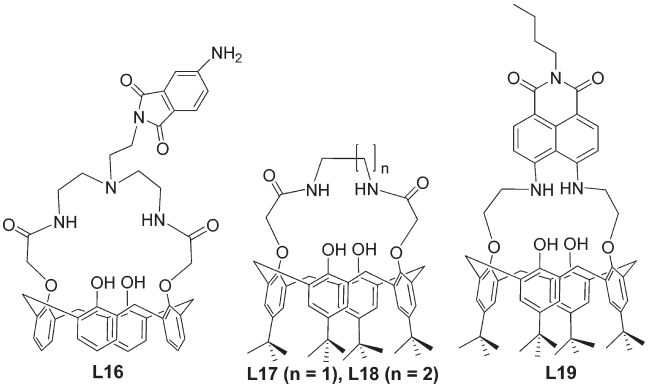

Figure 13. Schematic representation of the structures of **L16**, **L17**, **L18**, and **L19**.

3.2.2. Noncyclic Conjugates. A calix[4]arene appended with arylisoxazole unit at the lower rim (**L22**) shows Cu^{2+} receptor property by fluorescence quenching wherein the 10-chloroanthracenyl moiety has been integrated into this for monitoring the fluorescence changes (Figure 15).[84] **L22** forms a 1:1 complex with $K_a = 1.58 \times 10^4\ M^{-1}$ in $CH_3CN/CHCl_3$ (v/v = 1000:4). The Cu^{2+} undergoes autoreduction by the phenol, and the oxidized product can accommodate Cu^{+} as evidenced from the sharp NMR spectrum observed.

A derivative of β-amino-α,β-unsaturated ketone (**L23**) as well as its isoxazole precursor (**L24**) (Figure 16) were found to be selective toward Cu^{2+} by fluorescence enhancement and quenching, respectively.[85] In both cases, Cu^{2+} undergoes auto-reduction by phenolic-OH groups of the lower rim (Figure 16).

dx.doi.org/10.1021/cr1004524 |*Chem. Rev.* 2011, 111, 4658–4702

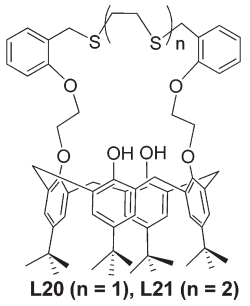

Figure 14. Schematic representation of the structures of **L20** and **L21**.

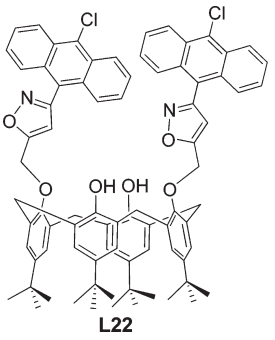

Figure 15. Receptor for Cu^{2+}.

The K_a values observed for Cu^{2+} were 17 200 and 2080 M^{-1}, respectively, for **L23** and **L24** in CH_3CN.

A 2,2′-bipyridyl conjugate, **L25** (Figure 17), forms a highly water stable mononuclear Cu^{+} complex with a possible tetrahedral geometry using its bipyridyl nitrogens.[86,87] The copper complex of **L25** exhibited significant stability in the presence of bovine serum albumin. The methyl ester derivative of **L25** [Zn(**L25**Es)] has been used in the isolation of a 1:2 ligand to Zn^{2+} complex, and the crystal structure showed one Zn^{2+} per each bipyridyl functionalized arm, where the zinc ion exhibits a tetrahedral geometry by the involvement of two nitrogens and two chlorides (Figure 17).

Shuttling of Cu^{2+}/Fe^{3+} between the two binding cores of a conjugate possessing 3-alkoxy-2-naphthoic acid (**L26**) has been demonstrated as a function of the pH of the solution (Figure 18).[88] This derivative shows a minimum fluorescence intensity when the pH of the medium was 5.6 and 6.9 in case of Fe^{3+} and Cu^{2+}, respectively. Upon increasing the pH, the carboxylic group undergoes deprotonation and acts as electron donor, resulting in fluorescence quenching through an eT mechanism. Further increase in pH results in the fluorescence enhancement, which may be due to the deprotonation of phenolic-OH, and the resultant phenolate moiety can coordinate Fe^{3+} and Cu^{2+}.

An amido-benzothiazole conjugate (**L27**)[89] (Figure 19) exhibits selective detection of Cu^{2+} among 11 different ions studied by forming a 1:1 complex. The DFT computations reveals a distorted trigonal bipyramidal geometry for the Cu^{2+} center in which O_2S_2 provides four coordination and the fifth one is from acetonitrile resulting in a NO_2S_2 core, where the bound oxygens were from amide C═O (Figure 19). The copper complex of **L27** ($[Cu(\mathbf{L27})]^{2+}$) further recognizes iodide by exhibiting a color change among the 14 anions studied, F^-, Cl^-, Br^-, I^-, ClO_4^-, SCN^-, AcO^-, SO_4^{2-}, CO_3^{2-}, NO_3^-, HSO_3^-, HPO_4^{2-}, NO_2^-, and N_3^-. The absorption spectral changes also confirm the recognition of iodide by ($[Cu(\mathbf{L27})]^{2+}$).

Bis-(2-picolyl)amide conjugate, **L28** (Figure 20a), showed selectivity toward Cu^{2+} among 10 other ions studied by forming

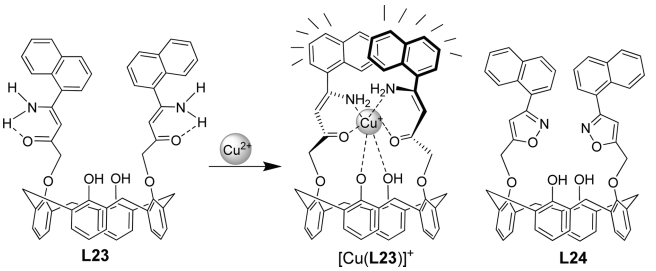

Figure 16. Schematic representation of the structure of **L23** (no excimer) and its Cu^{+} bound complex (excimer). Schematic structure of isoxazole derivative, **L24**, has also been shown.

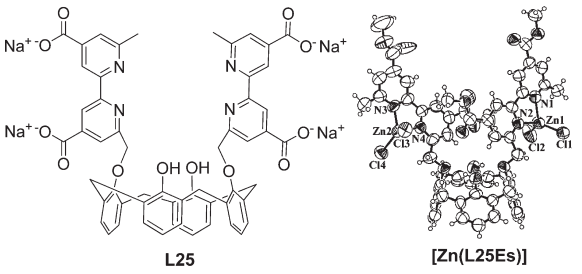

Figure 17. Schematic representation of the structure of **L25**. Single crystal X-ray structure of the Zn^{2+} complex of the methyl ester of **L25**, [Zn(**L25**Es)]. Reprinted with permission from ref 87. Copyright 2004 Wiley-VCH.

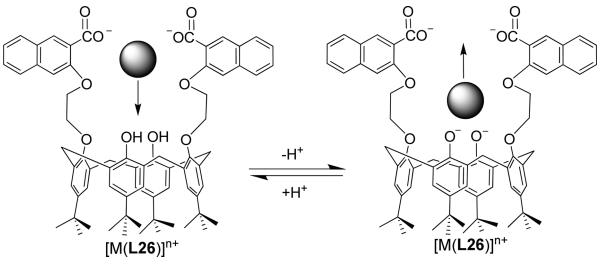

Figure 18. Variation in the metal ion coordination site as a function of the pH of the medium in case of **L26**.

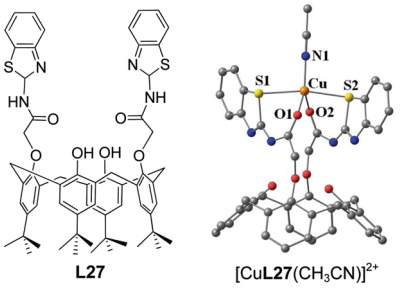

Figure 19. Schematic structure of **L27** and computationally optimized structure of the copper complex of **L27**, $[Cu(\mathbf{L27})(CH_3CN)]^{2+}$ (hydrogen atoms were removed for clarity). The *tert*-butyl groups of **L27** have been removed during the computation. Reprinted with permission from ref 89. Copyright 2010 Elsevier.

dx.doi.org/10.1021/cr1004524 |*Chem. Rev.* 2011, 111, 4658–4702

a 1:1 complex where the DFT computations revealed a highly distorted tetrahedral geometry for Cu^{2+} by coordinating through the four pyridyl nitrogens of the receptor (Figure 20b).[90] Changes observed in the microstructural features of **L28** and its Cu^{2+} complex in SEM and AFM clearly differentiate these two. The same conjugate exhibited selectivity toward Ag^{+} by ratiometric way wherein the fluorescence spectral changes observed were different from those observed in case of Cu^{2+}.[91] However, Cu^{2+} is a competitor to Ag^{+}. This may be explained from the computationally observed binding core of Ag^{+} being the same as that observed for Cu^{2+} (Figure 20b,c). In both complexes, conformational changes were required to be brought in the arms for accommodating these ions. TEM provided some differences in the nanostructural features of **L28** and its Ag^{+} complex.

A bishydroxamate derivative connected to pyrene as signaling moiety, **L29** exhibits sensitivity toward Cu^{2+} and Ni^{2+} in aqueous methanol depending upon the pH of the medium among other transition metal ions, Fe^{2+}, Co^{2+}, and Zn^{2+}, studied by the fluorescence quenching of both the excimer and the monomer emissions (Figure 21).[92] **L29** shows response to Cu^{2+} in HEPES medium, while Ni^{2+} requires a pH of 8 to exhibit ON/OFF fluorescence behavior with **L29**.

Calix[4]arene bearing two dansyl groups at 1,3-positions and two propyl groups at 2,4-positions (**L30**) exhibited a fluorescence quenching of 98% and 70% with Cu^{2+} and Hg^{2+}, respectively (Figure 22).[93] The **L30** forms a 1:2 (**L30**:Cu^{2+}) complex with Cu^{2+} and exhibits $\ln(K_a)$ of 4.19 and a lowest detection of 4×10^{-6} M in CH_3CN. The **L30** selectively forms complexes with Cu^{2+} even in the presence of other ions, which is evident form the competitive titration studies.

Most of the Cu^{2+} recognitions are generally observed as turn-off as a result of their paramagnetic nature except in some cases where turn-on fluorescence has been observed as a result of blocking the PET. Cu^{2+} complexes reviewed here were found to be in distorted trigonal bipyramidal geometry (N_3O_2, NO_2S_2) or distorted tetrahedral geometry (N_4) or distorted square planar (N_2O_2) (Figures 19, 20b,c). The proposed models for Cu^{2+} complexes show the possible binding by oxygens including carbonyls ones and also the nitrogens. While the nitrogen-rich core provides affinity and selectivity toward Cu^{2+}, the phenolic-OH moieties present in the vicinity of the binding core assist the autoreduction of Cu^{2+} to Cu^{+} followed by the binding of this ion to the oxidized semiquinone or quinone forms of the derivative (Figure 16). It has also been observed that lower rim phenolic-OH's, ether oxygens, and quinone oxygens together can provide binding cores toward Cu^{2+} (Figure 12). Thus, the donor groups such as N, O, and S can provide good coordination for Cu^{2+}. The stoichiometry of the complex formed in most of the cases has been found to be 1:1.

3.3. Monomer/Excimer Emissions in the Presence of Fe^{3+}

The monomer/excimer emissions of a dipyrenyl derivative of calix[4]arene, **L31**, are sensitive to the interaction of water through hydrogen bonding that disrupts the intramolecular ones to result in the excimer emission (Figure 23).[94] Even the presence of Fe^{3+} alters both the monomer and the excimer emissions perhaps through its interaction with phenolic and amide moieties of **L31**. At a pH of 6.1, Fe^{3+} associates with **L31** to give a K_a of 2.5×10^4 M^{-1} in aqueous CH_3CN.

3.4. Hg^{2+} Recognition

3.4.1. Cyclic Conjugates. Three closely related aza-crown receptors, **L32**, **L33**, and **L34** (Figure 24), have been shown to have high affinity toward Hg^{2+} based on either absorption or emission spectra.[95] An azophenol-type ionophore (**L32**) has

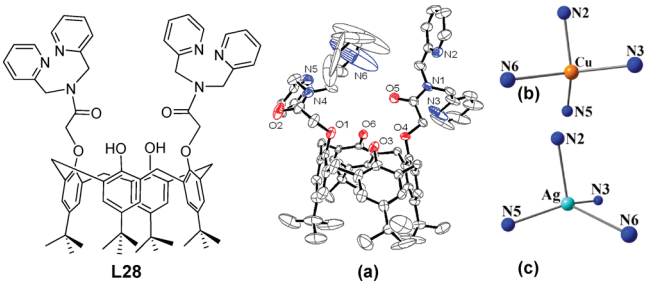

Figure 20. Schematic structure of **L28**. (a) Single crystal X-ray structure of **L28**. Computationally optimized binding cores of (b) Cu^{2+} and (c) Ag^{+} in the corresponding 1:1 complexes with **L28**. Reprinted with permission from ref 90. Copyright 2009 Elsevier.

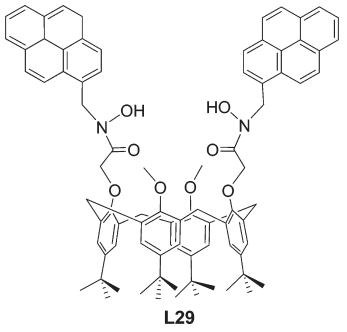

Figure 21. Schematic representation of the structure of **L29**.

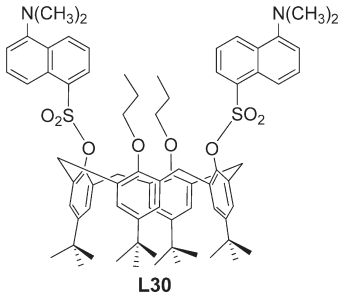

Figure 22. Schematic structure of **L30**.

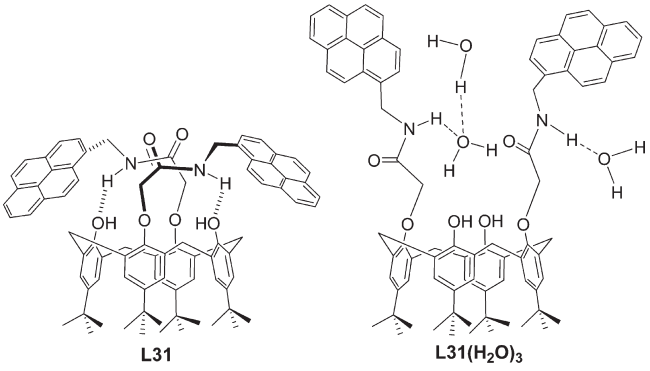

Figure 23. Schematic representation of the structures of **L31** and its water bound species, [**L31**$(H_2O)_3$] (from computational studies).

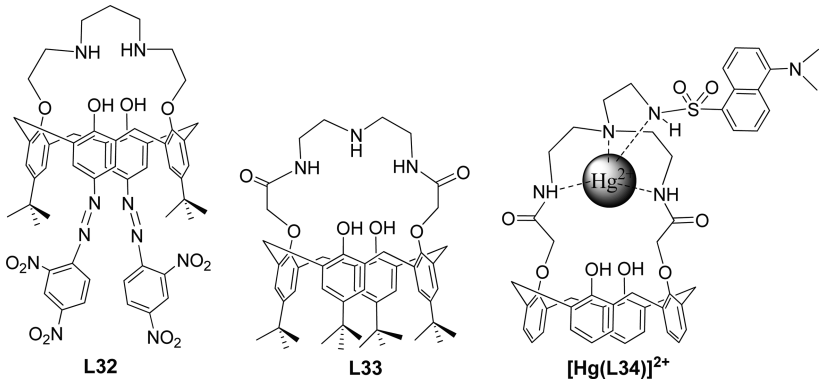

Figure 24. Schematic representation of the structures of **L32** and **L33** and proposed binding model for $[Hg(\mathbf{L34})]^{2+}$.

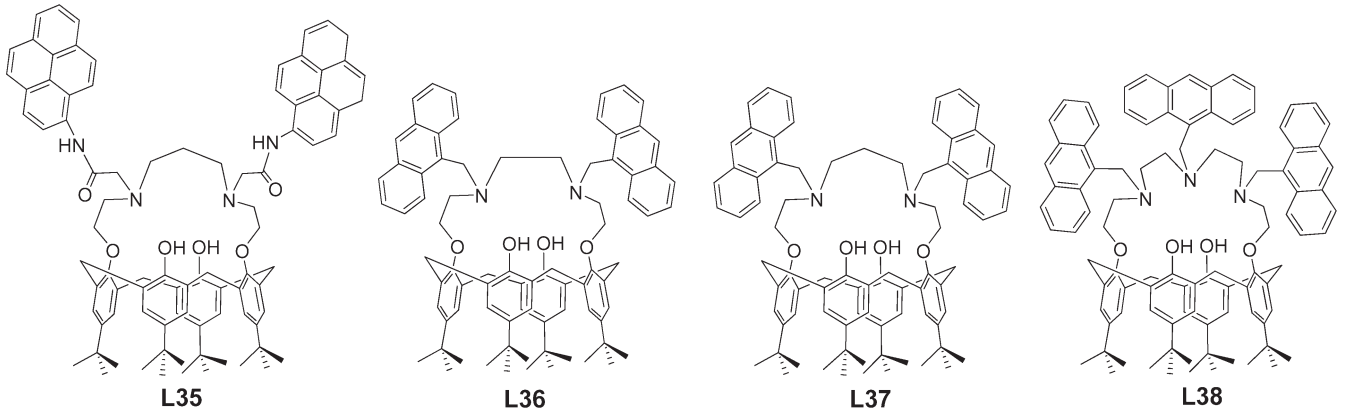

Figure 25. Schematic structures of different Hg^{2+} receptors, **L35**, **L36**, **L37**, and **L38**.

been shown to exhibit selective chromogenic behavior toward Hg^{2+} among a number of other ions, such as alakali, alkaline earth, transition, and heavy metal ions studied. Amido-crown conjugate of calix[4]arene, **L33**, showed selectivity toward Hg^{2+} by exhibiting a blue shift of 38 nm in UV−visible spectroscopy, while no changes were observed with other ions.[96] A cyclic-amido-dansyl conjugate (**L34**) forms a 1:1 complex by exhibiting high fluorescence sensitivity with Hg^{2+} through the formation of N_4 binding core (Figure 24); the heavy metal ions, such as Pb^{2+}, Cu^{2+}, Cd^{2+}, and Zn^{2+}, compete for Hg^{2+}.[97] No proposed structures were known for Hg^{2+} binding in case of **L32** and **L33**.

A calix[4]arene receptor appended with pyrenylacetamide, **L35** (Figure 25), detects Hg^{2+} through fluorescence quenching after a 100 equiv addition of the ion even in the presence of other ions such as alkali, alkaline earth, transition, and heavy metal ions, with an association constant of 4.5×10^4 M^{-1} in methanol.[98] The fluorescence emission of **L35** mainly originates from the monomer and weak excimer in methanol, while it is the reverse in 50% aqueous methanol. Upon interaction with Hg^{2+}, both the monomer and the excimer emissions of **L35** have been quenched, indicating an ON−OFF type receptor. A series of aza crown derivatives of calix[4]arene with an anthrancene fluorophore have been studied for their ability to detect Hg^{2+}.[99] The **L37** shows highest fluorescence enhancement toward Hg^{2+} as compared to **L38** and **L36** (Figure 25). The fluorescence of **L37** enhances in the presence of Cu^{2+} and Pb^{2+}, although this enhancement is much less than that of Hg^{2+} in a mixture of methanol−tetrahydrofuran. The nonselectivity of **L38** toward all of the ions is mainly due to the presence of more number of nitrogen donor centers in the system, indicating that only the presence of requisite number of ligating nitrogen centers is necessary for optimal binding. However, the selectivity is lost when the number of ligating centers is lower or higher than this. The higher selectivity of **L37** is attributable to the flexibility of the spacer unit present in **L37** as compared to **L36** that brings better coordination between Hg^{2+} and the nitrogen donor centers in the former.

3.4.2. Noncyclic Conjugates. An amido-benzimidazole conjugate (**L39**, Figure 26) exhibited Hg^{2+} selectivity (K_a = 20966 ± 873 M^{-1}) by forming a 1:1 complex among a number of other metal ions studied in 1:1 aqueous acetonitrile.[100] The necessity of the calix[4]arene unit and the nitrogen binding core has been demonstrated. The binding core has been delineated by ^1H NMR spectroscopy and the coordination features by the DFT computational calculations, which show a linearly coordinated N2···Hg···N5 core. The binding is further supported by the weak interactions extended from the amide carbonyl oxygens (Figure 26). The bent arm of **L39** undergoes major conformational changes in the presence of Hg^{2+} ion to make a suitable binding core. The TEM, AFM, and SEM studies of the isolated complex exhibited features different from those of the simple receptor (**L39**).

Amido-pyridylcalix[4]arene derivative, **L40**, has been studied for its complexation with Hg^{2+}, Zn^{2+}, and Ag^{+} using ^1H NMR spectroscopy and electrochemistry (Figure 27).[101] ^1H NMR spectral titration confirms the formation of the complex with

dx.doi.org/10.1021/cr1004524 |*Chem. Rev.* 2011, 111, 4658–4702

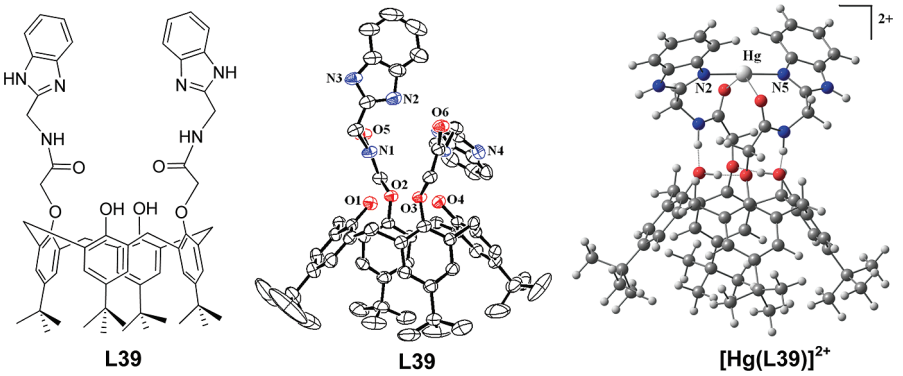

Figure 26. Schematic structure of **L39**. Single crystal X-ray structure of **L39** as ORTEP picture.[100] Computationally optimized structure of $[Hg(\mathbf{L39})]^{2+}$ complex.

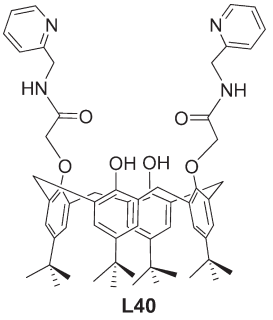

Figure 27. Schematical representation of the receptor **L40**.

Hg^{2+} through the involvement of both the pyridyl and the amide units. Interestingly, when the complex was prepared by heating a mixture of **L40** and Hg^{2+} in ethanol or methanol, it resulted in the cleavage of the amide bond, and the necessity of this ion for the cleavage has been clearly demonstrated. The Ag^{+} and Zn^{2+} also form complex with **L40** without undergoing any cleavage as proven by ^{1}H NMR studies. The fluorescence intensity of **L40** was quenched upon interaction with Hg^{2+}, Zn^{2+}, and Ag^{+}. The metal−ligand binding has also been supported by the electrochemical studies.

An amido-dansyl conjugate (**L41**) exhibit good extraction ability toward Hg^{2+} and found that Pd^{2+} is only the competitor for Hg^{2+} (Figure 28).[102−104] The **L41** also showed Hg^{2+} selectivity by fluorescence quenching as a result of electron transfer among the other ions studied, Na^{+}, K^{+}, Ca^{2+}, Cu^{2+}, Zn^{2+}, Cd^{2+}, and Pb^{2+}, in aqueous acetonitrile at pH = 4. It forms a 1:1 stoichiometric complex with Hg^{2+} with an association constant of 1.5×10^{7} M^{-1} in CH_3CN/H_2O (60:40 v/v). **L41** showed response toward Hg^{2+} even in the presence of other ions but for Pb^{2+}, which interferes to some extent. ^{1}H NMR spectral titration of this derivative with Hg^{2+} indicates that, upon complexation, calix[4]arene exists in the cone conformation. Time-resolved fluorescence titration has also been carried out to get more insight into the mercury complexation. The alkali and transition metal ion interactions of a series of calix[4]arenes possessing dansyl fluorophore (**L42**,**L43** and tetramethylammonium salt of **L41**, Figure 28) have been studied by absorption and fluorescence spectroscopy.[105] The metal ions, Fe^{3+}, Hg^{2+}, and Pb^{2+}, exhibit strong interaction with these conjugates by quenching the original fluorescence by 97%. A calix[4]arene functionalized with two dansyl fluorophores and two long alkyl chains of triethoxysilane groups (**L44**) that was placed in mesoporous silica showed the ability to sense Hg^{2+} in water by forming a 1:1 complex (Figure 28).[106]

The solvent-dependent recognition ability of thioether conjugate of calix[4]arene, **L45** (Figure 29), has been studied by ^{1}H NMR spectroscopy, electrochemistry, and thermodynamics.[107,108] Sensitivity of **L45** in the detection of Hg^{2+} is better than Ag^{+} by a factor of 2.2×10^{3} in acetonitrile, and it is exactly reverse in case of methanol, and no selectivity was observed in *N*,*N*-dimethylformamide. In the complex, Hg^{2+} forms a tetra-coordination by the involvement of two sulfurs of the pendant arms and two perchlorate ions, while Ag^{+} forms a supramolecular structure (Figure 29). CdSe/ZnS quantum dots (QDs) capped with thioether derivative of calix[4]arene, **L45**, exhibit selectivity toward Hg^{2+} among a number of ions studied and can be detected down to a concentration of 15 nM.[109]

Benzothiazole appended conjugate of calix[4]arene, **L46** (Figure 30), that was coated on glassy carbon electrode recognizes Hg^{2+} selectively in aqueous medium among alkali, alkaline earth, and transition ions using cyclic and square wave voltammetric techniques.[110] However, 500-, 50-, and 100-fold molar excess of Pb^{2+}, Ag^{+}, and Cu^{2+}, respectively, induce significant voltametric changes. The lowest concentration of Hg^{2+} that can be detected by **L46** was found to be 25 nM. Liquid membrane transport and silver selective electrode properties of a calix[4]arene appended with nicotinic moieties, **L47**, have been studied (Figure 30).[111] This derivative exhibits cation selectivity toward Ag^{+} and Hg^{2+} over other alkali, alkaline earth, transition, and ammonium ions studied.

A triazole linked 8-oxyquinoline conjugate (**L48**) exhibits selectivity toward Hg^{2+} by fluorescence quenching at a low pH (Figure 31).[112] While the K_a for the 1:1 complex is 8.5×10^{3} M^{-1} in case of Hg^{2+}, these are 1.2×10^{3} and 4.4×10^{3} M^{-1}, respectively, for Cu^{2+} and Fe^{2+} showing no greater selectivity in CH_3CN:H_2O (v/v 3:1). A NOR logic gate property has been proposed using the fluorescence intensity of **L48** in the presence of Hg^{2+} as a function of pH.

On the basis of the emission behavior, it has been possible to differentiate Hg^{2+} from that of other heavy ions, Pb^{2+} and Cd^{2+}, as shown by a terminal-NH_2 bound calix[4]arene conjugate, **L49** (Figure 32).[113]

The receptor, **L50**, a double branched calixarene conjugate bearing one amidopyrenylmethyl moiety and a rhodamine B unit (Figure 33), acts as 1:1 stoichiometric chemosensor for Hg^{2+}

dx.doi.org/10.1021/cr1004524 |*Chem. Rev.* 2011, 111, 4658–4702

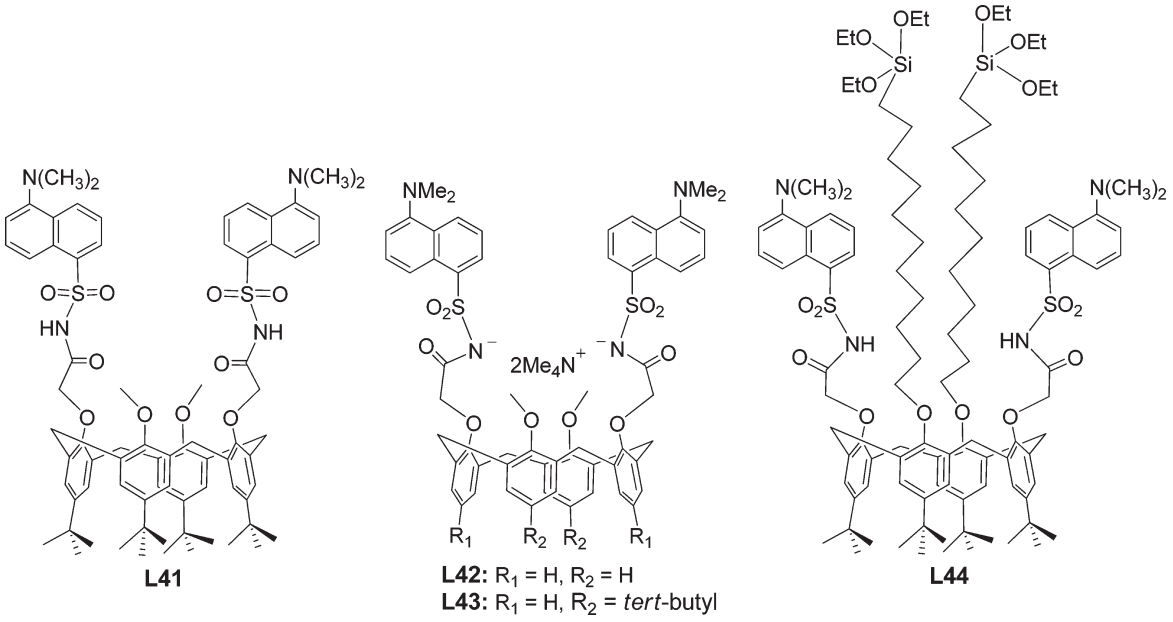

Figure 28. Schematic structures of **L41**−**L44**.

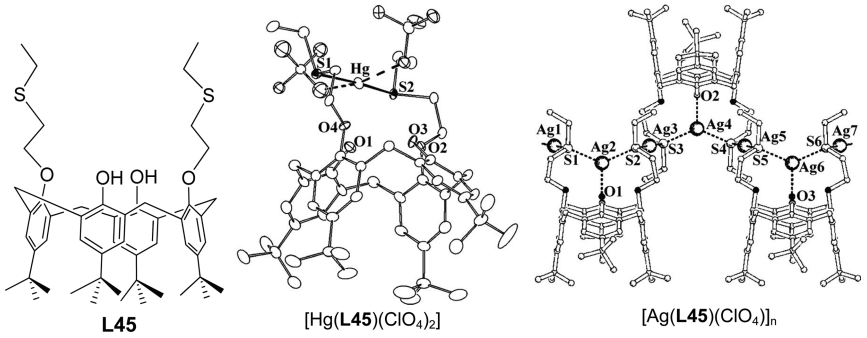

Figure 29. Schematic structure of **L45** and crystal structures of $[Hg(\mathbf{L45})(ClO_4)_2]$ and $[Ag(\mathbf{L45})(ClO_4)]_n$.[107]

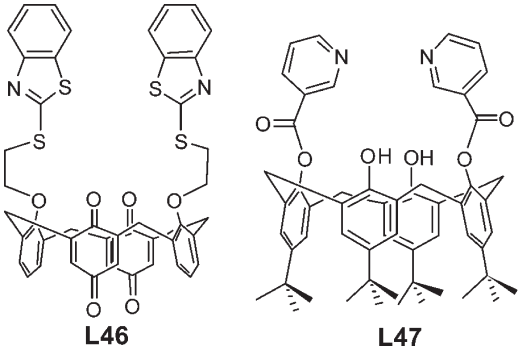

Figure 30. Schematic structures of **L46** and **L47**.

and Al^{3+}.[114] While Hg^{2+} opens the spirolactam ring of rhodamine to bind (tren-spirolactum), Al^{3+} binds unopened. Although this paper demonstrates the role of FRET, the role of calixarene moiety has not been addressed adequately.

Cyclic and noncyclic arms appended calix[4]arene bearing nitrogen, amide, or sulfur as donor groups detects Hg^{2+} with good selectivity among the other ions studied. Although Hg^{2+}

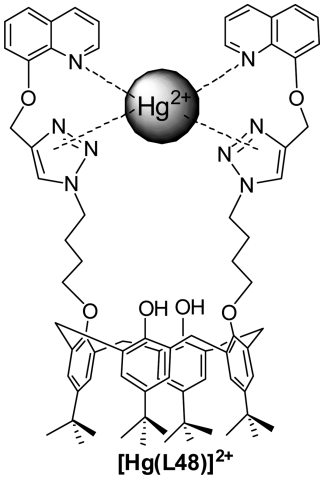

Figure 31. Proposed Hg^{2+} binding core present in **L48**.

favors linear coordination with ligands having nitrogen or sulfur, it has been found that in certain cases other donor centers, such as N, O of the arms or of the solvent, provide additional

dx.doi.org/10.1021/cr1004524 |*Chem. Rev.* 2011, 111, 4658–4702

stabilization by weak interactions (Figures 26 and 29). Aza-crown and amido-crown ether conjugates possessing preorganized binding cores exhibit good selectivity toward Hg^{2+} (Figure 24). The main binding core of Hg^{2+} that leads to the linear coordination obeys HSAB. It is important to note that the size of the cavity and the nature of the donor atoms are the two main factors, which determine the selectivity and binding efficiency of a conjugate toward a particular ion. This section also demonstrates the role of solvent in the selective recognition of Hg^{2+} over the other ions studied due to the difference in polarity of the same. Generally, Hg^{2+} interaction results in the fluorescence quenching of the receptor molecule as a result of the heavy metal atom effect, but in some cases the complexation leads to the enhancement of the fluorescence intensity due to the participation of a lone pair of nitrogens in the complexation, which was initially responsible for the fluorescence quenching. It is also possible to develop fluorescent sensors for Hg^{2+} by fluorescence enhancement using appropriate selection of the fluorophores, which function as FRET, PET, etc.

3.5. Pb^{2+} Recognition

A series of cyclic triazole linked calix[4]crown conjugates possessing both hard and soft ligating centers (e.g., **L51**, **L52**, **L53**, and **L54**) (Figure 34) exhibit selectivity toward alkali ions as well as Pb^{2+} depending upon the size of the crown as well as the number of hetero atoms present in it and their hard−soft base character.[115] The extraction abilities follow an order, $Li^+ > K^+ > Na^+ > Cs^+$, $Li^+ \gg Na^+ > K^+ > Cs^+$, $Li^+ > Cs^+ > Na^+ > K^+$, and $Li^+ \gg Cs^+ > K^+ > Na^+$, respectively, for **L51**, **L52**, **L53**, and **L54**. Among the four conjugates, only **L51** showed selective extraction with Pb^{2+} and not the others.

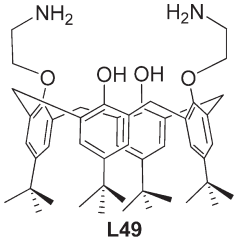

Figure 32. Schematic structure of **L49**.

The two β-ketoimine derivatives, which differ in their arm length, $-(CH_2)_2-$ (**L55**) and $-(CH_2)_4-$ (**L56**) (Figure 35), have been studied for extraction and the cation binding.[116] **L55** showed good extraction abilities toward Pb^{2+} among the ions studied at pH = 8, and the extraction is pH dependent. **L55** shows good affinity for Na^+, K^+, and Ca^{2+} at pH = 4.8 due to the electrostatic interaction between the cations and the cavity formed by the β-ketoimine group. Cation interaction studies of **L55** and **L56** results in similar changes with Hg^{2+}, Cu^{2+}, and Ag^+ as monitored by UV−vis spectroscopy, indicating that these cations are complexed by the β-ketoimine groups and the complexation is independent of the alkyl chain length.

A series of calix[4]arene-based amide derivatives have been studied in a PVC membrane for their Pb^{2+} selective electrode properties by potentiometry even in the presence of other competing ions.[117] Ag^+ has been found to be a competitor for Pb^{2+} in all of the cases. At low concentrations of K^+, Na^+, or NH_4^+, the electrodes modified with **L57**, **L58**, **L59**, and **L60** (Figure 36) act as Pb^{2+} sensors. Other calix[4]arene conjugates, **L61**−**L63** (Figure 36), exhibited high selectivity for Pb^{2+} even in the presence of other ions but in the absence of Ag^+. The electrode properties of these derivatives with dioctylphthalate as a plasticizer have also been studied, and it was found that the sensitivity of the response decreases in the order of **L60** > **L61**−**L63** > **L57** > **L59** ≥ **L58**, which is attributed to the variations present in the functional moiety.[118]

Fluorescence emission characteristics of amido-pyrenyl conjugates (**L64** and **L65**) exhibit a difference between Pb^{2+} and In^{3+} as can be seen from Figure 37.[119] A major difference between **L64** and **L65** is the ability of the former to make intramolecular hydrogen bonding and not the latter, due to the absence of phenolic-OH and its O-propyl derivatization in case of **L65**. Hence, the emission characteristics differ between **L64** and **L65** in the presence of Pb^{2+} and In^{3+}.

Pb^{2+} extraction and the detection were mainly observed with receptors bearing hard donor moieties such as oxygen in addition

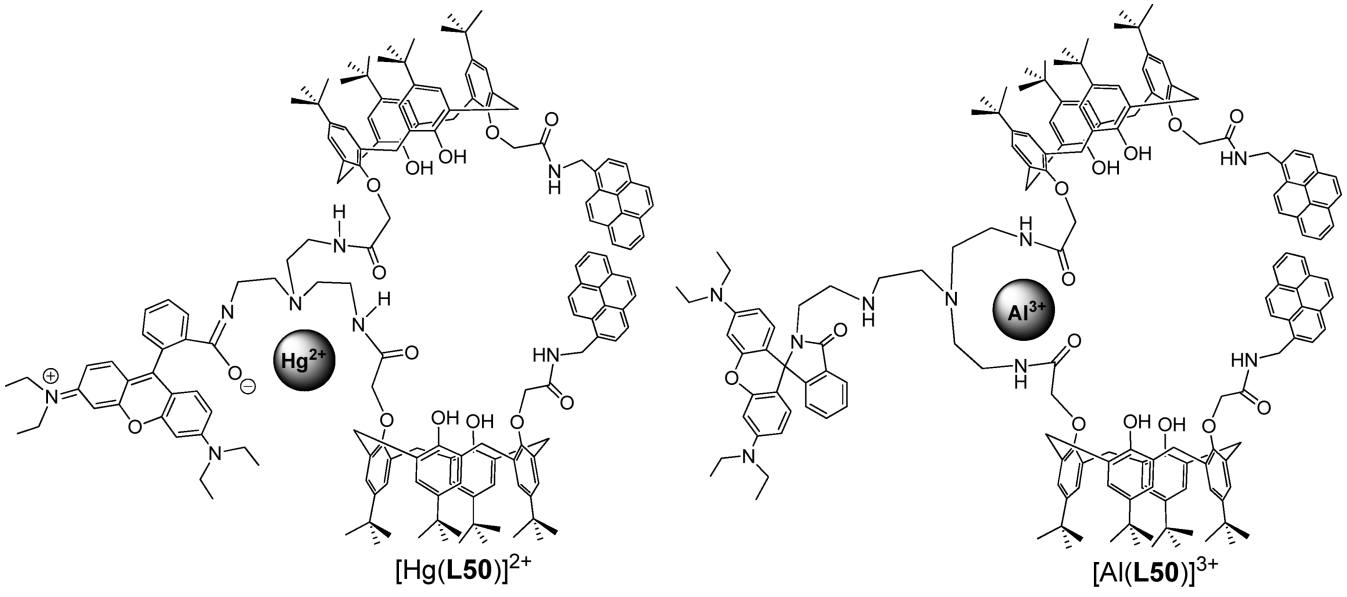

Figure 33. Proposed binding models for $[Hg(\mathbf{L50})]^{2+}$ and $[Al(\mathbf{L50})]^{3+}$ complexes.

dx.doi.org/10.1021/cr1004524 |*Chem. Rev.* 2011, 111, 4658–4702

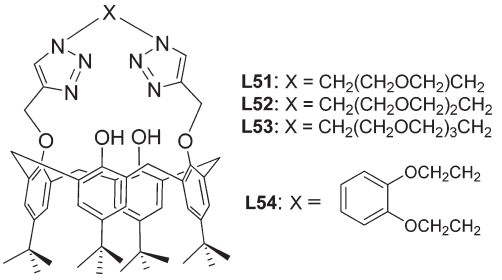

Figure 34. Schematic representation of triazole linked cyclic calix[4]arene conjugates, **L51**−**L54**.

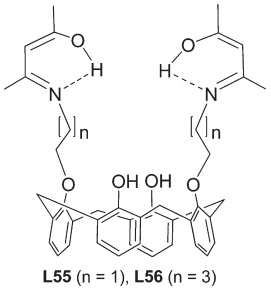

Figure 35. Schematic representation of **L55** and **L56**.

to the participation of phenolic-OH's, amide oxygen, or nitrogen centers (Figure 37). Pb^{2+} easily forms higher coordinations with the help of oxygen atoms of crown ether, phenolic-OH's, etc. Nitrogen containing triazole units also prefer transition metal ions as is evident from this section, and this indeed is based on the HSAB concept. It is also important to note that the pH of the medium has some role in the efficiency of extraction of Pb^{2+}. Attaching a fluorophore helps the derivatives to monitor the ion recognition by fluorescence spectroscopy (Figure 37).

3.6. Ag^+ Recognition

ortho-Schiff and *para*-Schiff base conjugates (**L66**−**L73**, Figure 38) have shown affinity toward Ag^+, but the *para*-isomer was found to be nonselective because of the absence of N_2O_2 binding core that was otherwise present in case of the *ortho*-derivative.[120] When an additional pyridyl moiety is present as in **L70**, the complex can show five or six coordination via the participation of two ether oxygens, two imine nitrogens, and one or both of the pyridine nitrogens (Figure 38). Among the *ortho*-derivatives, **L70** showed high affinity toward Ag^+ due to the presence of imine and aromatic nitrogens. Comparison of the data clearly suggests that the presence of a preorganized binding core is important in the selective recognition process. All of these derivatives exhibit good transport rates.

A 2,2′-bipyridine-substituted derivative of calix[4]arene, **L74** extracts Ag^+ from a mixture of lead and silver nitrate in neutral aqueous solution (Figure 39).[121] The silver complex of **L74** has been found to form a stable mononuclear complex. It has been suggested that the selective extraction of Ag^+ in the presence of Pb^{2+} is due to the tetrahedral mode of binding of Ag^+.

The presence of 2-bezothiazolylthioalkoxy at the lower rim (**L75**−**L80**, Figure 40) makes the ionophore suitable for the Ag^+ ion recognition, although some interference was observed in the presence of Hg^{2+} and not with the other dozen ions studied.[122,123] The selectivity exhibited by all of the receptors

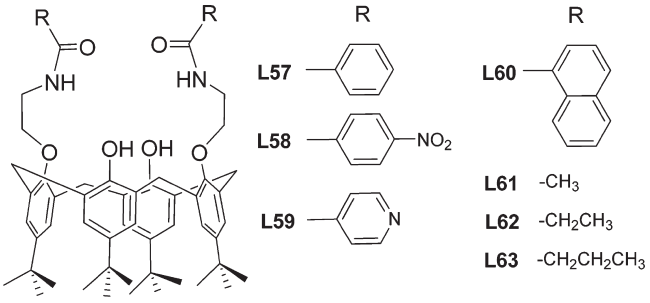

Figure 36. Schematic structures of **L57**−**L63**.

toward Ag^+ was irrespective of the tether length between the benzothiazolyl and the calix[4]arene. The HSAB characteristics seem to work well with this system.

All of the thio-conjugates, **L81**, **L82**, and **L83** (Figure 41), showed good ion selective electrode properties toward Ag^+ over the competing ions except for Hg^{2+}.[124] In case of **L83**, the ^{19}F NMR spectrum of the silver complex indicates the formation of a conformational equilibrium in solution where fluorine atoms are participating in ligation with the silver cation (Figure 41). Yet in the uncomplexed form, **L83** exists in a conformational equilibrium with some intramolecular weak hydrogen-bonding interaction between C−H and F.

A series of calix[4]arene conjugates possessing pyridyl moietiy (**L84**, **L85**, **L86**) (Figure 42) have been synthesized and were shown for their ion-selective electrode property toward Ag^+ over a number of alkali, alkaline-earth ions, lead, ammonium, and some transition metal ions, except Hg^{2+}.[125] Among the three conjugates studied, **L86** showed high selectivity toward Ag^+ and weak response to alkaline-earth ions, indicating the involvement of the ligation of Ag^+ through the $-PPh_2$ moiety.

Silver ion selective electrode property of a pyrimidine conjugate of calix[4]arene, **L87** (Figure 43), has been studied and found that it exhibits a detection limit of 1 μM.[126] This electrode works in the pH range of 3−7 and showed good Ag^+ selectivity over other alkali, alkaline earth, transition, and heavy metal ions.

A series of crown and one linear functionalized calix[4]arene (**L88**−**L93**, Figure 44) have been studied for their extraction abilities toward a number of alkali, alkaline earth, and transition metal ions.[127] Because of the flexibility, Ag^+ can access the sulfur donors in the linear calix[4]arene conjugate, **L88**, and therefore gives a higher extraction percentage as compared to the other conjugates, **L89** and **L90** (these two show similar extraction percentage with Ag^+). The calix[4]arene conjugate **L91** extracts Ag^+ as a results of its suitable cavity size. The extraction observed with **L92** was negligible due to the increased volume of cavity. Among all of these, **L93** bearing thiacrown with a pyridine moiety exhibited largest extraction of Ag^+.

The interaction of Ag^+ results in the chemical shifts of different protons of **L94** (Figure 45). However, the imine and the phenolic-OH of the corresponding calix[4]arene moiety of **L95** (Figure 45) experience significant chemical shift upon interaction with Ag^+.[128] A large chemical shift change was observed with **L95** as compared to **L94** when they interact with Ag^+. Therefore, in **L94** it may be the structural rearrangement rather than the direct binding that influences most, while it may be the direct binding in **L95** that brings change in the chemical shift.

The PVC membranes constructed using two different derivatives of bis-calix[4]arenes connected through phenyl (**L96**) or

dx.doi.org/10.1021/cr1004524 |*Chem. Rev.* 2011, 111, 4658–4702

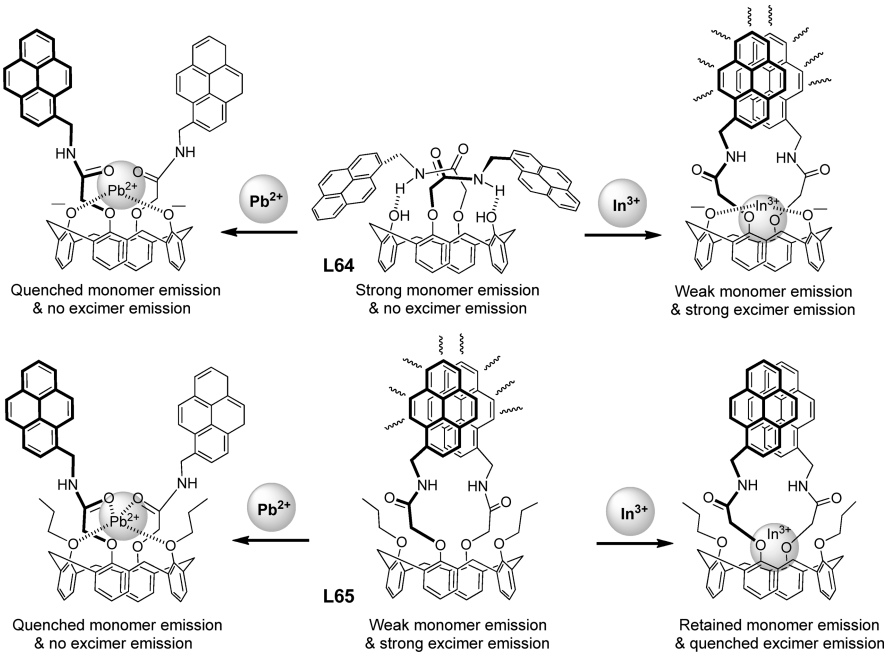

Figure 37. The mode of binding of **L64** and **L65** with Pb^{2+} and In^{3+}.

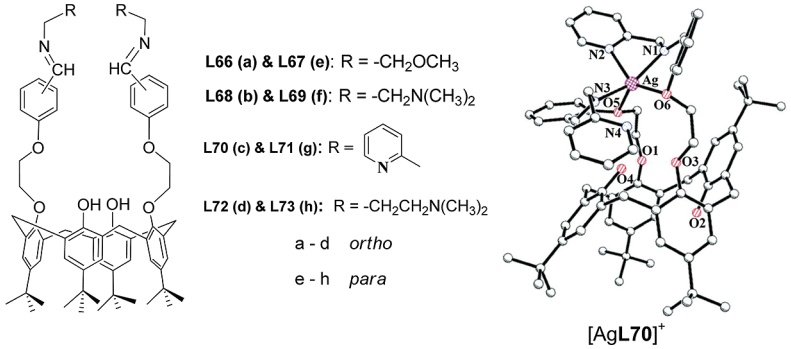

Figure 38. Schematic structures of *ortho*- and *para*-derivatives of calix[4]arene conjugates, **L66**−**L73**, and energy minimized structure of $[Ag(\mathbf{L70})]^+$ complex. Reprinted with permission from ref 120. Copyright 2004 Elsevier.

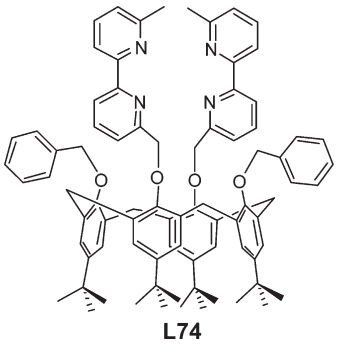

Figure 39. Schematic structure of **L74**.

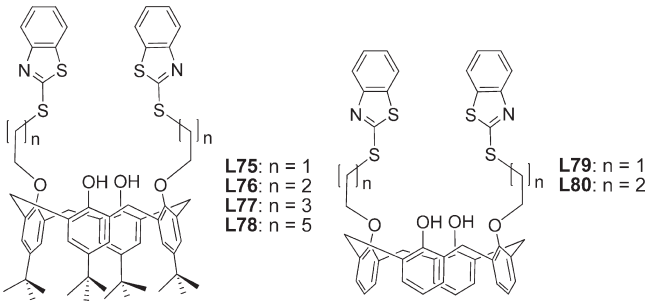

Figure 40. Schematic structures of **L75**−**L80**.

pyridyl (**L97**) (Figure 45) linkers exhibit better response toward Ag^+.[129] A higher Ag^+ selectivity with the pyridyl conjugate has been observed. The electrostatic interaction present between the metal ion and the aza crown cavity is responsible for the Ag^+ recognition.

The imine nitrogens, pyridine nitrogens, and soft donor groups such as sulfur are involved in the binding of silver ion. The Ag^+ complexes presented in this Review form tetrahedral geometry by the use of N4 core, and in some cases it can extend its coordination by the participation of nearby oxygens. Among the cyclic derivatives of calix[4]arene, the conjugates bearing both thiacrown and pyridine moiety together in one molecule showed excellent selectivity, and this indeed suggests the role of the soft donor moieties in efficient binding. The factors that are

dx.doi.org/10.1021/cr1004524 |*Chem. Rev.* 2011, 111, 4658–4702

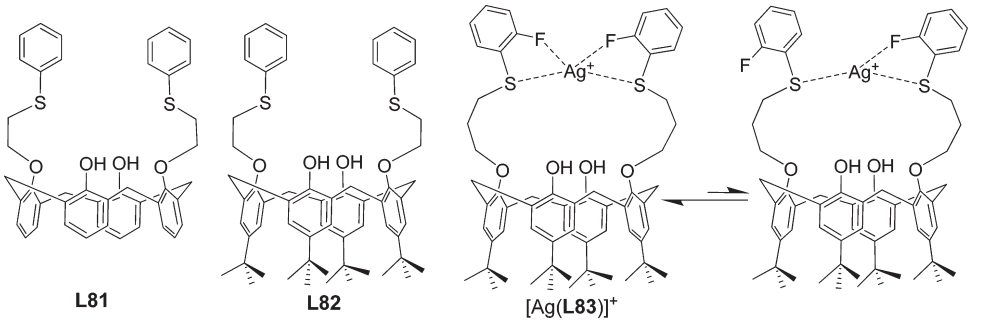

Figure 41. Schematic structures of **L81** and **L82** and Ag^+ binding model of **L83** in two of its resonance forms.

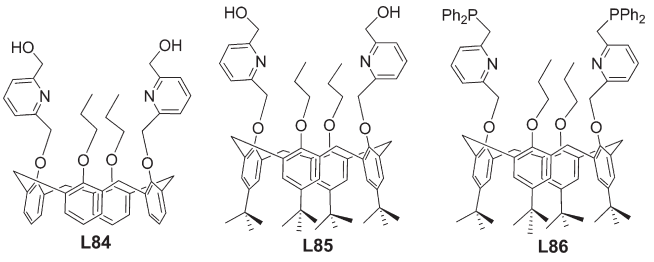

Figure 42. Schematic structures of **L84**−**L86**.

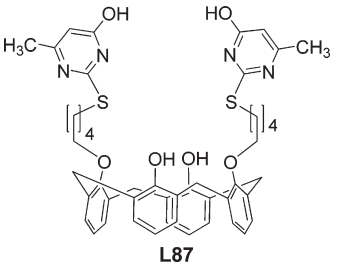

Figure 43. Schematic structure of **L87**.

responsible for the selective binding are the proper cavity size especially in case of cyclic conjugates. In most of the cases, ^1H NMR spectroscopy was used for studying the interaction between the receptor molecule and the Ag^+.

3.7. Al^{3+} Recognition

The tren-*N*-tricalix[4]arene appended pyrenyl fluorophore (**L98**) exhibits large fluorescence enhancement with Al^{3+} and less enhancement with In^{3+}.[130] From the ^1H NMR spectral titrations, it has been found that the interaction of **L98** with Al^{3+} is mainly through the tren-N part as can be seen from the Figure 46. The receptor molecule uses its nitrogen and oxygen moieties to satisfy six coordinations for Al^{3+} in its recognition.

3.8. Recognition of Alkali Metal Ions

Liquid−liquid extraction ability of a chiral calix[4]-(azoxa)crown-7, **L99**, exhibits Li^+ selectivity among the alkali metal ions, although the transition metal ions were also being extracted by this, due to its variable coordination core.[131] The ion binding is influenced by the size and the nature of hard and soft base character of the ligating centers present in the crown moiety and also the cation−π interactions present between metal ions and the carbonyl groups. Thus, while Li^+ is bound by three ether oxygens, the same receptor can extend higher coordination to transition ions as noted in case of **L99** (Figure 47).

The *o*-azo-benzene conjugate of calix[4]arene, **L100** (Figure 48), exhibits selectivity toward Na^+ and K^+ by the involvement of nitrogen of the diazo group.[132] Upon the complexation with K^+, the thermal equilibrium of the conjugate shifts toward the *trans*-isomer, while the complexation with Na^+ results in the *cis*-isomer.

Extraction of alkali ions as picrates by oxahexacyclic cage functionalized calix[4]arene conjugates (**L101**−**L104**) have been studied (Figure 49).[133] The conjugates **L101** and **L102** shows good Na^+ picrate extraction efficiency (with less percentage of extraction) as compared to the other metal picrates, while the highest K^+ extraction was observed with the receptors **L103** and **L104**, which were anchored with one or two $CH_2CH_2OCH_3$ units by using phenolic-OH moieties.

Calix[4]arene bearing two crown rings connected through a fluorophore, **L105** (Figure 50), shows Cs^+ and K^+ sensing ability in acidic and alkaline environments, respectively.[134] Under basic conditions, K^+ forms a complex with crown ring I, while Cs^+ requires acidic medium to interact with crown ring II, both by exhibiting fluorescence enhancement. In basic methanol, the fluorescence intensity of the receptor with different ions follows an order $K^+ > Rb^+ > Cs^+ > Na^+ > Li^+$, and in the acidic medium the trend is $Cs^+ > Rb^+ > K^+ > Na^+ > Li^+$. The fluorescence behavior of the receptor molecule also mimics the logic gate functions.

Double-calix[4]quinone conjugates have been studied for their selectivity toward alkali ions based on the variations observed in electrochemical potentials of the receptor system (Figure 51).[135,136] The conjugate **L106** exhibits selectivity toward Na^+ as a result of the optimal spatial fit of this ion within the cavity, while lower association constant and no complexation were observed with K^+ and Cs^+, respectively, due to the large size of these ions. Because its large cavity size, **L107** forms stable complexes with K^+ and Cs^+ but forms a weak complex with Li^+. Upon interaction with K^+, **L108** exists in cone conformation, but with Li^+ and Na^+ it results in the conformational changes (association constants could not be derived as a result of mixed conformation). In addition, **L108** exhibit low association constant and no complexation with K^+ and Cs^+, respectively, due to its smaller cavity size. On the basis of the association constants, the selectivity order of **L106** is $Na^+ > Li^+ \gg K^+$, and that of **L107** is $Cs^+ > K^+ > Na^+ \gg Li^+$. Both the **L107** and the **L108** exhibit significant electrochemical changes in the presence of alkali ions. The observed shift in the voltammograms depends upon the polarization ability of the metal ions. Among the three conjugates, **L108** showed switchable electrochemical binding toward Na^+ and K^+ with larger binding being observed with K^+ as a result of the polarizing ability of the $-OCH_3$ group.

L109 showed significant selectivity in solvent mixtures of varying polarity toward K^+ among group I metal ions and

dx.doi.org/10.1021/cr1004524 |*Chem. Rev.* 2011, 111, 4658–4702

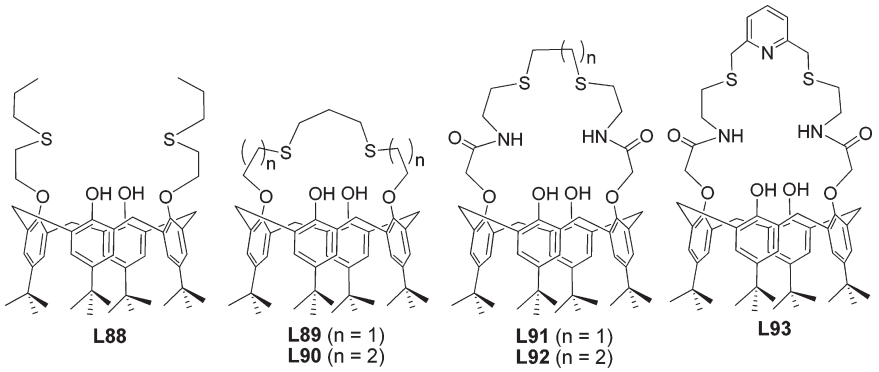

Figure 44. Schematic structures of **L88**−**L93**.

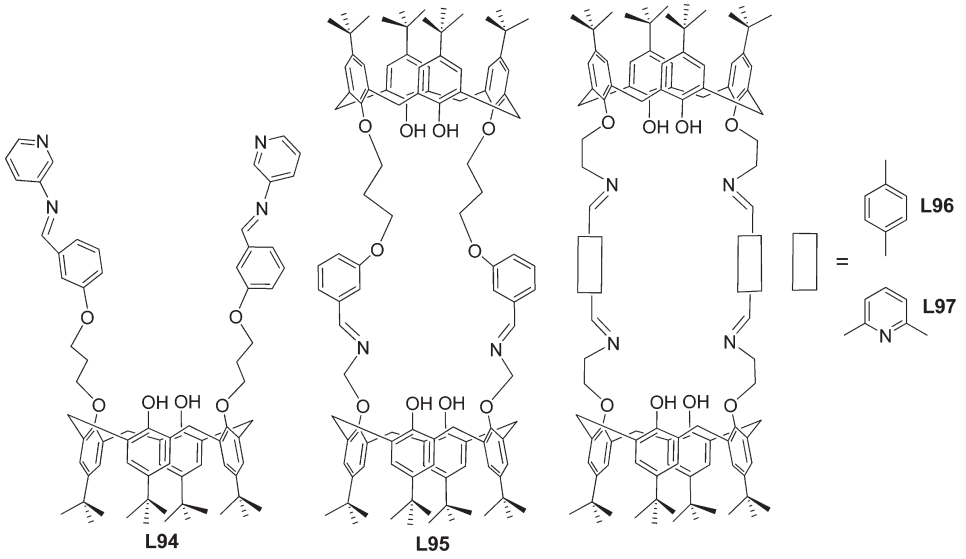

Figure 45. Schematic structures of **L94**−**L97**.

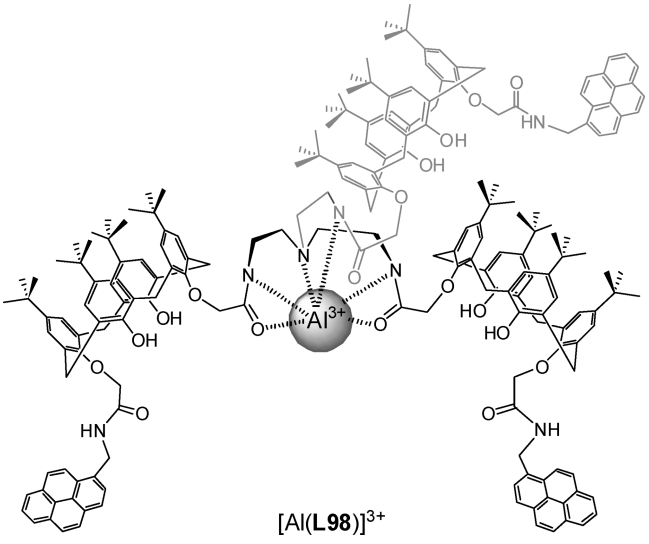

Figure 46. Schematic representation of Al^{3+} coordination with **L98**.

ammonium ion as studied by UV−vis and ^1H NMR spectroscopy (Figure 52).[137] The electrochemical recognition abilities of

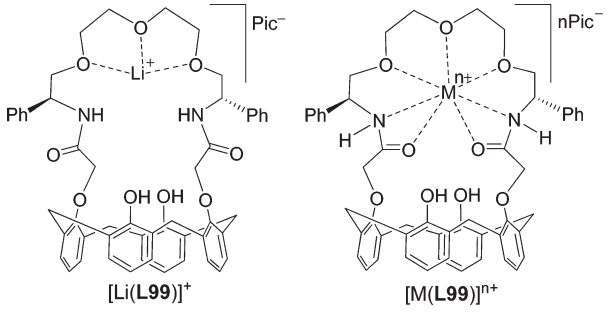

Figure 47. Proposed binding of $[Li(\mathbf{L99})]^+$ and $[M(\mathbf{L99})]^{n+}$.

calix[4]semitube diquinone, **L109**, have also been explored, and it recognizes both Na^+ and K^+. A series of double calix[4]diquinones connected by alkylene or pyridylene have been studied for their recognition toward alkali ions by spectroscopy and electrochemistry, in addition to establishing the structure by X-ray crystallogarphy and molecular modeling studies (Figure 52).[138,139] It has been found that the strength and the selectivity of ion binding depend upon the length and the nature of the bridging spacer groups. The selectivity of **L110** toward ions follows $Rb^+ > Cs^+ > K^+ \gg Na^+$, while it is $Cs^+ \gg Rb^+$ in

dx.doi.org/10.1021/cr1004524 |*Chem. Rev.* 2011, 111, 4658–4702

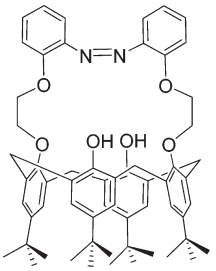

Figure 48. Schematic structure of **L100**.

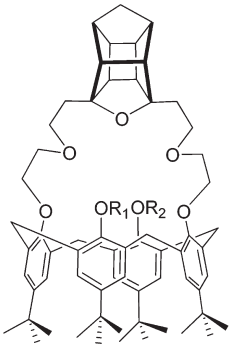

L101: $R_1 = R_2 = H$
L102: $R_1 = R_2 = CH_3$
L103: $R_1 = H$; $R_2 = CH_2CH_2OCH_3$
L104: $R_1 = R_2 = CH_2CH_2OCH_3$

Figure 49. Schematic structures of **L101**−**L104**.

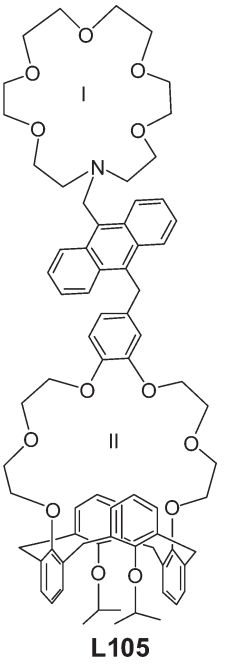

Figure 50. Schematic structure of **L105**.

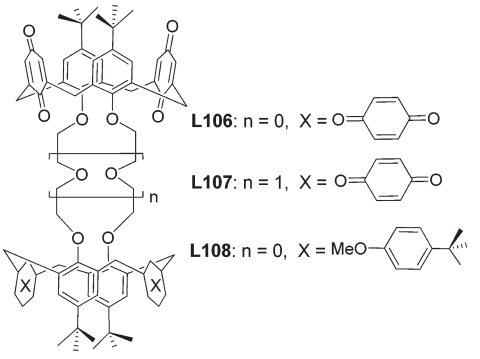

Figure 51. Schematic structures of **L106**−**L108**.

case of **L111** where no complexation was proposed with Na^+ and K^+ based on the association constants obtained from UV−vis titrations. The conjugate **L112** exhibits no selectivity toward any of the ions studied, while the selectivity of **L113** shows an order $Cs^+ > Rb^+ > K^+ \gg Na^+$, as a result of the enhanced rigidity of the linkages and the presence of two extra donor atoms. However, the binding of **L113** is weaker than that observed with either **L110** or **L111** due to the greater length of the bridging chains in **L113**. The crystal structure of the conjugate **L111** with Cs^+ exhibits eight coordination formed through four diquinone and four ether oxygens (Figure 52). Cs^+ also forms two strong bonds with quinone oxygens at the top rim of the two neighboring molecules and finally results in a 1-D polymeric chain. Molecular modeling has also been carried out to support the ion binding. From the X-ray structure and molecular modeling studies, it has been found that the cavity size of **L111** is complementary to the Cs^+ ion. The binding or the nonbinding nature of some of the ions with these conjugates has been further demonstrated by variable temperature ^1H NMR spectral titrations. These studies indicate that in case of **L110**, Na^+ cannot bind simultaneously to all eight donor atoms, while larger ions like Rb^+ can bind. The alkylene-linked host exhibits strong binding with ions if it can simultaneously coordinate to all eight oxygen donor atoms. All of the conjugates exhibit appreciable electrochemical recognition abilities with alkali ions such as Cs^+ and Rb^+.

A doubly bridged bis-calix[4]arene with pyridine, **L114**, exhibits higher extraction ability toward Rb^+ and Cs^+, in the order $Rb^+ > Cs^+ > K^+ > Na^+ > Li^+$, while its corresponding mono bridged derivative, **L115**, exhibits an extraction order $K^+ > Rb^+ \gg Na^+ > Cs^+ > Li^+$.[140] The molecular modeling studies suggest six coordination for the Rb^+ and only three coordination for K^+, respectively, with **L114** and **L115**, as can be seen from Figure 53.

Imine- and azo-functionalized calix[4]arenes (**L116**, **L117**, **L118**, Figure 54) exhibit selectivity through visual color change for Na^+, which binds stoichiometrically among a number of alkali ions studied.[141] All three conjugates showed larger association constants with Na^+, with the trend being **L117** > **L116** > **L118**, and the higher values observed are attributable to the presence of electron-withdrawing effect of the nitro group that enhances the ionization of the hydroxyl group to result in a stronger electrostatic interaction between the ion and the conjugate.

Two calix[4]arene-based bis-alkynyl bridged Au(I) isonitrile complexes having crown ether pendant have been studied for ion recognition properties.[142] Receptors **L119** and **L120** (Figure 55) recognize K^+ ($\log K = 5.8 \pm 0.1$) and Cs^+ ($\log K = 4.7 \pm 0.01$), respectively, in CH_2Cl_2:CH_3CN (1:1 v/v, 0.1 M nBu_4NPF_6) by sandwiching the ion using two benzo[15]crown-5 moieties resulting in Au···Au interaction from the arms of calix[4]arene. Geometry optimization also supports the sandwich formation with partial destruction of intramolecular hydrogen bonding present at the lower rim in calix[4]arene.

Calix[4]arene bearing pyridyl moiety, **L121** (Figure 56), shows good extraction ability with alkali ions but not with transition ions.[143] It also exhibits efficient dichromate extraction

dx.doi.org/10.1021/cr1004524 |*Chem. Rev.* 2011, 111, 4658–4702

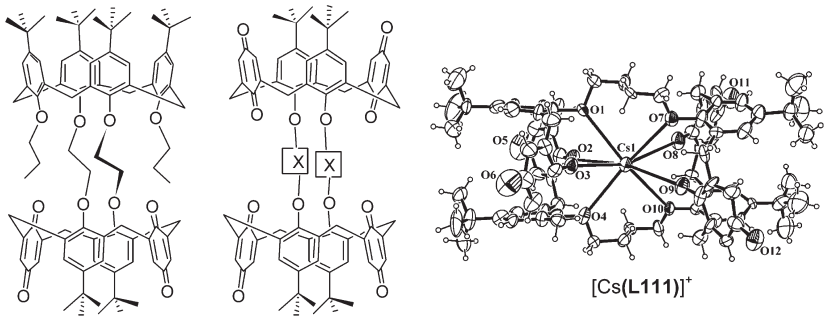

Figure 52. Schematic structures of **L109**−**113** and single crystal X-ray structure of [Cs(**L111**)]$^+$.[139]

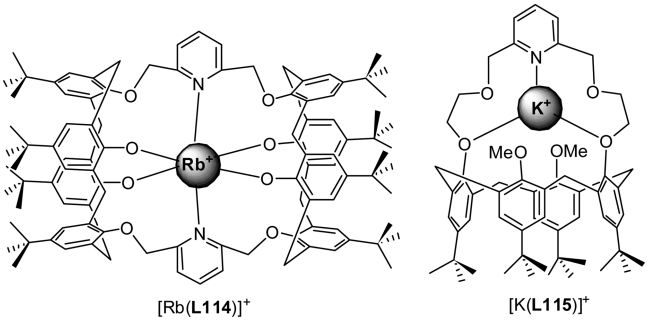

Figure 53. Line diagrams of the geometry-optimized structures of [Rb(**L114**)]$^+$ and [K(**L115**)]$^+$.

from aqueous into the dichloromethane layer at higher pH via the formation of a 1:1 complex.

The Cs^+ extraction ability of **L122** (Figure 57), a calix[4]arene bearing triazole and ester moieties, has been studied.[144] The extraction ratio was found to be $Cs^+/Na^+ = 10.5$. ^{1}H NMR spectroscopic studies suggest a higher extraction of this conjugate with alkali metal ions because of the presence of flexible triazole group, which facilitates the complexation between the ester group and the alkali ions by enhancing the flexibility of the cavity formed by the ester groups.

Alkali metal ions generally prefer oxygen-rich functional groups such as crown ether for their recognition as well as for extraction processes. Calix[4]diquinones can provide higher coordination number (even up to 10) toward Cs^+ and Rb^+ using quinone as well as ether oxygens. It is understood from the examples given in this Review that by incorporating suitable ligating groups containing hard soft donor sites along with suitable cavity size, the selectivity of a calix[4]arene derivative toward a particular alkali metal ion can be tuned. The electrostatic interactions present between the ion and the conjugate increase by introducing electron -withdrawing groups at appropriate positions in the receptor system.

3.9. Recognition of Alkaline Earth Metal Ions

A hydroxyamide conjugate of calix[4]arene, **L123** (Figure 58), forms a 1:1 complex with alkaline-earth ions, and Pb^{2+} and Zn^{2+} in acetonitrile as studied by ^{1}H NMR spectroscopy and conductometric titrations.[145] The interaction of **L123** with cations is mainly through the carbonyl, ethereal, and the hydroxyl oxygens of the pendant arms of the calix[4]arene. The strength of the complexation

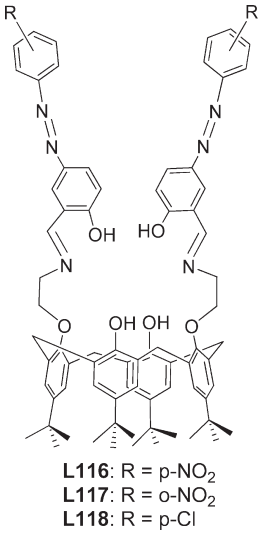

Figure 54. Schematic structures of **L116**−**L118**.

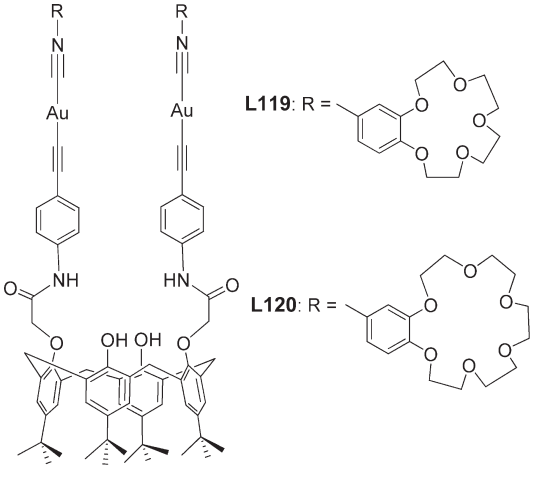

Figure 55. Schematic structures of **L119** and **L120**.

of **L123** in acetonitrile follows an order $Mg^{2+} > Ca^{2+} > Sr^{2+} > Ba^{2+}$, suggesting that the size affects the complexation.

The degree of interaction of diethylphosphate amine conjugate of calix[4]arene, **L124** (Figure 59), toward monovalent

dx.doi.org/10.1021/cr1004524 |*Chem. Rev.* 2011, 111, 4658–4702

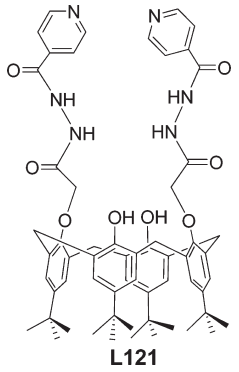

Figure 56. Schematic structure of **L121**.

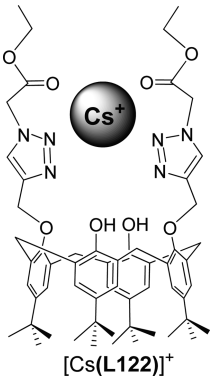

Figure 57. Schematic structure of [Cs(**L122**)]$^{+}$.

and divalent ions has been studied in acetonitrile, methanol, *N*,*N*-dimethylformamide, and propylene carbonate using ^{1}H NMR spectroscopy, conductance, and calorimetric measurements.[146] The monovalent ions did not exhibit complexation in any of these solvent systems, while divalent ions show interactions only in acetonitrile. The interaction of **L124** with alkaline-earth ions and Pb^{2+} results in the formation of 1:2 (cation:**L124**) complex, while it is a 1:1 complex with Cu^{2+}, Zn^{2+}, Cd^{2+}, and Hg^{2+}. Because alkaline-earth ions and Pb^{2+} prefer to form eight coordination, it requires two calix[4]arene moieties to come close to each other to satisfy the same coordination number and hence results in the formation of a 1:2 complex. The Ca^{2+} showed the highest stability constant with **L124** as compared to other ions studied due to the higher entropic contribution to the selectivity. All of the other ions were satisfied with either low coordination or soft donor centers.

Calix[4]arene functionalized with tetrazole at the lower rim and *p*-methoxyphenylazo substituent at the upper rim, **L125** (Figure 60), has been studied for its ion recognition by absorption spectroscopy.[147] **L125** showed high selectivity toward Ca^{2+} among 14 ions studied, while minimal responses were obtained with Cr^{3+} and Pb^{2+}. It forms 1:1 stoichiometric complex in CH_3CN by exhibiting color change upon the addition of Ca^{2+}. However, this derivative exhibited only Ca^{2+} selectivity when the titrations were carried out in CH_3CN/CH_3OH (9:1). The association constants observed for Ca^{2+} and Pb^{2+} were 9.1×10^4 and 8.4×10^3 M^{-1}, respectively, in CH_3CN. On the other hand, the corresponding *p*-nitrophenylazo conjugate, **L126** (Figure 60), does not exhibit any selectivity even though its association constants were found to be higher as compared to the

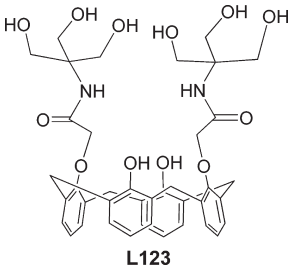

Figure 58. Schematic structure of **L123**.

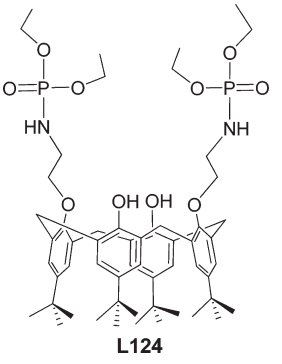

Figure 59. Schematic structure of **L124**.

methoxy derivative, **L125**. It is evident from the ^{1}H NMR spectra that Ca^{2+} interacts with both **L125** and **L126** through its two partially deprotonated hydroxyl azophenol groups and one of the two tetrazole groups. The presence of triazole moiety at the lower rim and the azo group at the upper rim in **L127** (Figure 60) leads to colorimetric sensing of Ca^{2+} and Pb^{2+} by forming a 1:1 complex, while exhibiting a 160−175 nm red shift in the absorption band.[148] The K_a values of 7.06×10^4 and 8.57×10^3 M^{-1} were found for Ca^{2+} and Pb^{2+}, respectively, in $CH_3CN/CHCl_3$ (1000:4 v/v). The ^{1}H NMR spectral titration results suggest the involvement of triazole and azophenol moieties by breaking the symmetry of **L127** upon interaction with Ca^{2+}, whereas it is symmetrical with Pb^{2+}. **L128** (Figure 60) exhibits selectivity toward cations, Ca^{2+}, Pb^{2+}, and Ba^{2+}, with association constants of 1.01×10^5, 6.35×10^4, and 2.53×10^4 M^{-1}, respectively, in $CH_3CN/CHCl_3$ (v/v 1000:4).[149] Color changes have also been observed where the original greenish color changes to bright yellow. ^{1}H NMR spectra show that Ca^{2+} is bound to two nitrogen atoms of the triazole units and two hydroxy-*p*-azophenol groups of **L128**, and the complexation results in the breakage of symmetry of the receptor molecule similar to that observed in case of **L127**.

The redox active monolayer of a calix[4]arene-disulfide-diquinone, **L129** (Figure 61), selectively recognizes Ba^{2+} in aqueous medium among a number of alkali and alkaline earth ions studied by voltammetry.[150] The detection limit and the association constant of the receptor-modified gold disk electrode were found to be 1.0×10^{-6} M and 9.8×10^4 M^{-1}, respectively, in 0.1 M HEPES buffer solution.

Alkaline earth metal ions utilizes the carbonyl, ethereal, and hydroxyl oxygens of the pendant arms for its binding, as is evident from the examples mentioned in this section. The triazole and tetrazole nitrogens in conjunction with the phenolic-OH's can provide efficient binding core toward Ca^{2+} as can be

dx.doi.org/10.1021/cr1004524 |*Chem. Rev.* 2011, 111, 4658–4702

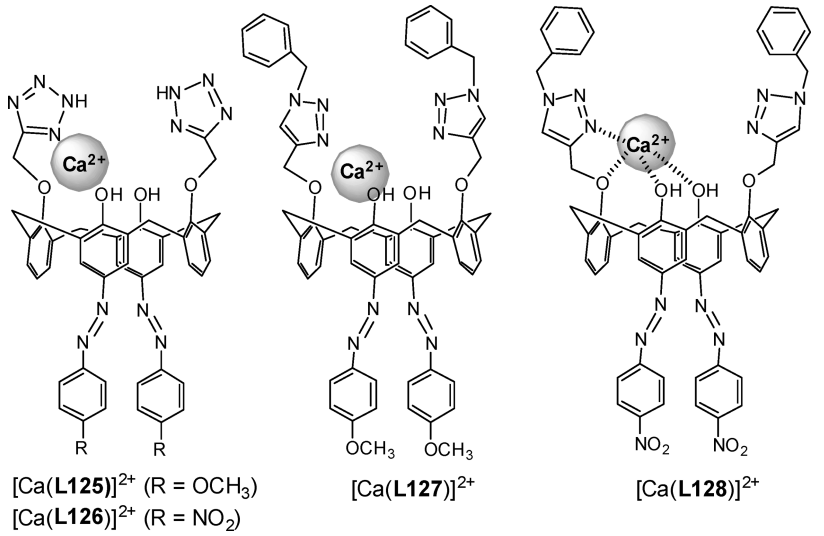

Figure 60. Proposed binding models for the Ca^{2+} complexes of **L125**, **L126**, **L127**, and **L128**.

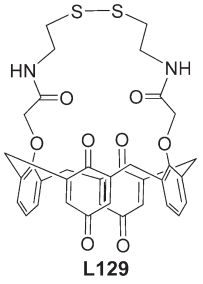

Figure 61. Schematic structure of **L129**.

seen from Figure 60. The symmetry of the calix[4]arene conformation changes upon ion coordination because the phenolic-OH participates in the binding. Colorimetric recognition of ions is also possible by introducing fluorophores appropriately.

3.10. Lanthanide Ion Recognition

The literature for the selective recognition of lanthanide ions includes the presence of two spirobenzopyran moieties in the lower rim of calix[4]arene by an ester linkage (**L130**, Figure 62).[151] **L130** shows high selectivity toward lanthanide ions, La^{3+}, Pr^{3+}, Eu^{3+}, Gd^{3+}, Dy^{3+}, Er^{3+}, and Yb^{3+}, even in the presence of other metal ions, Na^{+}, K^{+}, Ca^{2+}, Fe^{3+}, Cu^{2+}, and Zn^{2+}, in acetonitrile. Either in the UV or in the dark, the spirobenzopyran is in zwitterionic merocyanine form and binds to Eu^{3+} by electrostatic interaction, resulting in high fluorescence. However, this is exactly reverse under the visible light (Figure 62) where it exists in spirobenzopyran form and interacts with Eu^{3+} via coordinative bonds. The ligand to metal charge transfer (LMCT) between **L130** and Eu^{3+} in the spirobenzopyran form is weak as compared to the merocyanine form. Logic gate properties of this system have also been explored.

Another example for the lanthanide sensor is a *p-tert*-butylcalix[4]arene appended *o*-vanillin **L131** (Figure 63), which shows high selectivity to Eu^{3+} among the other lighter lanthanides, La^{3+}, Ce^{3+}, Pr^{3+}, Nd^{3+}, Sm^{3+}, and Gd^{3+}, studied by calorimetry in acetonitrile.[152] The effect of the substituent group, the size of the cavity, the type of the guest molecule, the spatial arrangement, and the orientation of the calix[4]arene donor atoms on lanthanide binding has been addressed by comparing calorimetric results of the Schiff's base derivative with its precursor molecules, bis(cyanomethyl)calix[4]arene and bis(2-aminoethoxy)calix[4]arene. **L131** shows high K_s for all of the lanthanide ions where Eu^{3+} is maximum, indicating the flexibility of the substituents and the proper size match between the arrangement of lower rim, and the donors of the side arm to Eu^{3+}.

The luminescence and energy transfer properties of **L11** in the presence of Eu^{3+} and Tb^{3+} have been explored.[153] The binding of Eu^{3+} by **L11** was determined on the basis of IR and phosphorescence spectra. The MM^{+} calculations supported 8-coordination about Eu^{3+} (Figure 63).

Photophysical properties of two calix[4]arene conjugates (**L132** and **L133**, Figure 64) with Tb^{3+} have been studied by UV−vis and fluorescence spectroscopy in acetonitrile.[154] As a result of intramolecular $\pi\cdots\pi$ stacking, **L132** forms a preorganized core by the use of eight oxygens as evident from the crystal structure and is responsible for better binding of Tb^{3+} as compared to **L133** where only intermolecular $\pi\cdots\pi$ stacking is present. UV−vis and fluorescence spectra of **L132** exhibited significant spectral changes upon interaction with Tb^{3+}, while no significant changes were observed when the titrations were carried out with **L133**.

Calix[4]arene conjugates appended with bisphosphonic acid (**L134**−**L136**) moiety have been studied for their lanthanide extraction properties (Figure 65).[155] The extraction efficiencies of the receptor molecules decrease with increasing length of the CH_2 spacer and also decrease as the acidity rises. The extraction ability also increases significantly with decreasing the ionic radius of Ln^{3+}. The conjugate **L135** exhibits good extraction ability with all of the lanthanides as compared to the other receptor molecules.

Sequestering abilities of a few calix[4]arene derivatives (**L137**−**L139**, Figure 66) have been demonstrated toward UO_2^{2+} by UV−vis spectroscopy in aqueous medium under different pH conditions. **L139** showed higher complexation ability with UO_2^{2+} at a pH of 9.0.[156] ^{1}H NMR spectral titrations have also been carried out with **L139** to establish the complexation properties.

A series of acid-amide conjugates of calix[4]arene have been synthesized, and their lanthanide extraction abilities have been

dx.doi.org/10.1021/cr1004524 |*Chem. Rev.* 2011, 111, 4658–4702

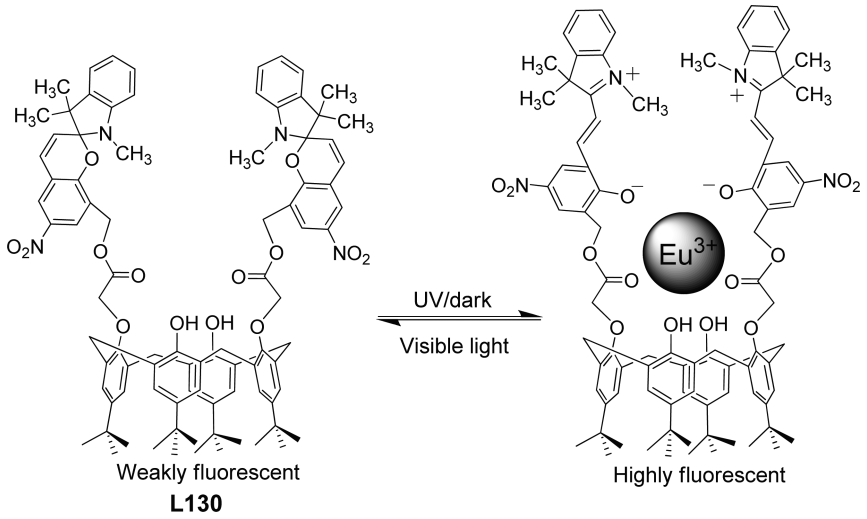

Figure 62. Eu^{3+} binding with **L130** under UV light and release of **L130** from the complex under visible light.

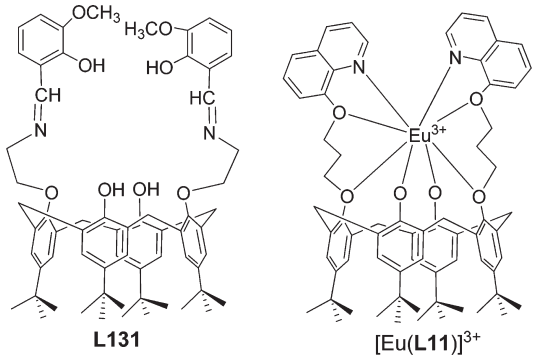

Figure 63. Schematic structure of **L131**, and the proposed binding model of Eu^{3+} with **L11** obtained on the basis of molecular mechanics calculations.

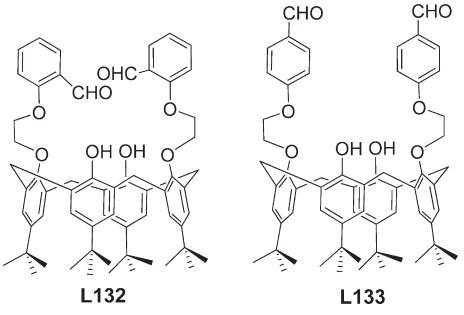

Figure 64. Schematic structures of **L132** and **L133**.

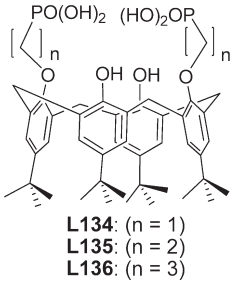

Figure 65. Schematic structures of **L134**−**L136**.

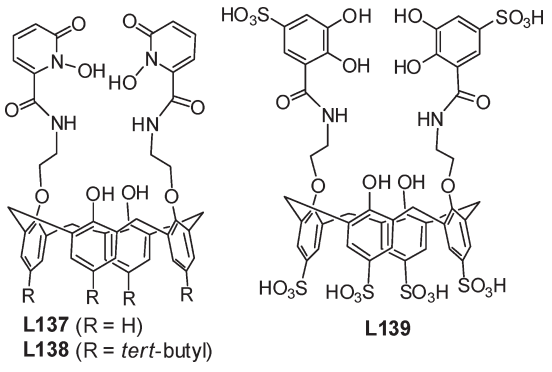

Figure 66. Schematic structures of **L137**−**L139**.

studied (Figure 67).[157] The conjugates **L143** and **L144** exhibit higher extraction efficiency over the other conjugates, with 90% of uranyl extraction being observed with **L143** at 1:1 metal:calix ratio at pH = 7.0. At the same ratio, the conjugate **L141** exhibited 60% extraction, while **L140** and **L142** need a 1:25 ratio for good extraction. The uranyl extraction ability has been increased at lower pH in **L143** and **L144** due to the presence of an electron-withdrawing group and the removal of *tert*-butyl groups, respectively. The crystal structure of **L142** with La^{3+} and Na^{+} has been demonstrated where both of the complexes were dinuclear in which La^{3+} forms eight coordination while sodium forms only six coordination (Figure 68). It has been found that while the larger lanthanide ions form a 2:2 complex, the smaller ones form a 1:1 complex, and the ions of intermediate size exist in solution as a dynamic mixture of 2:2 and a 1:1 complexes with these conjugates.

A series of ferrocene conjugates possessing ester-amide (**L145**−**L147**) and acid-amide (**L148**−**L150**) moieties form 1:1 complexes with lanthanides (Figure 69).[158] The ester-amide conjugates (**L145**−**L147**) exhibit large potential shift as compared to the acid-amides (**L148**−**L150**), and those with spacer (**L147**) show the largest anodic shift in the lanthanide electrochemical recognition studies. Among the acid-amide conjugates, **L148** shows maximum changes with Lu^{3+}. It has been found that the length of the alkyl spacer has some effect on the electrochemical

dx.doi.org/10.1021/cr1004524 |*Chem. Rev.* 2011, 111, 4658–4702

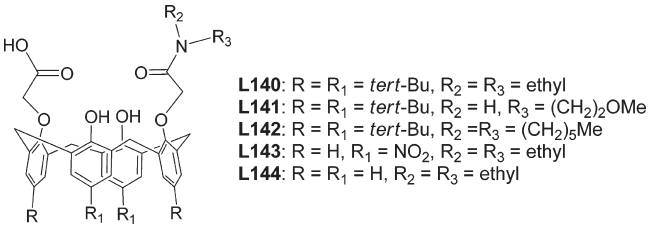

Figure 67. Schematic structures of **L140**−**L144**.

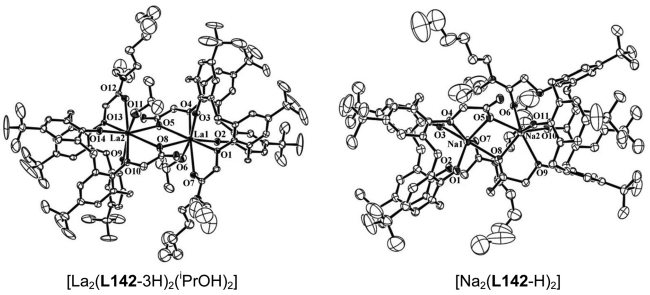

Figure 68. Crystal structures of $[La_2(\mathbf{L142}\text{-}3H)_2(^{i}PrOH)_2]$ and $[Na_2(\mathbf{L142}\text{-}H)_2]$. Reprinted with permission from ref 157. Copyright 2002 The Royal Society of Chemistry.

responses of bis-calix[4]arene conjugates (**L151**−**L153**) toward lanthanides where the largest shift was observed with the molecules having the longer chain length (Figure 69).

An electrochemical sensor for uranium has been synthesized by self-assembled ensembles of a disulfide conjugate of calix[4]arene 1,3-diacid, **L154**, on a polycrystalline gold (Figure 70).[159] The electrochemical response that is related to the microscopic changes at the electrode surface is proportional to the concentration of uranium present in the solution.

A series of ruthenium(II) bipyridyl complexes containing one, two, or six lower rim acid-amide-modified calix[4]arene moieties have been prepared, and their photophysical characteristics have been studied using different spectral techniques (Figure 71).[160] Absorption spectral titrations with Eu^{3+}, Tb^{3+}, and Nd^{3+} (Ln^{3+}) in CH_3CN indicate that **L155** initially forms a 2:1 (**L155**:Ln^{3+}) and finally converts to a 1:1 complex at higher (<0.5) ratios of lanthanide ions. The conjugate, **L156**, forms an initial 1:1 complex followed by the formation of a 1:2 (**L156**:Ln^{3+}) complex, while **L157** accommodates at least five Ln^{3+} upon binding. The emission spectrum of ruthenium moiety has been perturbed upon the interaction of lanthanide ions depending upon the nature of the host metal complex and the lanthanide ion. The emission intensity of the receptor has been quenched upon interaction with Nd^{3+}, while the ruthenium bipyridyl moiety showed an enhancement in the emission with Tb^{3+} and finally with Eu^{3+}. While **L155** and **L157** exhibited quenching, receptor **L156** showed enhancement in the fluorescence intensity.

The complexation of Eu^{3+} by calix[4]arene capped with DTPA bridges (**L158**−**L160**) has been studied by mass spectroscopy (Figure 72).[161] The molecular modeling of the Eu^{3+} complex of **L160** shows nine coordination about the metal ion where the ligations are derived from the carboxylates and the aliphatic amines.

The luminescence properties of Eu^{3+} and Tb^{3+} complexes of a series of calix[4]arene appended with one or two bipyridines (**L161**−**L165**) have been studied (Figure 73).[162] All of the derivatives exhibited bathochromic shift in the absorption upon complexation with Eu^{3+} and Tb^{3+}. The association constant obtained for **L161** and **L162** with Eu^{3+} complexes showed 2 orders of magnitude higher than the simple 18-crown-6. The photophysical properties of the free conjugates and their Eu^{3+} and Tb^{3+} complexes exhibit high molar absorption coefficients proportional to the number of bipyridine units.

Lanthanides generally look for oxophilic centers for its coordination. Free carboxylic acid groups and other oxygen- and/or nitrogen-rich centers provide good binding cores for the lanthanide ion detection and/or extraction. The pH and the electron-withdrawing and -donating character of the functionalized groups have an important role to play in lanthanide sensing. The detection of lanthanides can be monitored using electrochemistry by incorporating the redox active groups into the calix[4]arene unit.

4. ANION RECEPTORS

The calix[4]arene-based anion receptors are synthesized by introducing functionalities such as amide, urea, or thiourea, which can interact with anions through hydrogen bonding. Incorporation of fluorophores into such binding cores would be of great use in monitoring the binding aspects. This Review focuses on the recognition of inorganic and organic anions by lower rim 1,3-diconjugates of calix[4]arene.

4.1. Inorganic Anions

4.1.1. Fluoride Recognition. A selective colorimetric and fluorescent sensor for F^- over Cl^-, Br^-, I^-, CH_3COO^-, HSO_4^-, $H_2PO_4^-$, and OH^- has been synthesized by attaching 1-amidoanthraquinone unit on both the arms at the lower rim of calix[4]arene, **L166** (Figure 74).[163] This derivative senses F^- by inhibiting excited-state intramolecular proton transfer (ESIPT) in CH_3CN with an association constant of 279 M^{-1} by forming a 1:1 complex. During binding, **L166** forms intramolecular H-bonds, N−H···F (or deprotonation), resulting in the delocalization of π-electrons in the fluorophore. ^1H NMR spectral titrations suggest proton transfer between the conjugate and F^- through amide NH groups. Coumarin appended calix[4]arene through amide linkage, **L167** senses F^- through NH···F interactions via fluorescence quenching (Figure 74).[164] The interaction has been further supported by ^1H NMR spectral titrations. In the absorption spectra, the original band of the coumarin showed a red shift and exhibits a new band at 408 nm. Fluorescence titrations were carried out by exciting at two wavelengths, 335 and 408 nm. In case of the former, it results in the quenching of 420 nm band and exhibits a new band at 508 nm due to the PET from F^- to coumarin, while in the latter it results in the fluorescence enhancement when compared to all other anions. Association constant sobtained for F^- and $CH_3CO_2^-$ were 1.08×10^4 and 3.77×10^2 M^{-1}, respectively, in CH_3CN. Visual color change has also been observed when F^- interacts with **L167**. The studies were suggestive of H-bonding followed by the deprotonation of amide NH. When the two free OH groups of **L167** were alkylated with propyl moiety, the resultant derivative exists in 1,3-alternate conformation and loses selectivity by exhibiting equal response toward $CH_3CO_2^-$ and $H_2PO_4^-$.

An amide-based calix[4]arene derivative bearing pyrene and nitrophenylazo moieties exhibited F^- recognition as studied by UV−vis and fluorescence spectroscopy.[165] The interaction of

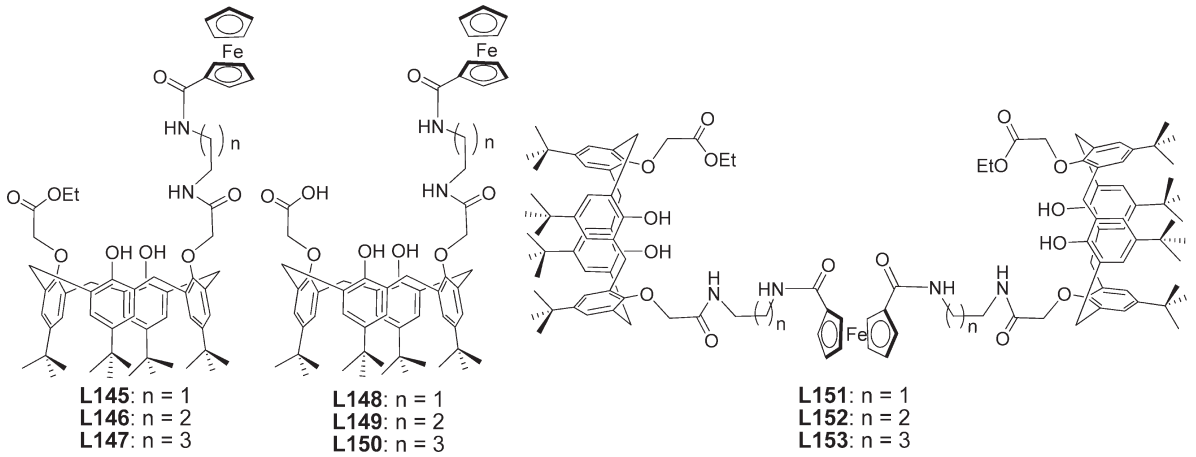

Figure 69. Schematic structures of **L145**−**L153**.

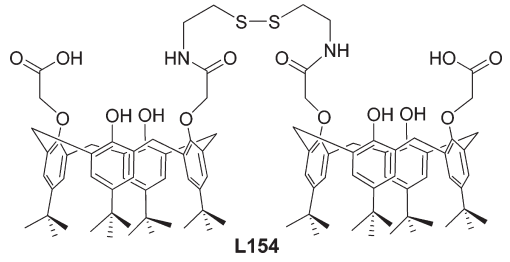

Figure 70. Schematic structure of **L154**.

F^- with **L168** and **L169** has been found to be through the amide and the phenolic protons, respectively, due to the orientation of the pyrenyl moieties present in these as modeled by computational calculations (Figure 75). Both of the conjugates exhibit strong color change with F^- as compared to the CH_3COO^-. Because of the direct linking of pyrenyl moiety to the amide group, **L168** exhibits an excimer band, while **L169** does not. Initial addition of F^- to **L168** results in the fluorescence quenching of the excimer that originated from the pyrene, and in the presence of an excess amount of F^- (<300 equiv), it results in the formation of a new excimer band and exhibits a decrease in the monomer emission.

L128 shows dual sensing by giving visual color change toward both Ca^{2+} and F^-, and it changes from light green to blue upon interaction with F^- (Figure 76).[149] Association constants observed with F^-, AcO^-, and $H_2PO_4^-$ were found to be 4.38×10^4, 2.5×10^4, and 5.5×10^3 M^{-1}, respectively, in CH_3CN:$CHCl_3$ (v/v 1000:4). One new absorption band was observed during the interaction of **L128** with F^-, AcO^-, and $H_2PO_4^-$ at 626, 618, and 622 nm, respectively, with the absorption intensity being varied in the order $F^- > AcO^- > H_2PO_4^-$. The amount of bathochromic shift observed upon interaction of **L128** with these anions is dependent on the extent of deprotonation followed by the complexation of the azophenol unit. **L128** shows INHIBIT logic gate with YES logic function by using Ca^{2+} and F^- as inputs. ^{1}H NMR spectroscopy supports F···H−O interactions.

A calix[4]arene-based conjugate containing hydrazone functionalities, **L170**, exhibits anion binding toward F^- among Cl^-, Br^- I^-, $H_2PO_4^-$, HSO_4^-, AcO^-, ClO_4^-, and PF_6^-.[166] The **L170** initially forms a 1:1 and a 2:1 (F^-:**L170**) complex at 1 and 2 equiv of F^-, respectively, through hydrogen bonding and finally undergoes deprotonation at the NH moiety and results in the formation of $[HF_2]^-$, which is supported by absorption and ^{1}H NMR spectroscopy studies (Figure 76). The **L170** exhibits colorimetric detection of F^- in DMSO−CH_3CN (0.5:9.5 v/v).

4.1.2. Chloride Recognition. A series of urea and thiourea derivatives of calix[4]arene have been studied for their anion recognition by ^{1}H NMR spectroscopy.[167] Among the four derivatives (**L171**−**L174**), the **L172** exhibits large chemical shifts in its −NH protons, suggesting the interaction of anion through these groups (Figure 77). The stability of the receptor with anions follow an order $Cl^- > Br^- > H_2PO_4^- > CH_3CO_2^-$. The other derivatives (**L171**, **L173**, and **L174**) possessing free OH group did not show any significant anion binding because of the presence of intramolecular hydrogen bonding between the urea/thiourea and phenolic-OH groups. Similarly, the low association observed with thiourea derivatives as compared to that of the urea is attributable to the high intra- and intermolecular hydrogen-bonding ability of the former.

Two azo functionalized derivatives bearing thiourea moiety have been studied for their ionophoric properties by chloride-selective electrode (Figure 77).[168] Among the two derivatives (**L175** and **L176**), the ion selective electrode based on **L175** exhibits good selectivity toward Cl^- as compared to the classical Hofmeister series with a detection limit of $\log[Cl^-] = -4.02$ and in a concentration range from 1.5×10^{-4} to 1.0×10^{-1} M.

Calix[4]arene-based rotaxanes have been synthesized for anion recognition studies. The rotaxane [**L178**·Cl] contains a conformationally flexible pyridinium axle, while [**L177**·Cl] is composed of a preorganized one (Figure 78).[169] The crystal structure of [**L177**·Cl] shows that chloride anion is tetrahedrally coordinated with respect to the amide protons, but central aryl protons also form close contact. The PF_6^- bound conjugate, [**L177**·PF_6], shows selectivity for chloride over other anions in the order $Cl^- > Br^- > H_2PO_4^- > OAc^-$ in $CDCl_3/CD_3OD$ (1:1), while this loses its selectivity in $CDCl_3/CD_3OD/D_2O$ (45:45:10) and cannot differentiate the Cl^- from that of the Br^-. The complex [**L178**·PF_6] exhibits weak anion binding in $CDCl_3/CD_3OD$ (1:1) and cannot differentiate the Cl^- from that of the Br^-.

The cooperative ion-pair binding of a series of calix[4]-diquinones with group I metal ions and chlorides was demonstrated in CH_3CN by using ^{1}H NMR and UV−vis spectroscopy and computational modeling studies (Figure 79).[170,171] The calix[4]diquinone receptors, **L179** and **L180**, exhibit Cl^-

dx.doi.org/10.1021/cr1004524 |*Chem. Rev.* 2011, 111, 4658–4702

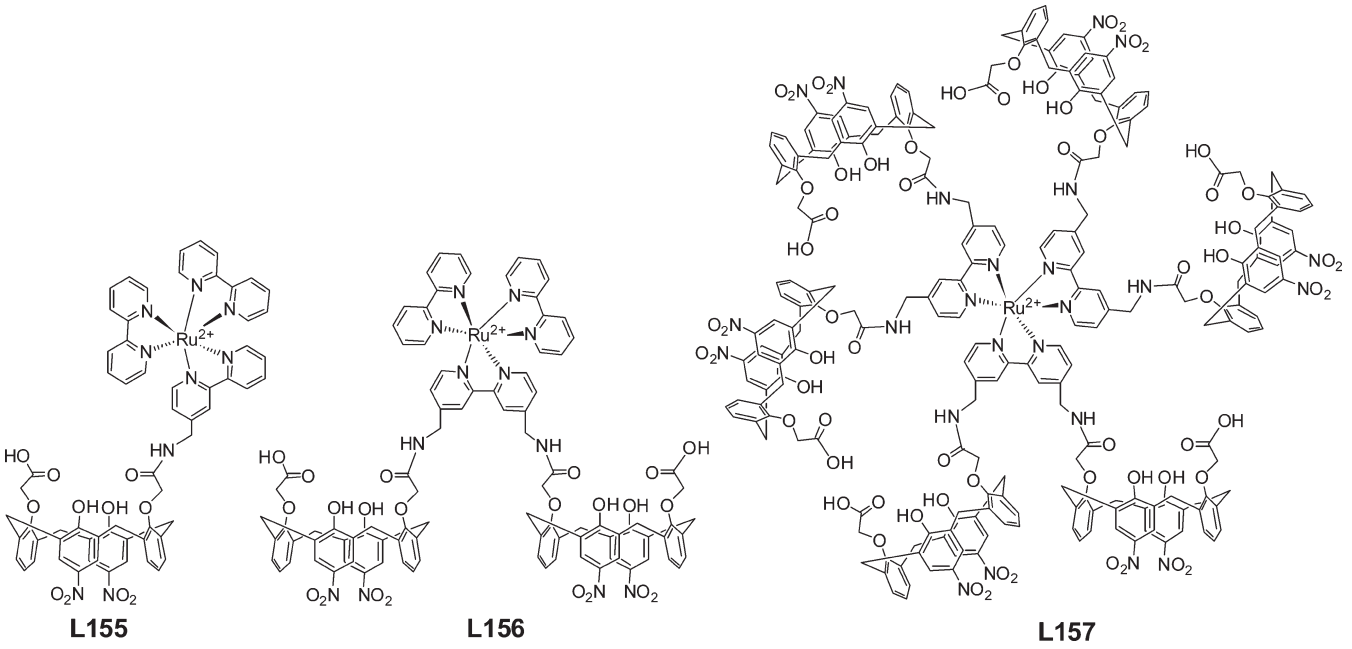

Figure 71. Schematic structures of **L155**−**L157**. The counter anion in all the three molecules are $2(PF_6^-)\cdot 2H_2O$.

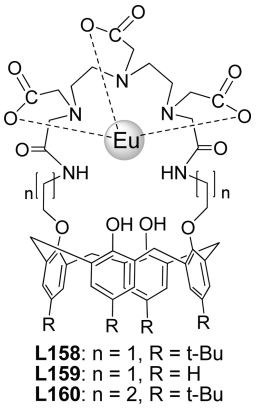

Figure 72. Proposed binding model of Eu^{3+} with **L158**−**L160**.

recognition in the presence of alkali cations. Both **L179** and **L180** show AND logic gate properties with coordinating ions as inputs. Cation-induced anion binding results in the conformational changes in **L179** and **L180**. The cation binding of **L180** is higher as compared to **L179** due to the presence of NO_2 group, which increases the acidity of the amide group and enhances the Cl^- recognition in the former. A cooperative binding has also been observed in a competitive solvent mixture, CD_3CN/D_2O (98:2), and the coordinating ability of halide in the presence of cations follows a trend $Cl^- > Br^- > I^-$ in both of the cases. The strength of the anion binding in case of **L179** also depends on the nature of the cation present, and this follows $TBA^+ \ll Li^+ < Rb^+ < Cs^+ < K^+ < Na^+ < NH_4^+$ for Cl^- {TBA is tetrabutylammonium}. The anion binding strengths of **L181**, **L182**, and **L183** are in the order of $Cl^- > Br^- > I^-$ toward halides, and the anion binding constants of the receptor follow the order **L181** < **L183** < **L182**. In case of K^+, Rb^+, and Cs^+ containing ion pairs, **L181** binds more strongly to Br^- and I^- as compared to **L182** and **L183**. Similar to the anion binding, the cation binding has also been observed with all of the cations including NH_4^+ and Na^+ only in the presence of Cl^- in case of **L179** and **L180**, but the K^+ binding was observed with the free receptor.

4.1.3. Iodide Recognition. A conjugate in which anthracene connected to both of the arms through triazole moiety, **L184**, exhibits anion recognition in methanol as studied by fluorescence spectroscopy (Figure 80).[172] The fluorescence intensity of this derivative in various solvents follows the order $CH_3OH < CH_3CN < THF \cong CHCl_3$. While TBABr, TBAI, LiBr, and LiI exhibit fluorescence enhancement, the TBAHS (tetrabutylammonium hydrogen sulfate) exhibits fluorescence quenching. Maximum fluorescence intensity was observed upon the addition of iodide salts.

A diamine derivative of calix[4]arene, **L49**, has been found to be selective toward iodide among the halide ions irrespective of the countercation as studied by fluorescence emission spectroscopy.[173] On the basis of various studies, it has been suggested that iodide occupies the arene cavity (Figure 81). This receptor detects I^- even in the presence of all of the competing ions.

4.1.4. Chromate Recognition. A series of amide derivatives have been synthesized, and their extraction properties toward $Cr_2O_7^{2-}/HCr_2O_7^-$ into aqueous and dichloromethane phases have been studied (Figure 82).[174] Because of the presence of protonable amine moieties, **L187** and **L188** were found to be good extractants as compared to **L185** and **L186** at low pH.

A series of amide-based calix[4]arene conjugates have been studied for liquid−liquid extraction of dichromate anion ($Cr_2O_7^{2-}/HCr_2O_7^-$) at different pH's (Figure 83).[175] Among the three derivatives, **L189** showed the highest extraction at lower pH due to the presence of more hydrogen-bonding sites, amide nitrogen, carbonyl, and oxa-oxygens. Further, the structure of **L189** is nonflexible due to the presence of bridging 1,8-dioxa octyl unit, wherein the protonation of amide oxygens is also possible. The **L191** binds to chromate ions at low pH due to the presence of protonable amine moieties, but its extraction ability is

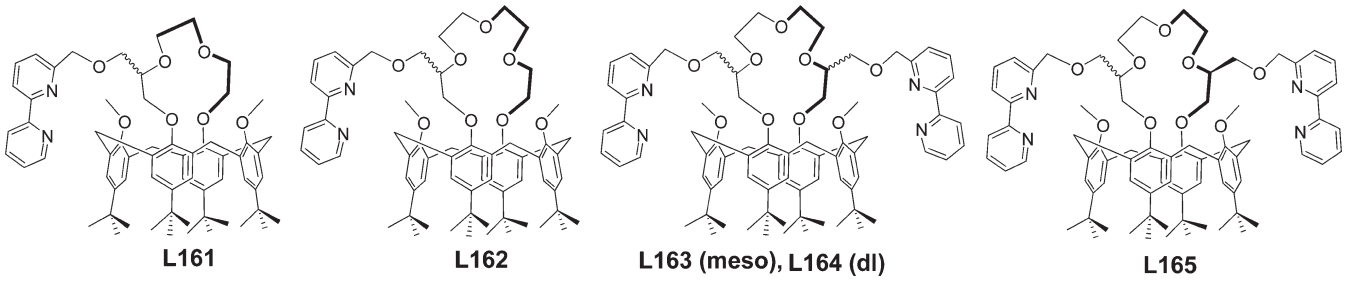

Figure 73. Schematic structures of **L161**−**L165**.

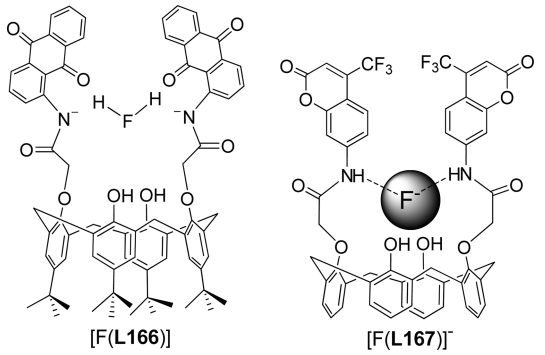

Figure 74. Proposed F^- binding with **L166** and **L167**.

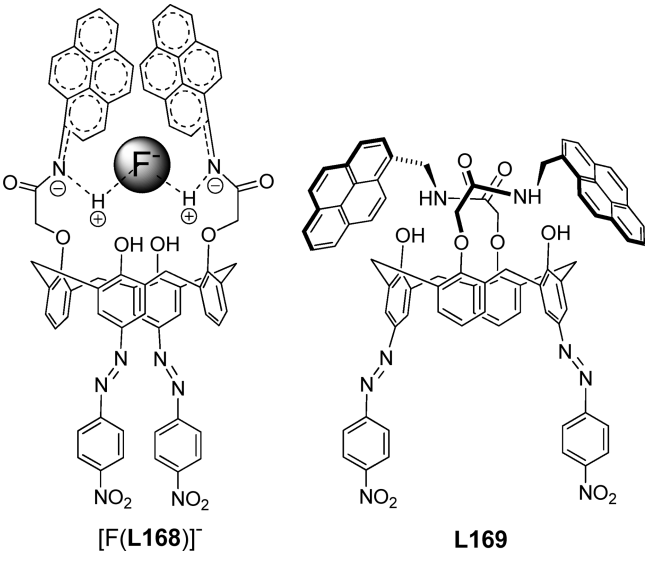

Figure 75. Proposed binding model of F^- with **L168**, and schematic structure of **L169**.

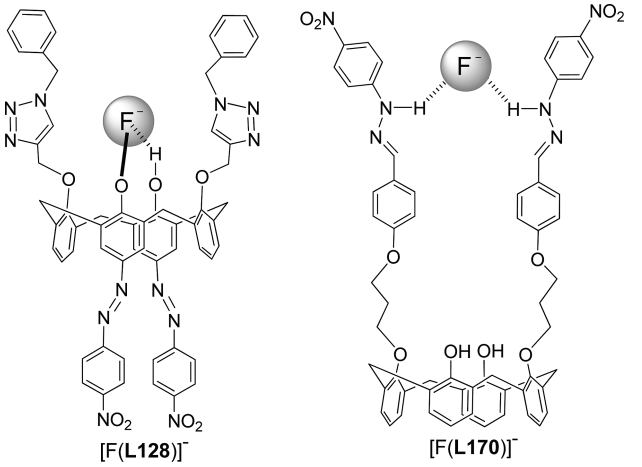

Figure 76. Proposed binding of F^- with **L128** and **L170**.

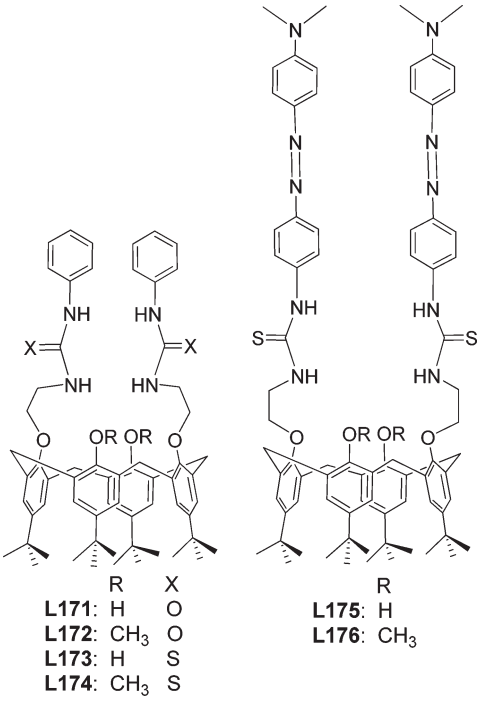

Figure 77. Schematic structures of the receptor molecules, **L171**−**L176**.

low due to the flexible arms present as compared to **L189** where the arms were cyclized. However, no extraction was observed with **L190** due to the steric hindrance of the bulky groups present in this system.

4.1.5. HSO_4^- and HSO_3^- Recognition. Calix[4]diquinone possessing phenylurea (**L192**) has been studied for its anion binding characteristics by ^1H NMR spectroscopy and electrochemistry (Figure 84).[176,177] From the spectroscopy studies, it has been found that the binding strength and the selectivity of binding follow an order $HSO_4^- > H_2PO_4^- > CH_3CO_2^- > Cl^- > Br^- > I^-$, ClO_4^-, where HSO_4^- forms a 1:1 complex with this derivative. During the titration, HSO_4^- coordinates to NH

dx.doi.org/10.1021/cr1004524 |*Chem. Rev.* 2011, 111, 4658–4702

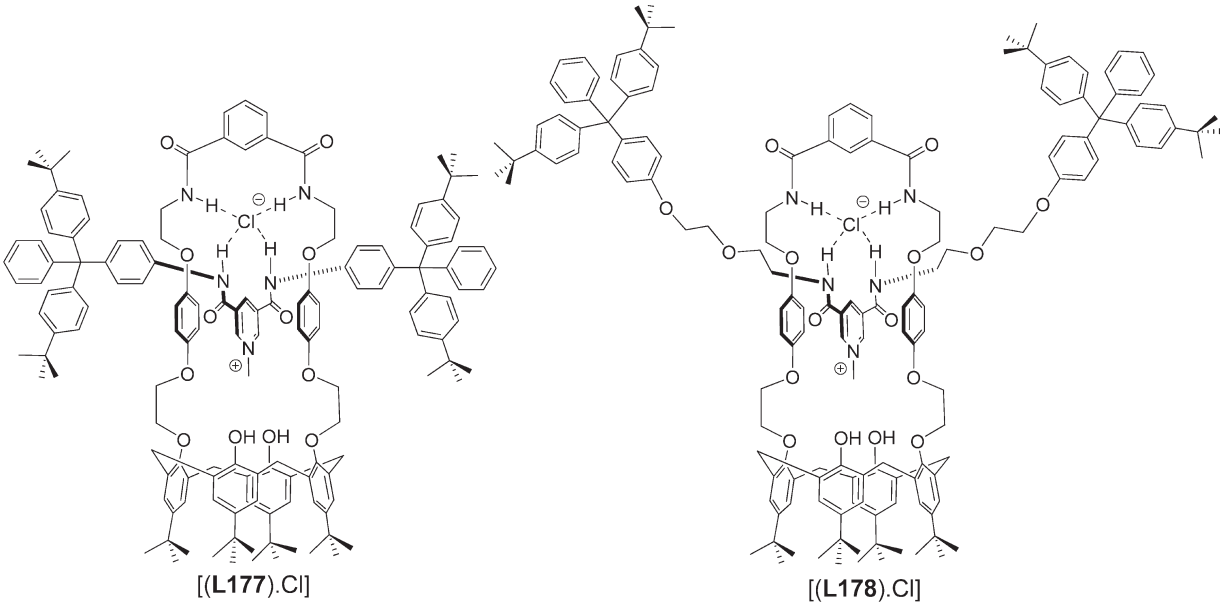

Figure 78. Proposed models for the binding of Cl^- with **L177** and **L178**.

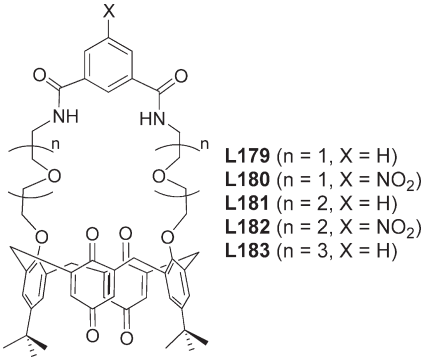

Figure 79. Schematic structures of **L179**−**L183**.

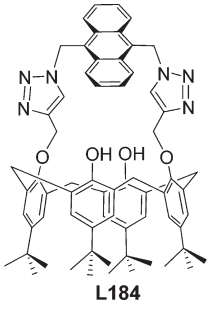

Figure 80. Schematic structure of **L184**.

protons of calix[4]diquinone as well as quinone moiety through hydrogen bonding. The HSO_4^- sensing by two calix[4]arene derivatives (**L193** and **L194**, Figure 84) possessing urea moiety over $H_2PO_4^-$, Cl^-, Br^-, I^-, ClO_4^-, and $CH_3CO_2^-$ has been studied by ^1H NMR spectroscopy and electrochemistry. The K_a values of **L193** and **L194** toward different anions follow $HSO_4^- \gg H_2PO_4^- > CH_3CO_2^- > Cl^-$ and $HSO_4^- \gg CH_3CO_2^- \approx H_2PO_4^- > Cl^-$, respectively. Among the two conjugates, **L194** showed highest binding toward HSO_4^- due to the presence of additional hydrogen bonding by the phenolic-OH's of

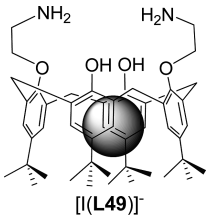

Figure 81. Proposed species for the interaction of I^- with **L49**. The sphere inside the calix[4]arene cavity represents I^-.

calix[4]arene, which is absent in **L193**. The cathodic shift in the quinone/semiquinone redox couple observed during the cyclic voltametry studies of **L193** with anions follows an order $HSO_4^- > H_2PO_4^- > CH_3CO_2^- > Cl^- > Br^-, I^-, ClO_4^-$.[178]

A series of semicarbazone and thiosemicarbazone appended calix[4]arene conjugates (**L195**−**L198**) have been studied for their anion recognition properties toward a variety of anions, Cl^-, Br^-, I^-, ClO_4^-, $H_2PO_4^-$, and PF_4^- in $CDCl_3$ by ^1H NMR spectroscopy (Figure 85).[179] Among the four conjugates, **L195** showed selectivity toward HSO_4^-, while the others did not show due to the absence of imine-hydrogen and/or their poor solubility. **L195** forms a 1:1 complex with HSO_4^- as a result of the hydrogen bonding as can be seen from the binding model (Figure 85), and this complex exhibits a K_a of 4.5×10^3 M^{-1} in $CDCl_3$.

4.1.6. Phosphate Recognition

4.1.6.1. Recognition of Phosphate by Uncomplexed Calix[4]arene Conjugates. Lower rim calix[4]arene substituted with α-hydroxyamide, **L199** (Figure 86), showed promising selectivity for $H_2PO_4^-$ and *N*-tosyl-(L)-alanate over Cl^-, Br^-, and HSO_4^- as studied by ^1H NMR spectroscopy.[180] The K_a values for this binding have been found to be 5413 and 1590 M^{-1}, respectively, for $H_2PO_4^-$ and *N*-tosyl-(L)-alanate in $CDCl_3$ by forming a 1:1 complex in each case.

A series of ferrocene linked calix[4]arene through amide and urea moieties (**L200**−**L202**) have been explored for their anion binding properties by ^1H NMR spectroscopy and by electrochemical methods (Figure 87).[181] The importance of the ion

dx.doi.org/10.1021/cr1004524 |*Chem. Rev.* 2011, 111, 4658–4702

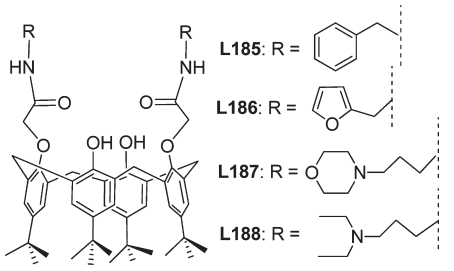

Figure 82. Schematic structures of **L185**−**L188**.

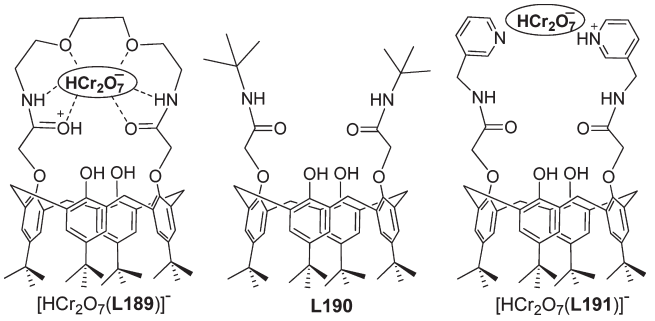

Figure 83. Proposed interaction of **L189** with dichromate anion. Schematic structures of **L190**. Proposed interaction of **L191** with dichromate anions.

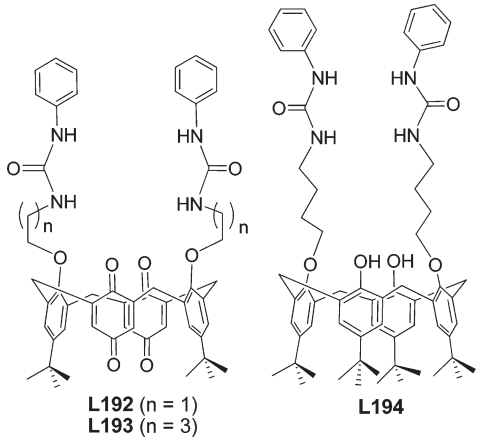

Figure 84. Schematic representation of **L192**, **L193**, and **L194**.

pairing effect on the electrochemical recognition has been explored. The receptors **L200** and **L202** did not show any significant binding as compared to **L201** when titrated with different anions, NO_3^-, SO_4^{2-}, Cl^-, and CH_3COO^-. The **L201** forms a 1:1 complex with $H_2PO_4^-$ yielding K_a of 36 M^{-1} in CD_2Cl_2 as studied by ^1H NMR spectroscopy. All three receptors showed significant electrochemical response only with $H_2PO_4^-$ and not with the other anions studied.

Calix[4]arenes bearing a bis-pyridinium and pyridinium bridge (Figure 88) have been studied for anion recognition with $H_2PO_4^-$, Cl^-, Br^-, and HSO_4^- by ^1H NMR spectroscopy.[182] The **L203** and **L204** form a 1:2 ($L:X^-$) complex with anions, while it is 1:1 in case of **L205**. **L203** exhibits highest stability toward $H_2PO_4^-$ (45 225 M^{-1}). **L204** and **L205** exhibit affinity toward Cl^- (1150, 1015 M^{-1}) over other anions in DMSO-d_6.

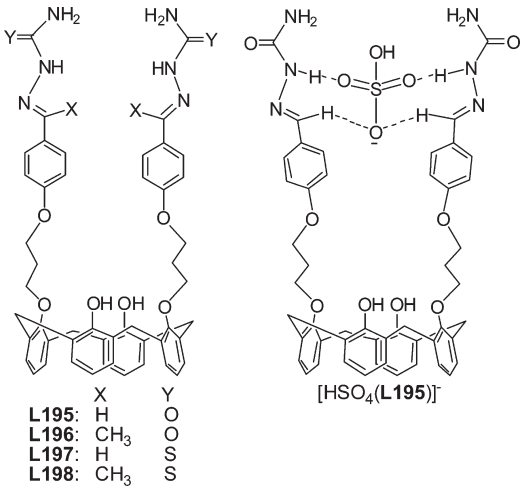

Figure 85. Schematic structure of **L195**−**L198** and proposed binding model of HSO_4^- with **L195**.

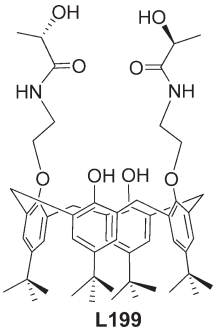

Figure 86. Schematic structure of **L199**.

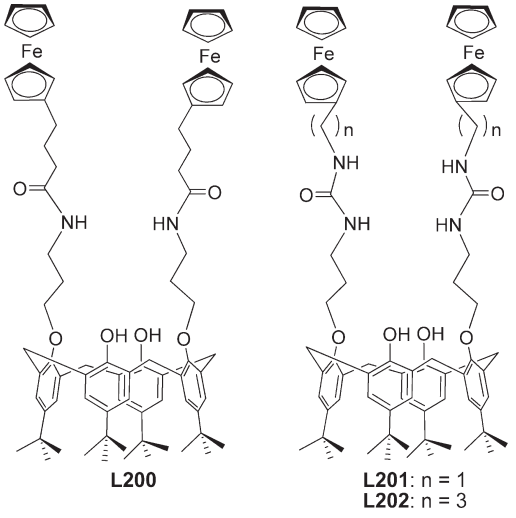

Figure 87. Schematic structures of the receptor molecules **L200**, **L201**, and **L202**.

Electrochemical studies of **L203** with $H_2PO_4^-$ and Cl^- also support the conclusions derived from ^1H NMR spectroscopy.

The **L123** interacts with fluoride and dihydrogen phosphate, giving a 1:1 complex.[145] Molecular modeling calculations suggest that the dihydrogen phosphate mainly interacts with this

dx.doi.org/10.1021/cr1004524 |*Chem. Rev.* 2011, 111, 4658–4702

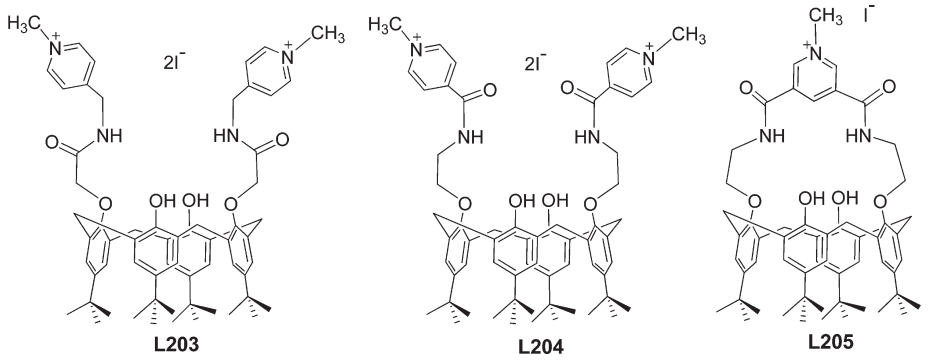

Figure 88. Schematic structures of I^- complexes of **L203**, **L204**, and **L205**.

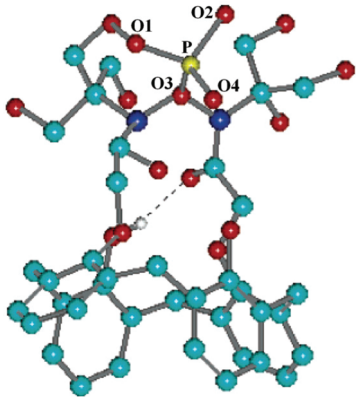

Figure 89. Equilibrium structure of $[H_2PO_4(\mathbf{L123})]^-$ complex as obtained from molecular modeling studies.[145]

conjugate by hydrogen bonding through two amides and one OH of the functionalized arm (Figure 89).

Another phenylureido derivative of calix[4]quinone, **L206** (Figure 90), showed interaction with various anions, and their binding follows a trend, $H_2PO_4^- \gg HSO_4^- > CH_3CO_2^- > Cl^- > Br^-$, as obtained from ^1H NMR spectral titrations.[183] Upon interaction with Na^+, calixarene protons undergo changes in the chemical shift. As a result of the cooperative effect, the strength of Cl^- and Br^- binding has been increased by 20- and 7-fold, respectively, in the presence of Na^+ ion. Electrochemical experiments indicate an effective binding of $H_2PO_4^-$ over other anions studied.

Anion recognition properties of alkyltriphenylphosphonium (Figure 91) toward Cl^-, Br^-, HSO_4^-, $CH_3CO_2^-$, $H_2PO_4^-$, SCN^-, ClO_4^-, and $Cr_2O_7^{2-}$ have been studied in two different solvent systems using ^1H and ^{31}P NMR spectroscopy.[184] The **L207** showed maximum change in ^1H and ^{31}P NMR spectroscopy for SCN^- as compared to the other anions in the series. The complexation of SCN^- has been further supported by FAB-mass. The K_a value of **L208** with different anions follows an order, $H_2PO_4^- > HSO_4^- \gg Cl^- > Br^- > CH_3CO_2^- > ClO_4^-$. Both derivatives exhibit a 1:1 complex with the anions.

A tetraamide derivative of calix[4]arene, **L209**, showed fluorescence enhancement with $H_2PO_4^-$ with K_a of 5.48×10^9 M^{-2} by forming a 1:2 (**L209**:$H_2PO_4^-$) complex in CH_3CN (Figure 92).[185] However, F^- shows fluorescence quenching

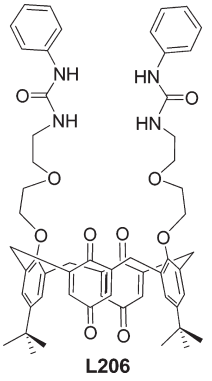

Figure 90. Schematic structure of **L206**.

through the formation of a 1:2 complex and yields a K_a of 2.02×10^6 M^{-2}. The ^1H NMR spectral titrations explain the multiple hydrogen-bonding interaction of $H_2PO_4^-$ with the amide, sulfonamide groups, OH, and several CH protons of **L209**, and that resulted in the high selectivity of this guest species.

Calix[4]arene possessing cyclopeptide moiety, **L210** (Figure 93), at the lower rim exhibits molecular recognition toward phosphomonoester (4-nitrophenyl phosphate) as studied by UV−visible and ^1H NMR spectroscopy.[186] The absorption spectral changes observed indicate the interaction of 4-nitrophenyl phosphate with the calix[4]arene conjugate. This forms a 1:1 complex, and the K_a was found to be 3.9×10^3 M^{-1} in DMSO. The guest interacts with the conjugate through hydrogen bonding mainly to the amide hydrogens.

4.1.6.2. Recognition of Phosphate by a Metal Complex of Calix[4]arene Conjugate. The detection of pyrophosphate has been carried out using a copper complex of **L211** (Figure 94) with pyrocatechol violet as indicator in 80/20 (v/v%) CH_3CN/H_2O buffered with HEPES at pH 6.4.[187] Upon interaction with pyrophosphate, the mixture changes its color from green to yellow, indicating the displacement of pyrocatechol violet from the complex. The formation of a stoichiometric complex between **L211** and pyrophosphate has been shown by mass spectrometry, and the complex exhibits K_a of 5.2×10^5 M^{-1} {80/20 (v/v%) CH_3CN/H_2O buffered with HEPES at pH 6.4}. No color change was observed with other anions, F^-, Cl^-, Br^-, I^-, $H_2PO_4^-$, AcO^-, BzO^-. However, ADP and ATP show behavior similar to that of the pyrophosphate, but not the AMP. Absorption studies have been carried out to account for the color changes observed during the interaction.

dx.doi.org/10.1021/cr1004524 |*Chem. Rev.* 2011, 111, 4658–4702

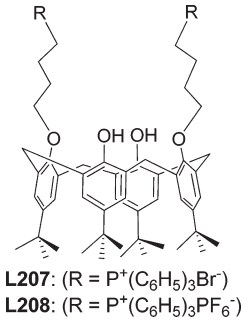

L207: (R = $P^+(C_6H_5)_3Br^-$)
L208: (R = $P^+(C_6H_5)_3PF_6^-$)

Figure 91. Schematic structures of **L207** and **L208**.

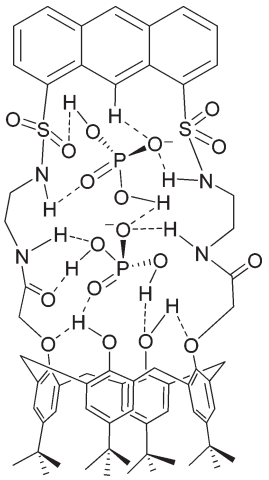

$[H_2PO_4(\mathbf{L209})]^-$

Figure 92. Proposed binding model of **L209** with $H_2PO_4^-$.

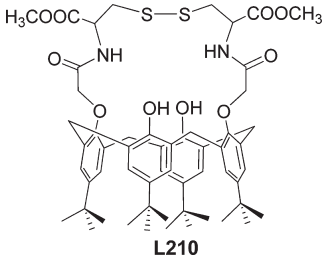

L210

Figure 93. Schematic structure of **L210**.

Conjugates capable of exhibiting hydrogen bonding can interact with anions selectively. The F^- mainly binds to the amide −NH's through hydrogen bonding, and in some cases this is followed by the deprotonation of −NH protons. The interaction of F^- through the phenolic-OH's and urea moieties has been reported in the literature. The Cl^- recognition using thiourea and metal-mediated calix[4]arene conjugates has been known. The aromatic cavity of the calix[4]arene is suited to recognize I^- ion. Of course, the I^- ion can also be sensed by following the spectral changes observed with the Cu^{2+} complexes of some receptor molecules. The pH of the medium also plays an important role in the extraction of anions as shown in case of the chromate. Urea and amide conjugates of calix[4]arene

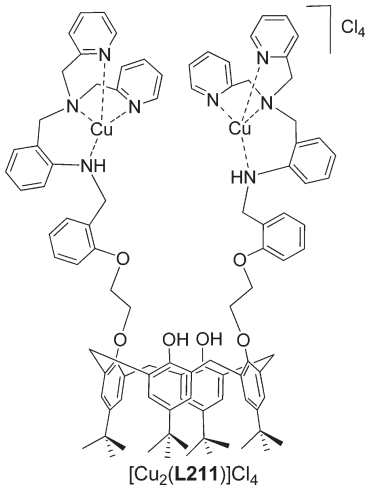

$[Cu_2(\mathbf{L211})]Cl_4$

Figure 94. Proposed binding model of $[Cu_2(\mathbf{L211})]Cl_4$.

showed good selectivity toward various phosphates and sulfates. The free-OH groups present in the calix[4]arene derivatives can also provide additional hydrogen-bonding sites toward the guest molecules as can be seen from Figure 92. The electron-withdrawing groups, which can increase the acidity at the anion binding site, also enhance its binding efficiency.

4.2. Organic Anions

4.2.1. Acetate Recognition. Bridged urea derivatives of calix[4]arene and calix[4]quinone exhibited good selectivity toward CH_3COO^- as compared to Cl^-, HSO_4^-, and $H_2PO_4^-$ as studied by ^1H NMR spectroscopy.[188] Among the four derivatives (Figure 95), **L214** exhibits highest selectivity toward CH_3COO^-, and the K_a order was found to be **L214** > **L213** > **L215** > **L212**, which may be attributed to the presence of quinone moiety and the flexible alkyl bridge. However, when this flexible alkyl bridge is being replaced by the *m*-phenylidene bridge as in **L215**, it exhibits almost equal affinity toward both HSO_4^- and CH_3COO^-.

The Ru^{2+} and Re^+ bipyridyl-based calix[4]arene and calix[4]quinone conjugates (**L216** to **L219**) exhibit selectivity toward acetate in 1:1 stoichiometry, and the order of the selectivity follows $AcO^- > Cl^- > H_2PO_4^-$, as deduced on the basis of the K_a data obtained from ^1H NMR spectroscopy (Figure 96).[189] Among the four derivatives, **L216** shows large K_a with acetate due to the presence of the quinone moiety as well as the positive charge present on the complex.

Quinone bis-calix[4]arene derivative (**L220**, Figure 97) exhibits good selectivity toward acetate and benzoate with the formation of a complex having a ligand to anion ratio of 1:2, among all of the anions, chloride, bromide, iodide, acetate, and benzoate, studied by ^1H NMR spectral titrations.[190]

Anion recognition studies of an amidourea based calix[4]arene, **L221** (Figure 98), have been carried out by UV−visible spectroscopy.[191] Interaction of CH_3COO^-, F^-, and $HP_2O_7^{3-}$ with the calix[4]arene conjugate results in the formation of 1:1 complex initially followed by 1:2 (**L221**:anion) at higher equivalents to give a visual color change in case of F^- and $HP_2O_7^{3-}$. However, the interaction of $H_2PO_4^-$ with **L221** results in only a 1:1 complex.

The Cu^+ complex of **L23** ($[CuL23]^+$) exhibits fluorescence changes toward CH_3COO^- and F^- (Figure 99) among various

dx.doi.org/10.1021/cr1004524 |*Chem. Rev.* 2011, 111, 4658–4702

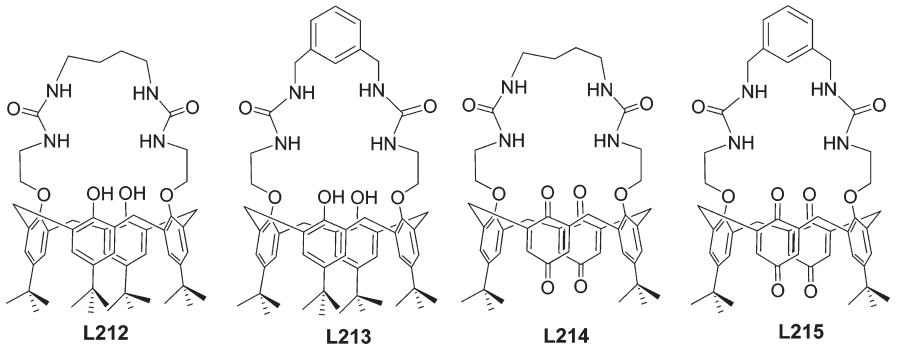

Figure 95. Schematic structures of acetate receptors.

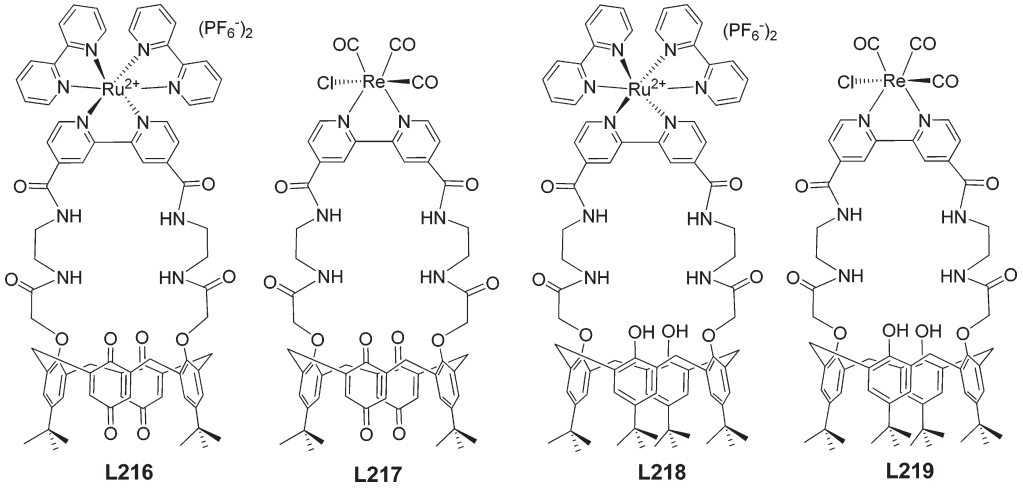

Figure 96. Schematic structures of acetate receptors, **L216**−**L219**.

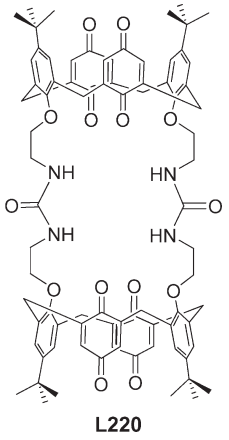

Figure 97. Schematic structure of **L220**.

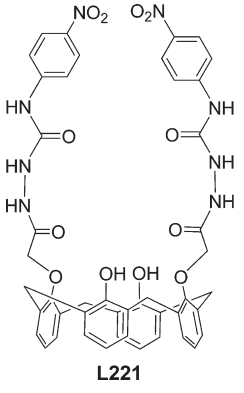

Figure 98. Schematic structure of **L221**.

anions studied, Cl^-, Br^-, I^-, HSO_4^-, $H_2PO_4^-$, and NO_3^-, while its precursor **L24** does not (Figure 16).[85] Recognition of these anions is also being accompanied by a color change from yellow to beige in case of CH_3COO^- and F^-, and the corresponding association constants were found to be 159 000 and 59 900 M^{-1}, respectively, in CH_3CN.

4.2.2. Recognition by Dicarboxylates. Calix[4]arene conjugate bearing thiourea and amide (**L222** and **L223**) selectively recognizes dicarboxylate anions, malonate, succinate, glutarate, and adipate over AcO^-, $H_2PO_4^-$, Cl^-, Br^-, and I^- in DMSO as studied by UV−visible, fluorescence, and ^1H NMR spectral titrations.[192] Both of the conjugates form stoichiometric complexes with all of the dicarboxylates through multiple hydrogen bonding (Figure 100), and the sensitivity of the recognition depends on the chain length, and the selectivity follows an order adipate > glutarate > succinate > malonate, based on their K_a values. The conjugate **L222** undergoes color change from yellow to red when it interacts with dicarboxylate anions.

dx.doi.org/10.1021/cr1004524 |*Chem. Rev.* 2011, 111, 4658–4702

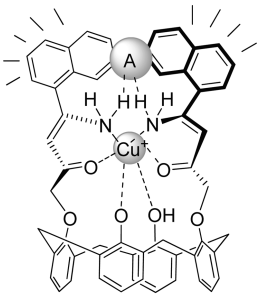

Figure 99. Possible anion binding mode of [Cu(**L23**)(A)], where A represents anion.

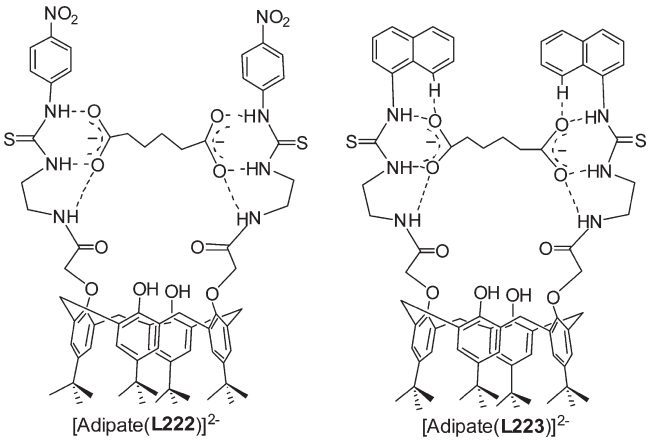

Figure 100. Possible adipate ion binding models in case of **L222** and **L223**.

Calix[4]arene functionalized with aminobenzimidazole, **L224**, exhibits high selectivity toward pimelate through fluorescence enhancement in CH_3CN with a K_a of $(7.2 \pm 0.13) \times 10^5$ M^{-1} and a detection limit of 1 μM.[193] A number of other dicarboxylates, such as malonate, succinate, glutarate, adipate, and suberate, exhibit lower K_a. Both pimelate and suberate form 1:1 complexes, while others were found to form 1:2 (receptor to the guest), as is evident from the Job's plots. The mode of dicarboxylate coordination has been proposed on the basis of ^{1}H NMR spectral titrations (Figure 101).

Membrane transportation properties of a series of calix[4]arene derivatives toward dicarboxylic acids and α-hydroxycarboxylic acids have been studied (Figure 102).[194] The conjugate bearing the pyridyl moiety, **L228**, exhibits greater efficiency of carrying oxalic acid among all of the conjugates. Both COOH groups of the substrate form hydrogen bonds with the nitrogen of the pyridyl ring as is evident from the computational calculations (Figure 102a). The absorption intensity of **L228** follows an order oxalic > glycolic > tartaric > succinic acids. The conjugate **L225** exhibits maximum transfer rate with oxalic, hydroxycarboxylic, and dicarboxylic acids. Oxalic acid binds only through the amide nitrogen, while the malonic acid uses both hydroxy and amide groups (Figure 102b−d). The involvement of the hydroxyl group in case of **L225** has been studied by comparing the results with **L226** where it does not show any mass transfer. The conjugate **L227** shows transfer only to sodium acetate, while **L230** transfers to both glutamic acid and sodium

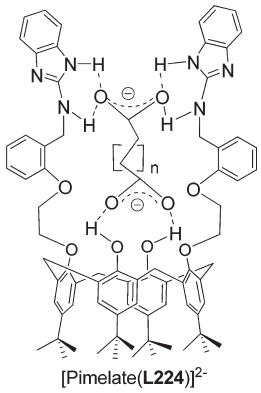

Figure 101. Possible pimelate ion bound **L224**.

acetate. To prove the role of the substituents required for the selective extraction, studies were also carried out with **L229** where interactions are possible only through hydroxyl groups at the lower rim. The **L229** does not exhibit any response due to its electron-deficient character of the substituents and its inability to act as a proton donor or proton acceptor.

Acetate sensing has been possible with the bridged urea moieties, the double calix[4]quinones possessing amide functionalities, and the metal-mediated ones. In the case of capped conjugates, the flexibility of the alkyl group, which determines the efficiency of binding, can be seen from Figure 95. Dicarboxylate recognition requires several hydrogen-bonding sites in the receptor systems where the distance between the two binding sites should match the length of the guest molecule. In addition to this, the pH value of the solvent is an important factor in sensing dicarboxylates. The electronic factor of the substituents also influences the ability of anion binding.

4.3. Chiral Recognition by Calix[4]arene Conjugates

Chiral recognition is an important subject not only in the field of supramolecular chemistry, but also in biomedical applications. Four chiral calix[4]arene conjugates were synthesized for the enantiomeric recognition of different amino acid derivatives and were studied by UV−vis spectroscopy in $CHCl_3$ (Figure 103).[195] Thermodynamic parameters, such as binding constant, enthalpy, entropy, and free-energy changes, have been derived. It has been found that all of the receptor molecules (**L231**−**L234**) exhibit higher K_a values toward enantiomers of Phe−OMe than Ala−OMe as a result of $\pi\cdots\pi$ interaction of the former with the receptor (Figure 103). Among the four derivatives, **L233** showed maximum binding with L-Phe−OMe·HCl followed by **L231**. Therefore, the factors that are responsible for enantioselective recognition are the multiple hydrogen bonding, the steric hindrance, the structural rigidity, and the $\pi\cdots\pi$ stacking, etc., as reported in the literature.

Chiral calix[4]crown bearing 1,2-diphenyl-1,2-oxyamino residue, **L235** (Figure 104), exhibits good chiral recognition between the enantiomers of mandelic acid as studied by ^{1}H NMR spectroscopy with the ratio of association constant of (*S*)- and (*R*)- being $K_{a(S)}/K_{a(R)}$ = 102 in $CDCl_3$; that is, the enantioselectivity observed was almost 98%.[196] Chiral calix[4]azacrown possessing L-valine, **L236** (Figure 104), has shown different recognition ability toward D- and L-forms of the tartaric acid derivative with association constants of $(9.83 \pm 0.43) \times 10^3$ and $(5.04 \pm 0.28) \times 10^3$ M^{-1}, respectively, in $CHCl_3$ and exhibit different conformations with different guest species.[197]

dx.doi.org/10.1021/cr1004524 |*Chem. Rev.* 2011, 111, 4658–4702

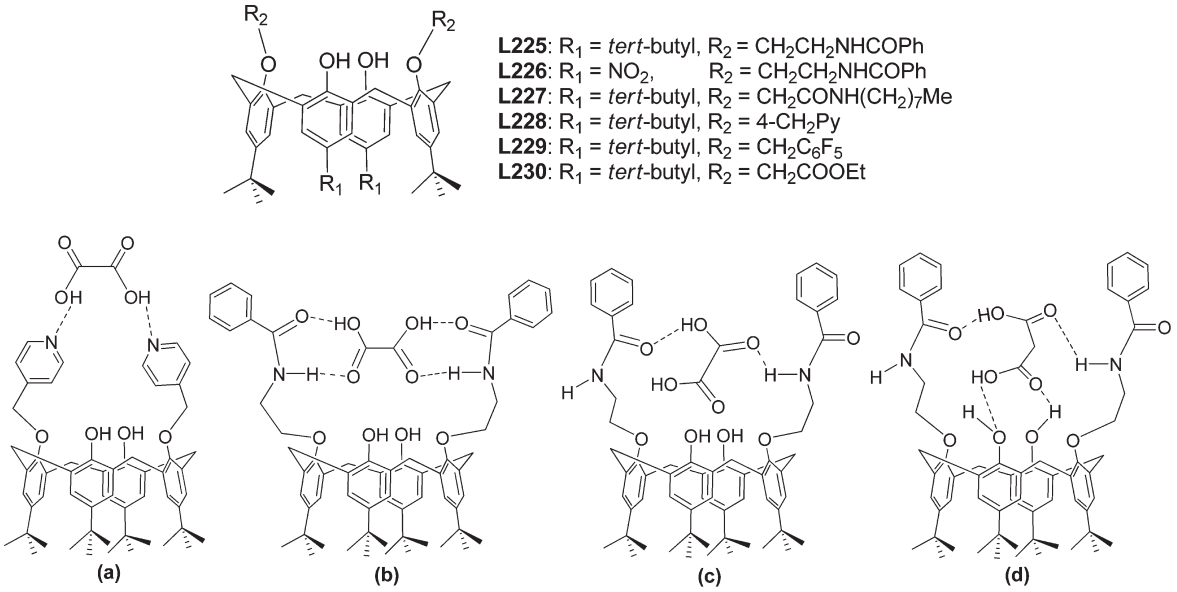

Figure 102. Schematic structures of **L225**−**L230**. (a) Oxalic acid bound species of **L228**. Two different binding modes of oxalic acid in **L225** are shown in (b) and (c). (d) Schematic structure of **L225** bound to malonic acid.

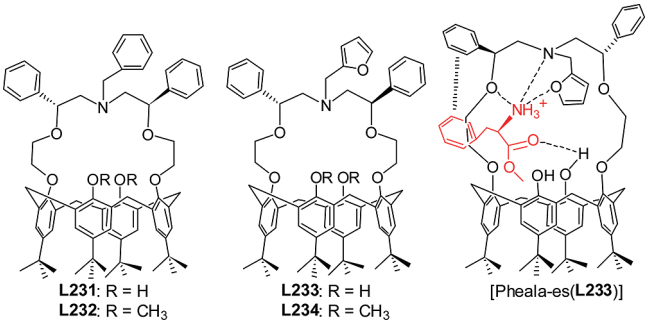

Figure 103. Schematic structures of **L231**−**L234** and the proposed binding model of N-protonated methyl ester of phenylalanine with **L233**.

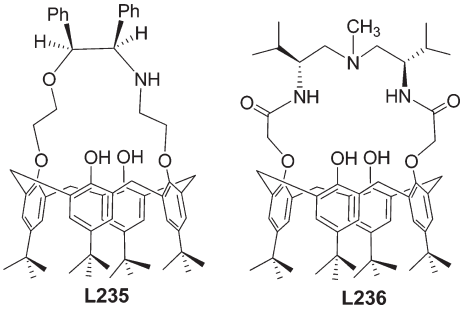

Figure 104. Schematic structures of **L235** and **L236**.

Calix[4]arene bearing tartaric ester moieties has been studied for chiral recognition using ^{1}H NMR spectroscopy. Among the four derivatives (Figure 105), **L238**, **L239**, and **L240** exhibit enantioselective recognition toward *rac*-SerOMe and 1,2-propanediol.[198] Extraction properties of **L237** and **L238** have also been studied, but none of these show any selectivity toward the esters of α-amino acids.

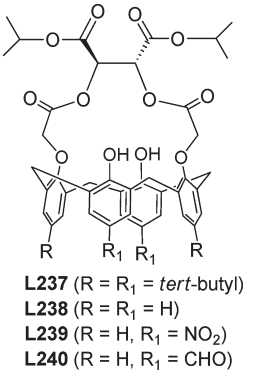

Figure 105. Schematic structures of **L237**−**L240**.

Chiral calix[4]arene functionalized at the lower rim with amino acid residues has been studied for their complexation toward anions, Cl^-, $H_2PO_4^-$, HSO_4^-, and *N*-tosyl-(L)-alaninate, by ^{1}H NMR spectroscopy.[199] Among the three receptor molecules studied (Figure 106), **L243** exhibits the highest K_a with *N*-tosyl-(L)-alaninate, and the trend follows an order *N*-tosyl-(L)-alaninate > Cl^- > Br^- ≈ HSO_4^- > $H_2PO_4^-$. However, the K_a in case of **L241** and **L242** follows: *N*-tosyl-(L)-alaninate > Cl^- and Cl^- > *N*-tosyl-(L)-alaninate > Br^-, respectively. All of these derivatives form a 1:1 complex with the anions studied. Although the receptor is chiral, no chiral recognition has been reported.

The enantioselective recognition abilities of a series of calix[4]arene conjugates bearing L-tryptophan have been studied by fluorescence and ^{1}H NMR spectroscopy (Figure 107).[200] **L244** shows fluorescence quenching of 48% with D-Ala as opposed to 10% with L-Ala even after 155 equivalent addition of these. While **L245** exhibits selectivity toward D-mandelate with $\Delta I_D/\Delta I_L = 8.0$, **L246** shows good enantioselective recognition toward D-malate by fluorescence enhancement of the excimer band of this conjugate with D/L selectivity of $K_{a(D)}/K_{a(L)} = 4.95$. Among the three conjugates, highest association was observed with **L245**

dx.doi.org/10.1021/cr1004524 |*Chem. Rev.* 2011, 111, 4658–4702

toward different guests as compared to **L244** and **L246**. The results of the fluorescence titrations were supported by ^{1}H NMR spectroscopy, and the stoichiometry of the complex was found to be 1:1. The chiral recognition has been attributed to the structural preorganization, steric effects, and multiple hydrogen bonding present in **L244** and **L245**.

Chiral recognition of L- or D-α-phenylglycinate ions among the other enantiomers of mandelate and dibenzoyl tartrate has been studied by UV−vis (DMSO) and ^{1}H NMR ($CDCl_3$) spectroscopy using **L247** and **L248** (Figure 108).[201] Both of the receptors form a 1:1 complex with L- or D-α-phenylglycine anion, and the corresponding $K_{a(L)}/K_{a(D)}$ = 4.76 and 2.84, respectively, in DMSO for **L247** and **L248**, and hence **L247** is the better among the two. The colorless solution of **L247** has been changed to yellow and saffron, respectively, upon interaction with L- and D-α-phenylglycine. However, the colorless solution of **L248** changes to saffron during its interaction with both enantiomers of phenylglycine. The good enantioselective recognition of α-phenylglycinate by **L247** is attributed to its steric effects, better preorganized structure, and good hydrogen-bonding ability.

Calix[4]arene functionalized with chiral moiety along with anthracenyl group exhibits a chiral recognition toward enantioselective malate as studied by fluorescence quenching in $CHCl_3$, and the results were supported by ^{1}H NMR spectroscopy.[202] Both receptors (**L249** and **L250**, Figure 108) showed good selectivity toward D-malate as compared to L-malate, and the corresponding quenching efficiencies ($\Delta I_D/\Delta I_L$) are 1.75 and 1.53, respectively, for **L249** and **L250**. The fluorescence quenching is attributable to PET. Both receptors form a 1:1 complex with malate, and the $K_{a(D)}/K_{a(L)}$ values are 4.34 and 10.41, respectively, for **L249** and **L250** in $CHCl_3$.

Chiral calix[4]arene bearing hydrazide and dansyl groups (**L251** and **L252**, Figure 108) exhibits enantioselective recognition toward the anions of L-amino acid as compared to D-amino acid, which is evident from the quenching efficiency and higher K_a observed.[203] The results were supported by ^{1}H NMR spectral titrations. The quenching efficiency of **L251** toward L- and D-Ala was $\Delta I_L/\Delta I_D$ = 5.0, while it was only 2.5 toward Phe. Similarly, **L252** showed $\Delta I_L/\Delta I_D$ values of 2.5 and 5.7 with Ala and Phe anions.

The conformational properties and enantioselective recognition abilities of a bisurea conjugate of calix[4]arene possessing L-amino acid, **L253** (Figure 109), have been studied by ^{1}H NMR spectroscopy and molecular modeling.[204] **L253** exhibits significant enantioselectivity of K_a^D/K_a^L = 4.14 by a three-point interaction with *N*-acetyl-D-phenylalaninate as evident from the molecular modeling (Figure 109).

The enantioselective recognition of *N*-acetyl-aspartate using a calix[4]arene-based chiral receptor by fluorescence quenching has been studied in DMSO (Figure 110).[205] The association constants of the receptor **L254** toward the L and D forms of aspartate were found to be 126 and 854 M^{-1}, respectively, in DMSO. Upon interaction with 35 equiv of *N*-acetyl-L- or -D-aspartate, **L254** exhibits quenching of 35.6% and 9.6%, respectively, by forming a 1:1 complex. The D-form of the guest species shows 45% quenching with **L255**, while it was only 37% in case of L-form where the equivalents of D- and L-forms were 175 and 160, respectively. The K_a values observed for **L255** with L- and D-aspartate were 959 and 148 M^{-1}, respectively. The selectivities of the two receptors, **L254** and **L255**, toward *N*-acetyl-aspartate were $K_{a(D)}/K_{a(L)}$ = 6.74 and $K_{a(L)}/K_{a(D)}$ = 6.48, respectively, and thus exhibit exactly an opposite selectivity among the two. The binding has been further supported by comparing the results obtained from appropriate control molecules.

The enantioselective recognition abilities of **L256** and **L257** (Figure 110) toward two amino alcohols, phenylglycinol and phenylalaninol, have been carried out in DMSO using fluorescence and ^{1}H NMR spectroscopy.[206] Both **L256** and **L257** exhibit fluorescence enhancement with L- and D-phenylglycinol, and the corresponding K_L/K_D values were found to be 4.85 and

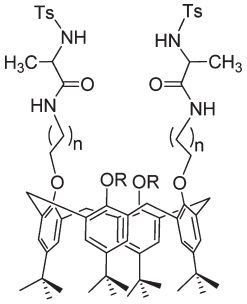

L241 (R = H, n = 1)
L242 (R = H, n = 3)
L243 (R = C_3H_7, n = 3)

Figure 106. Schematic structures of some chiral calix[4]arene receptors for the chiral recognition.

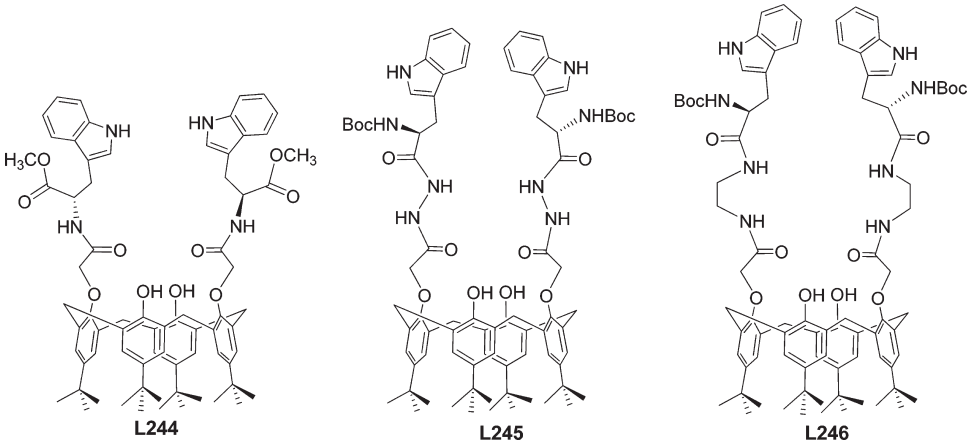

L244 **L245** **L246**

Figure 107. Schematic structures of **L244**, **L245**, and **L246**.

dx.doi.org/10.1021/cr1004524 |*Chem. Rev.* 2011, 111, 4658–4702

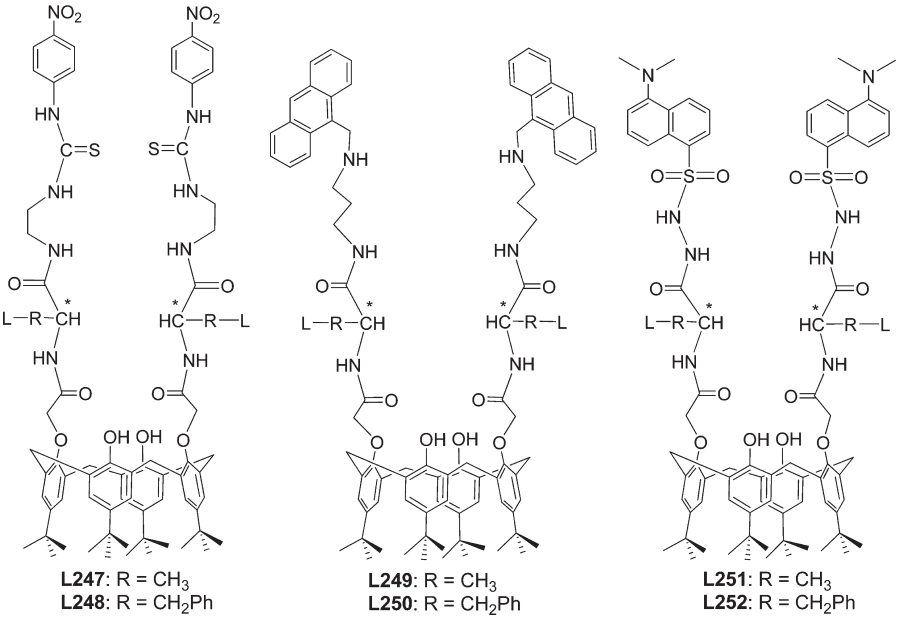

Figure 108. Schematic representation of **L247**−**L252**.

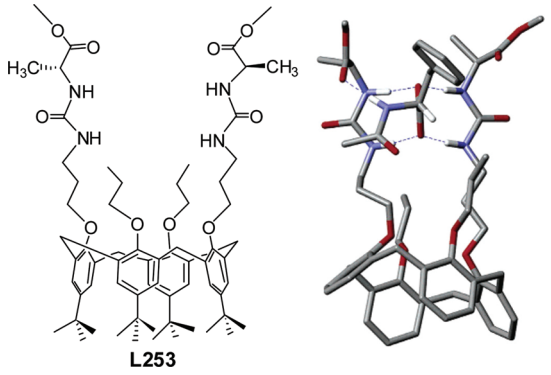

Figure 109. Schematic structure of **L253** and the energy minimized structure of **L253** (*tert*-butyl group is being replaced by hydrogen for optimization) with *N*-acetyl-D-phenylalaninate.[204]

0.51, respectively. The observed K_L/K_D values for **L256** and **L257** with L- and D-diphenylalaninol were 1.44 and 0.83, respectively. Both conjugates form a 1:1 complex with the guest molecules, and their interaction with phenylglycinol is mainly through the $\pi\cdots\pi$ stacking between the aromatic ring of phenylglycinol and that of the naphthalene of the receptor molecules.

Liquid-phase extraction studies of the methyl esters α-amino acid, such as L- and D-forms of SerO−Me, AlaO−Me, and PheO−Me, have been studied using chiral diamide conjugates of calix[4]arene, **L258**−**L261** (Figure 111).[207] All of the receptors exhibit significant extraction toward α-amino acid methylesters without any enantioselectivity. The proposed mode of binding of the receptor molecule with an ammonium cation belonging to the amino acids is given in Figure 111. The extraction ability of **L258** and **L260** is slightly higher than that of **L259** and **L261** due to a better preorganization and fixed cone conformation in the former, whereas the latter ones are more flexible.

Three chiral bicyclodipeptide bearing calix[4]arenes, **L262**, **L263**, and **L264** (Figure 112), as chiral coatings for gas sensors were studied where all of the conjugates exhibit selectivity for the (*R*)-methyl lactate as compared to the (*S*)-enantiomer by using quartz crystal microbalance method.[208]

Chiral calix[4]arenes bearing optically pure α,β-amino alcohol groups (**L265** and **L266**) at the lower rim showed efficient chiral recognition ability and high enantioselectivity between the enantiomers of carboxylic acids, such as mandelic acid (**g1**), 2-hydroxy-3-methylbutyric acid (**g2**), and 2,3-dibenzoyltartaric acid (**g3**) as studied by ^{1}H NMR spectroscopy (Figure 113).[209] Interactions of the receptor molecule and all of the guest molecules result in 2:1 complexes except for **L265** with **g3** where it shows a 1:1 complex. The data show that (*S*)-**g1**, (*S*)-**g2**, and L-**g3** with **L265** and **L266** results in higher association constants as compared to the corresponding enantiomers (*R*)-**g1**, (*R*)-**g2**, and D-**g3**, respectively.

A series of chiral calix[4]arene derivatives (**L267**−**L272**) (Figure 114) have been synthesized, and their complex formation with antibiotic levofloxacin (Lfx) has been studied by quantum mechanical calculations at the density functional and semiempirical levels.[210] It has been found that the calix[4]arene−Lfx interaction mode is determined by the substituents present at the upper and the lower rims of calix[4]arene. The calix[4]arene with strong electron-withdrawing group, NO_2 (**L272**), forms a stable complex with the guest species.

A calix[4]arene bearing two sugar moieties through amide linkage has been synthesized, and its complexation properties with three sugar derivatives have been studied (Figure 115).[211] The conjugate, **L273**, undergoes self-aggregation in nonpolar solvents as is evident from the ^{1}H NMR spectroscopy. The K_a's observed for **L273** upon complexation with 1-*O*-octyl-α-D-glucopyranoside, 1-*O*-octyl-β-D-glucopyranoside, and 1-*S*-octyl-β-D-thioglucopyranoside were 650, 1050, and 1000 M^{-1}, respectively, in $CDCl_3$. The almost similar association constants observed for α- and β-forms of the sugar explain that the configuration at the C1 is not important for the complexation.

Several calix[4]arene conjugates appended with chiral moiety exhibited enantioselective recognition toward neutral and anionic

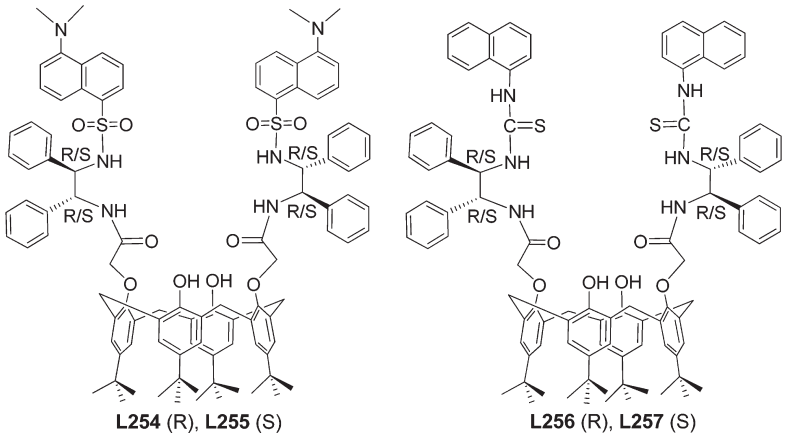

Figure 110. Schematic structures of **L254**−**L257**.

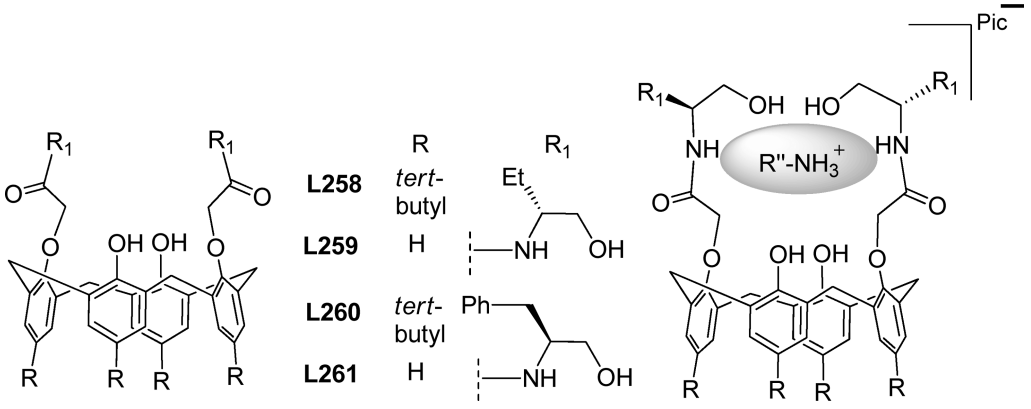

Figure 111. Schematic structures of **L258**−**L261** and proposed structure of the species of the receptor with an ammonium cation belonging to an amino acid.

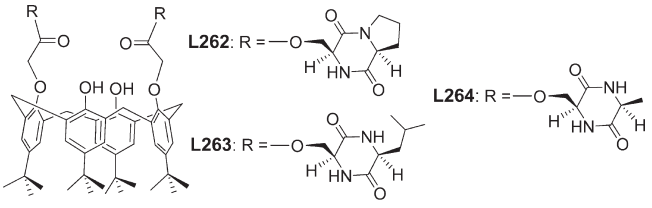

Figure 112. Schematic structures of chiral calix[4]arene conjugates.

chiral organic species. The enantioselective recognition of D-malate, L- or D-α-phenylglycine, L-alanine, and *N*-acetyl aspartate has been demonstrated by 1,3-diconjugates of calix[4]arene. Therefore, it is evident from the literature that the calix[4]arenes functionalized with chiral moieties, which complement the substrates, are useful for the selective recognition of the enantiomers. The other important aspects of the enantioselective recognition are the steric hindrance, the structural rigidity, and the $\pi\cdots\pi$ stacking between the host and the guest.

5. AMINO ACIDS AND OTHER MOLECULAR RECOGNITION

5.1. Recognition of Amino Acids by Uncomplexed Calix[4]arene Conjugates

Aminoacids are present in the cell in the free state as well as in the peptides and proteins as building blocks. The detection of

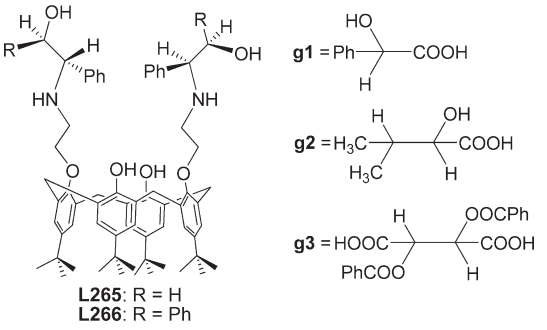

Figure 113. Schematic structures of **L265** and **L266**, and the guest molecules, **g1**, **g2**, and **g3**.

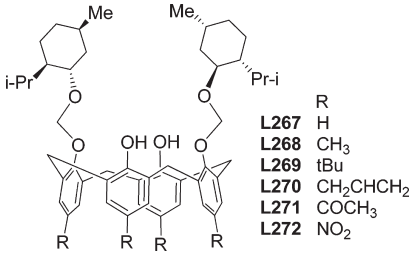

Figure 114. Schematic structures of **L267**−**L272**.

dx.doi.org/10.1021/cr1004524 |*Chem. Rev.* 2011, 111, 4658–4702

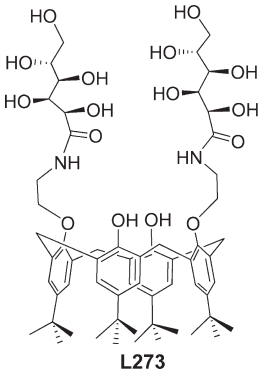

Figure 115. Schematic structure of **L273**.

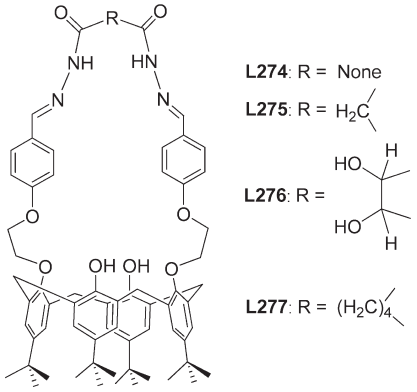

Figure 116. Schematic structures of **L274**−**L277**.

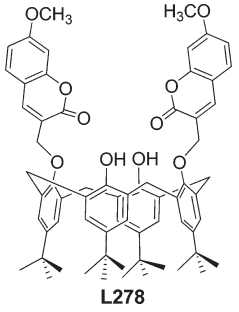

Figure 117. Schematic structure of **L278**.

these in their free or in their protein bound form is important in biology as was already given in the Introduction.

A series of calix[4]azacrowns bearing acylhydrazone group, **L274**−**L277** (Figure 116), have been synthesized, and the extraction abilities of various α-amino acids, Gly, Trp, His, Lys, Pro, Thr, IIe, and Arg, have been studied.[212] All of the conjugates exhibit similar extraction behavior, indicating that the complexation ability is independent of the length of the crown ether chain. Among the four conjugates, **L275** showed highest extraction with tryptophan by forming a 1:1 complex, and this has been further supported by UV−vis spectroscopy.

A coumarin appended conjugate, **L278** (Figure 117), recognizes L-tryptophan by forming a 1:1 complex with equilibrium constant of 111 M^{-1} via fluorescence enhancement among a number of D- and L-forms of amino acids, Ser, Tyr, Trp, Met, His, Cys, and

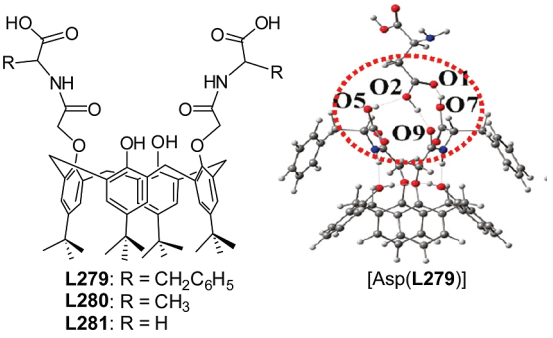

Figure 118. Schematic structures of **L279**−**L281**. The DFT-optimized structure of **L279** with Asp.[214]

Ala, as studied by UV−visible and fluorescence spectroscopy in a 1:1 DMF:acetonitrile mixture.[213]

The molecular recognition properties of **L279** (Figure 118) possessing terminal −COOH moiety exhibit fluorescence turn-on behavior only toward guest molecules bearing −COOH groups such as Asp, Glu, GSH (glutathione reduced), and GSSG (glutathione oxidized).[214] **L279** forms a 1:1 complex with Asp and Glu by exhibiting a K_a of 532 and 676 M^{-1}, respectively, in H_2O:CH_3CN (v/v 1:1). The fluorescence studies of **L280** and **L281** with Asp, Glu, GSH, and GSSG also resulted in the same behavior as that observed with **L279**, revealing that the recognition is independent of the side chain of the receptor molecule. The role of the terminal −COOH of the receptor and the guest molecules was demonstrated by studying the corresponding ester derivatives of both, where no fluorescence response was observed with increasing concentrations of the guest species. Computational calculations demonstrate the presence of three hydrogen-bond interactions between two arms of **L279** and Asp/Glu/GSH (Figure 118). The spherical cluster formation and the aggregational behavior between the **L279** and Asp or Glu have been demonstrated based on SEM, AFM, and DLS studies, which are further supported by the computational calculations. The nanosphere formation of **L279** with GSH-coated Ag-nanoparticles has been established by TEM and AFM studies. The studies were also extended to monitor interaction of **L279** with proteins, BSA/HSA, which shows uniform-spherical particles, and this is found to be dependent on the presence of the amido-arm as well as the side chain of the receptor.

The solid-state structure of the complex formed between **L282** (Figure 119) and L-lysine has been demonstrated where lysine forms a 1-D ladder network in the lattice.[215] The asymmetric unit of the complex is composed of four **L282**, three lysines, two molecules of ethanol, and seven water molecules (Figure 119). All four independent molecules of the receptors are in cone conformation, and the phenolic oxygens are involved in intramolecular hydrogen bonding except in one case where hydrogen bonding is present between the water molecule and the unsubstituted phenolic oxygen atom. Also, the L-lysine exhibits three different conformations. The dimeric units of the calixarenes from the neighboring layers form hydrogen bonds with −OH groups of the oxyphosphoryl units.

5.2. Recognition of Amino Acid by Metal Complexes of the Calix[4]arene Conjugates

Among the20 naturally occurring amino acids, [Zn(**L3**)] (Figure 2) provides response to Asp, Cys, His, and Glu by fluorescence quenching, as these amino acids can chelate using

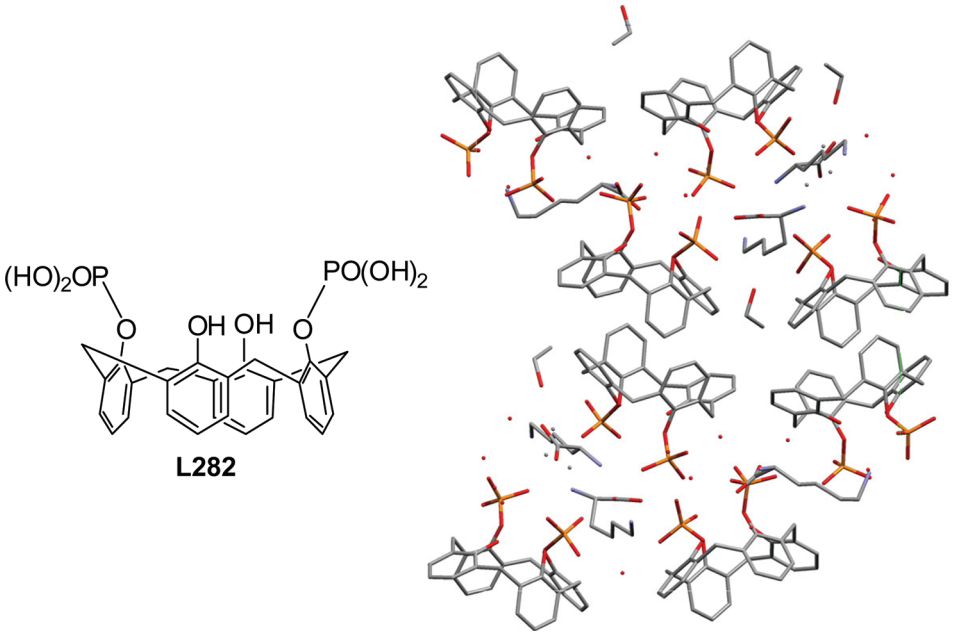

Figure 119. Schematic structure of **L282**. Molecular packing diagram of the complex of **L282** with L-lysine. Several water (red points) and ethanol molecules are present in the crystal lattice. Reprinted with permission from ref 215. Copyright 2006 Elsevier.

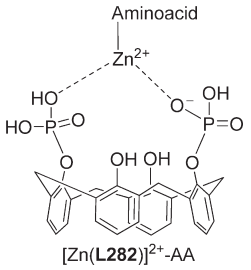

Figure 120. Proposed binding model of zinc complex of **L282** with an amino acid.

their side-chain moieties and hence impart selectivity toward these amino acids.[216] During the titration, the Zn^{2+} was found to be displaced from the complex as a result of the protonation of the bound [Zn(**L3**)] followed by chelation by the added amino acid, in addition to having $\pi\cdots\pi$ interactions between the arm-aromatic component of **L3** and the aromatic side chain of the amino acids. Because these amino acid residues are present in proteins, transfer of Zn^{2+} from [Zn(**L3**)] to the protein was studied by absorption and fluorescence spectroscopy, the conformational changes by CD, and the aggregation aspects by atomic force microscopy, as was carried out using some α-helical and β-sheet proteins.

Among the 20 natural amino acids, [Zn(**L5**)] (Figure 3) showed maximum quenching with a few, and this follows a trend, Cys > Asp ≫ His, depending upon the chelating ability of the amino acid.[70] The fluorescence quenching of the complex is due to the protonation of Zn^{2+} coordination sphere followed by the formation of a complex of Zn^{2+} with amino acid. The removal of Zn^{2+} by the amino acid has been further supported by absorption titrations.

The Ag^{+} complex of **L28** ($[Ag(\mathbf{L28})]^{+}$), in turn, recognizes Cys ratiometrically among the 20 naturally occurring amino acids studied with the release of Ag^{+} followed by the formation of its cysteine complex as shown by absorption, mass spectrometry, and TEM studies.[91] The minimum detection limit has been found to be 514 ppb, and this system exhibits INHIBIT logic gate (Figure 20).

The interaction of **L282** with seven amino acids, Ala, Asp, Arg, His, Lys, Ser, and Cys, in the presence and absence of different metal ions, Na^{+}, K^{+}, Mg^{2+}, Ca^{2+}, Cu^{2+}, Ni^{2+}, and Zn^{2+}, have been studied by ESI MS.[217] In the absence of these cations, His exhibits highest affinity toward **L282**. Decomplexation of the amino acid was observed in the presence of Na^{+} and K^{+}; however, the interaction between the other ion and **L282** resulted in either decomplexation or ternary complex formation. Competitive titration experiments of **L282**, Zn^{2+}, and all seven amino acids by ESI MS show the selective ternary complex formation only with histidine. ^{1}H NMR spectroscopic results indicate that there is no direct interaction between phosphate groups of **L282** and His in the presence of Zn^{2+}, and the amino acid interaction is possible only through Zn^{2+} as can be seen from Figure 120.

Amino acid recognition is generally achieved either by the direct interaction of the properly functionalized 1,3-diconjugate of calix[4]arene with amino acid or by the displacement mechanism where amino acid replaces the metal ion from the complexes of the receptor conjugates. Conjugates of calix[4]arene appended with dihydroxyphosphate moiety have been studied for their amino acid recognition and complexation properties.

5.3. Recognition of Other Molecular Species

Calix[4]arene functionalized with guanidinium groups, **L283**, forms stable monolayers at the air−water interface and exhibits different binding behavior with 5′-AMP^{-} and 5′-GMP^{2-} as studied by $\pi-A$ isotherms, relaxation curves, and UV, CD, IR, and XPS of the LB films.[218] The interaction of the receptor molecule with these is mainly through the complementary hydrogen bonding and electrostatic interactions in 1:1 and 2:1

dx.doi.org/10.1021/cr1004524 |*Chem. Rev.* 2011, 111, 4658–4702

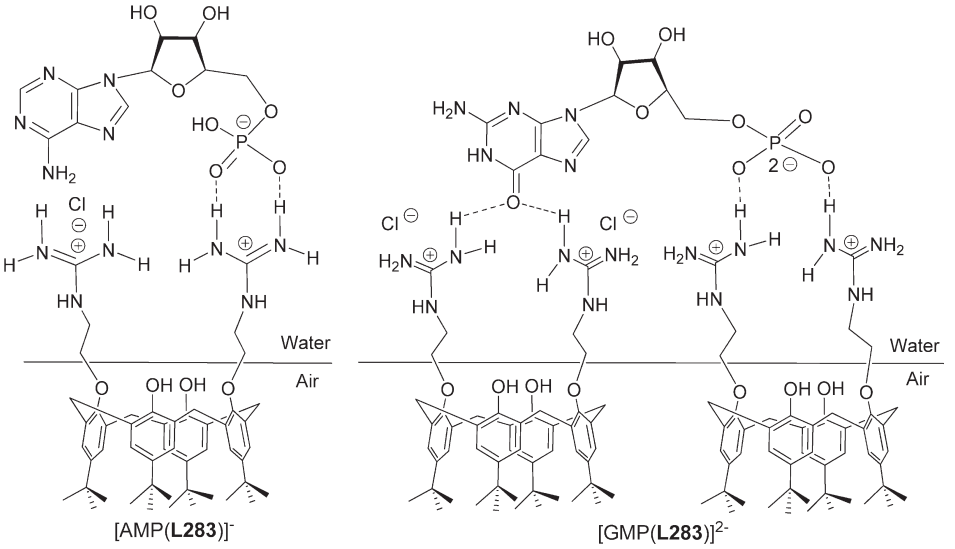

Figure 121. Schematic representation of the species of interaction of **L283** with nucleotides, 5′-AMP^{-} and 5′-GMP^{2-}, at the air−water interface.

molar ratios with K_a values of $(1 \pm 0.5) \times 10^6$ and $(6 \pm 1) \times 10^5$ M^{-1}, respectively, in aqueous solution (Figure 121).

The crystal structures of **L282** with dimethyl ammonium and tetra-methyl ammonium cations have been demonstrated.[219] In the unit cell, two molecules of calix[4]arene diphosphate, three dimethyl ammonium cations, one tetra-methyl ammonium cation, and one DMF molecule were present. The species of the recognition can be seen from the lattice structure shown in Figure 122.

Solid-state aspects of a calix[4]arene-based dihydroxyphosphonic derivative (**L282**) with various guest molecules have been explored.[220] **L282** forms a complex with 1,10-phenanthroline where the structural motif is composed of eight molecules of calixarene, which form intermolecular hydrogen bonds and which are stacked by π---π interaction (Figure 123). The monoprotonated 1,10-phenanthroline dimers exhibit face-to-face stacking with the aromatic ring of the calix[4]arene conjugate and CH---C interactions. Hydrogen-bond interactions exist between the protonated nitrogen atom of the trapped 1,10-phenanthroline and deprotonated hydroxyl of the phosphoric acid.

The solid-state structural characteristics of melamine monocation complexes of **L282** have been established. In the unit cell of the complex, one molecule of **L282**, nine water molecules, and one molecule of ethanol were present.[221] Also in the solid state, the melamine cations are aligned parallel to the in-layer arrangement of the calixarene. The protonation of one of the aromatic nitrogen atom of melamine accounts for the charge equilibrium.

The formation of an aqua-channel system by **L282** has also been reported. In the crystal structure, **L282** exists in the dimeric form and is arranged in a head-to-head fashion by intermolecular π---π interactions (Figure 124).[222] The lattice is mainly composed of 12 calix[4]arene dihydroxyphosphoric acids, 12 propane diammonium cations, 12 ethanol, and 40 water molecules arranged in a triagonal fashion to form a hexameric tube with radius and depth of 15 and 16 Å, respectively. Finally, these form a channel with a length of 40 Å that is occupied by the water molecules and further assembles through the propane diammonium cations and ethanol molecules. The diammonium cations exhibit two hydrogen

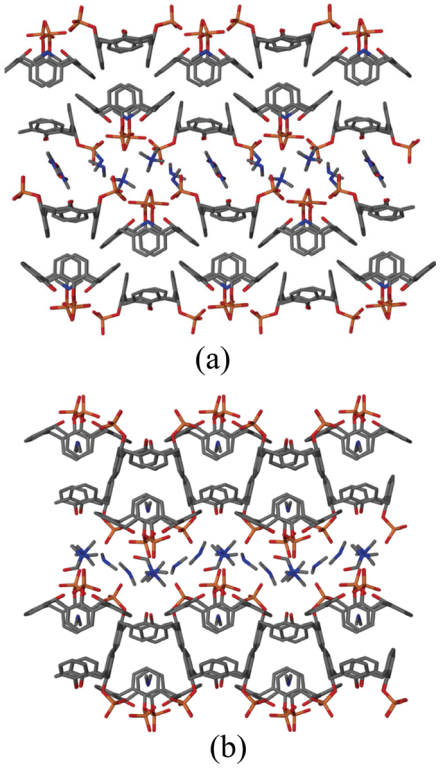

Figure 122. The molecular packing of **L282** complexed with dimethyl ammonium and tetra-methyl ammonium cations: (a) along the *c* axis and (b) along the *b* axis. Blue color shows ammonium cations, and the red color shows the lower rim. Reprinted with permission from ref 219. Copyright 2008 Elsevier.

bonds with the $-OPO(OH)_2$ of one of the triangular units, and by one hydrogen bond to a $-OPO(OH)_2$ of the other subunit.

Therefore, appropriately derivatized calix[4]arne bearing units, which are complementary to the guest species, are developed and studied for their properties. Calix[4]arenes derivatized with dihydroxyphosphate moiety crystallize with several molecular species, and their single crystal X-ray structures have been established.

dx.doi.org/10.1021/cr1004524 |*Chem. Rev.* 2011, 111, 4658–4702

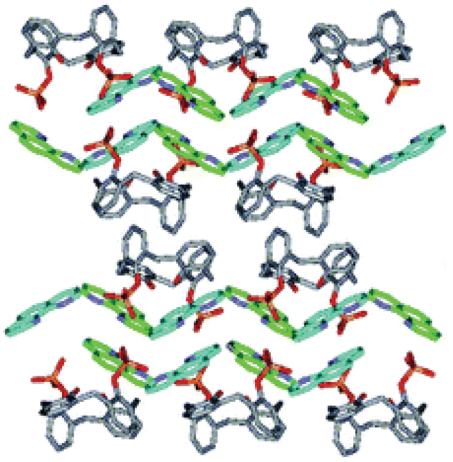

Figure 123. Molecular packing diagram of the complex of **L282** with 1,10-phenanthroline along the *c* axis. Green and blue represent phenonthroline moieties. Reprinted with permission from ref 220. Copyright 2004 The Royal Society of Chemistry.

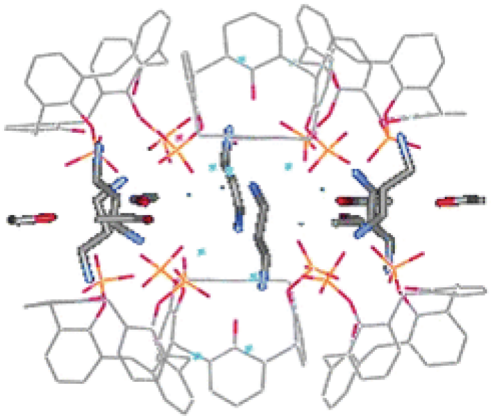

Figure 124. The structural motif is formed by the connection of one hexagonal assembly along the [111] direction to one another via six propane diammonium cations and six ethanol molecules in the hydrophobic zone of **L282**. Reprinted with permission from ref 222. Copyright 2003 The Royal Society of Chemistry.

The structures indicate the formation of suparmolecular assemblies stabilized by hydrogen bonds and π---π interactions.

6. CONCLUSIONS AND FUTURE PERSPECTIVES

It is quite evident from the literature that the functionalized calix[4]arenes are good candidates for the selective recognition of ions and molecular species as concluded and correlated appropriately in each subsection of this Review. This can be achieved by derivatizing these with appropriate functional groups possessing nitrogen, oxygen, or sulfur ligating centers, which in turn provide suitable coordination to different metal ions. The interaction zone should possess moieties such as amide, amine, triazole, nitrile, urea, thiourea, carboxylic acid, phosphine, or metal-based macrocycles, etc., for the recognition of anions. Chiral calix[4]arenes are excellent receptors for the enantioselective detection of amino acids and other chiral species. It has been found from the literature that a preorganized binding core and/or a binding core that can be formed spontaneously in the presence of guest species utilizing the flexibility of the arms is required for the selective detection of ions and molecular species. Various studies in the literature clearly demonstrate that the calix[4]arene is indeed essential for the selective recognition of ions and molecular species, where the sensitivity can be achieved by incorporating appropriate reporter moieties . Generally, it has been found that the variations brought in the spacer length and the changes brought in the electronic environment (with the introduction of withdrawing or donating groups) can alter the selectivity and sensitivity of a receptor toward a particular ion or a molecular species. This will influence the spectral behavior of the receptor molecule and thereby elicit variation in the intensity and/or the wavelength of the absorption or the emission spectral studies.

Thus, this Review clearly explains the inherent advantage of 1,3-diconjugates of calix[4]arene for the same. The conjugates mentioned in this Review showed selectivity toward biologically relevant ions, Zn^{2+}, Ni^{2+}, Cu^{2+}, Fe^{2+}, Fe^{3+}, Ca^{2+}, and Na^{+}, and toxic ions, Cd^{2+}, Hg^{2+}, Pb^{2+}, and Ag^{+}, and few others including lanthanides. The anions and molecular species, halides, acetate, benzoate, phosphate, pyrophosphate, bisulfate, thiocyanate, *N*-tosyl-alanate, dicarboxylate, chromate, pimelate, phosphomonoester, etc., have also been shown to be recognized by 1,3-diconjugates of calix[4]arene. There are some reports in the literature for chiral species as well as amino acid recognition, which were covered in this Review. Because the glyco-calix conjugates are a special kind of hybrid molecules, which are suitable for various biological studies including in the field of lectins and glycosidases, these were not considered in the present Review as the same were reviewed recently.[21,32,33] In the literature, there are several examples of ion and molecular recognition aspects being demonstrated based on the microscopic features of the corresponding nanospecies. These were deliberately avoided from being incorporating in this Review because such studies deserve an independent review on its own. A literature survey performed keeping all these aspects in mind resulted in over 275 conjugates of 1,3-disubstituted calix[4]arene during the past 10 years. Of these, >50% conjugates were found to exhibit metal ion recognition, while ~40% conjugates exhibit anion recognition. The latter one is inclusive of ~10% of chiral recognition systems.

The present Review demonstrates the ion and molecular recognition properties of 1,3-diconjugates of calix[4]arene. These recognitions were carried out in different solvent systems by using various spectroscopy techniques, and in some cases the species of recognition have been demonstrated by single crystal X-ray structure determination and/or by computational modeling studies. Although there are several reports in the literature for the selective detection of cations, the anionic ones are rather limited. This may be attributed to the varied size, shape, and charge characteristics of the anion, which demands higher and specific contacts with the receptor for the recognition, as compared to the almost spherical cationic species. Therefore, much greater efforts are required to develop suitable receptors for anions. Among the cation receptor systems, the receptors for the selective recognition or the extraction of lanthanide and/or toxic ions are rather scarce in the literature, which deserves additional support. Another aspect that requires further attention is the aqueous solubility of calix[4]arene conjugates. Although the host−guest properties of few calix[4]arene conjugates have been studied in the aqueous medium, further demonstrations still await use of these in the area of ion and molecular recognition.

The outcome of such exercise will advent the sensing properties in biological fluids or medium. Although it is possible to demonstrate the ion/molecular recognition properties of a receptor system by several spectroscopy techniques, the exact mode of binding can be obtained only from the single crystal X-ray structures of these complexes. Therefore, additional efforts are required in crystallizing these complex species and studying their structures by single crystal XRD. Higher level computational modeling will be of great advantage where the species of recognition could not be studied by crystal structure due to the lack of the formation of single crystals.

In addition to this, it is possible to build more binding sites on the calix[4]arene platform by introducing various donor groups in the vicinity of the lower rim phenolic group of calix[4]arene to provide higher coordination for lanthanides and other demanding ions. Thus, among the cation receptors, further developments are warranted particularly to take care of the aqueous solubility, large working window for pH, and their utilization in biological and ecological conditions. All of these receptors primarily possesses O- and N-binding centers, but are mostly deprived of carboxylato- and/or thiolato-moieties that may be required to mimic the selective recognition of metal ions by the corresponding apo-proteins. It is hoped that the future literature would carry greater contributions to fulfill these deficiencies. Therefore, the synthesis, characterization, and ion and molecular recognition properties of 1,3-diconjugates of calix[4]arene provide further challenges to the synthetic chemists as well as spectroscopists, because such conjugates not only supply the requisite binding cores but also are flexible enough to accommodate various ions and/or molecular species, which demand diverse features of interactions and geometry. Such study will certainly find a place in the contemporary research on the conjugates of calix[4]arene.

AUTHOR INFORMATION

Corresponding Author

*Phone: +91 22 2576 7162. Fax: +91 22 2572 3480. E-mail: cprao@iitb.ac.in.

BIOGRAPHIES

Roymon Joseph, born in Kerala, India (1980), received his Bachelor's degree (2001) and Master's degree (2003) from St. Berchmans' College Changanacherry affiliated to Mahatma Gandhi University Kottayam, Kerala. He received his doctoral degree from the Indian Institute of Technology Bombay in 2010 under the supervision of Prof. C. P. Rao. His graduate research has focus on the synthesis, characterization, and ion and molecular recognition properties of calix[4]arene conjugates. His Ph.D. thesis was awarded the Excellence in Thesis Work by IIT Bombay and Outstanding Thesis Award by Eli Lilly & Company. Currently he is working as a research associate in the same research group and will be soon moving to the United States as postdoctoral fellow. His research interests are in the area of supramolecular chemistry, ion and molecular recognition, and bioinorganic chemistry.

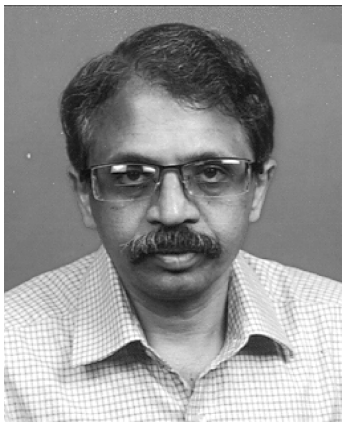

Chebrolu Pulla Rao obtained his Master's degree (1977) from Indian Institute of Technology Madras, and Ph.D. degree (1982) from Indian Institute of Science Bangalore under the joint supervision of Professors C. N. R. Rao and P. Balaram. After one year of Research Associateship with Prof. C. N. R. Rao, he shifted to the research groups of Prof. R. H. Holm at Harvard University (1983−1985), followed by Prof. S. J. Lippard (1986−1987) at Massachusettes Institute of Technology as a postdoctoral fellow. Since 1988, he has been on the Chemistry Faculty at Indian Institute of Technology Bombay and has been a full Professor since 1998. His research interests are broad-based and well extend into the areas of bioinorganic chemistry, including metallation of proteins and glyco-targeting, all using small molecular model systems (viz., calixarenes and carbohydrates) as well as proteins and enzymes, where some of these resulted in the development of ion and molecular sensors as well as materials.

ACKNOWLEDGMENT

C.P.R. acknowledges the financial support by DST, CSIR, and BRNS-DAE. R.J. thanks UGC for his research fellowships. We thank Dr. Amitabha Acharya and Mr. Rakesh Kumar Pathak for some help during the preparation of this Review. We thank all four reviewers and the associate editor for their valuable comments and suggestions.

LIST OF ABBREVIATIONS

ADP	adenosine diphosphate
AFM	atomic force microscopy
AgNP	silver nanoparticles
AMP	adenosine monophosphate
ATP	adenosine triphosphate
BOC	di-*tert*-butyl dicarbanate
BSA	bovine serum albumin
CD	circular dichroism
DFT	density functional theory
DLS	dynamic light scattering

DTPA	diethylenetriamine pentaacetate
EPR	electron paramagnetic resonance
ESI MS	electro spray ionization mass spectrometry
ESIPT	excited-state intramolecular proton transfer
eT	electron transfer
FAB	fast atom bombardment
FRET	fluorescence resonance energy transfer
GMP	guanosine monophosphate
GSH	glutathionine reduced
GSSG	glutathionine oxidized
HEPES	4-(2-hydroxyethyl)-1-piperazineethanesulfonic acid
HSA	human serum albumin
ICT	internal charge transfer
K_a	association constant
K_s	stability constant
LB films	Langmuir−Blodgett film
LMCT	ligand to metal charge transfer
PET	photo electron transfer
ppm	parts per million
QD	quantum dots
SEM	scanning electron microscopy
TBA	tetrabutyl ammonium
TEM	transmission electron microscopy
TGA	thermal gravimetric analysis
XPS	X-ray photoelectron spectra

REFERENCES

(1) Gutsche, C. D. *Calixarenes*; Royal Society of Chemistry: Cambridge, U.K., 1989.

(2) Mandolini, L.; Ungaro, R. *Calixarenes in Action*; Imperical College Press: London, 2000.

(3) Shinkai, S. *Tetrahedron* **1993**, *49*, 8933.

(4) (a) Gutsche, C. D.; Muthukrishnan, R. *J. Org. Chem.* **1978**, *43*, 4905. (b) Gutsche, C. D.; Iqbal, M.; Stewart, D. *J. Org. Chem.* **1986**, *51*, 742.

(5) Vicens, J.; Harrowfield, J. *Calixarenes in the Nanoworld*; Springer: Dordrecht, The Netherlands, 2007.

(6) Dalgarno, S. J.; Thallapally, P. K.; Barbour, L. J.; Atwood, J. L. *Chem. Soc. Rev.* **2007**, *36*, 236.

(7) Ikeda, A.; Shinkai, S. *Chem. Rev.* **1997**, *97*, 1713.

(8) (a) Inokuchi, F.; Miyahara, Y.; Inazu, T.; Shinkai, S. *Angew. Chem., Int. Ed. Engl.* **1995**, *34*, 1364. (b) Ma, J. C.; Dougherty, D. A. *Chem. Rev.* **1997**, *97*, 1303. (c) Ikeda, A.; Tsuzuki, H.; Shinkai, S. *J. Chem. Soc., Perkin Trans. 2* **1994**, 2073.

(9) (a) Bryan, J. C.; Chen, T.; Levitskaia, T. G.; Haverlock, T. J.; Barnes, C. E.; Moyer, B. *J. Inclusion Phenom. Macrocyclic Chem.* **2002**, *42*, 241. (b) Ungaro, R.; Pochini, A.; Andreetti, G. D.; Domiano, P. *J. Chem. Soc., Perkin Trans.* **1985**, 197. (c) Andreetti, G. D.; Ungaro, R.; Pochini, A. *J. Chem. Soc., Chem. Commun.* **1979**, 1005.

(10) (a) Liu, L.; Zakharov, L. N.; Golen, J. A.; Rheingold, A. L.; Watson, W. H.; Hanna, T. A. *Inorg. Chem.* **2006**, *45*, 4247. (b) Haddadi, H.; Alizadeh, N.; Shamsipur, M.; Asfari, Z.; Lippolis, V.; Bazzicalupi, C. *Inorg. Chem.* **2010**, *49*, 6874. (c) Vigalok, A.; Zhu, Z.; Swager, T. M. *J. Am. Chem. Soc.* **2001**, *123*, 7917. (d) Giannini, L.; Caselli, A.; Solari, E.; Floriani, C.; Chiesi-Villa, A.; Rizzoli, C.; Re, N.; Sgamellotti, A. *J. Am. Chem. Soc.* **1997**, *119*, 9198. (e) Hascall, T.; Pang, K.; Parkin, G. *Tetrahedron* **2007**, *63*, 10826.

(11) (a) Atwood, J. L.; Barbour, L. J.; Jerga, A.; Schottel, B. L. *Science* **2002**, *298*, 1000. (b) Ananchenko, G. S.; Udachin, K. A.; Dubes, A.; Ripmeester, J. A.; Perrier, T.; Coleman, A. W. *Angew. Chem., Int. Ed.* **2006**, *45*, 1585. (c) Ananchenko, G. S.; Udachin, K. A.; Ripmeester, J. A.; Perrier, T.; Coleman, A. W. *Chem.-Eur. J.* **2006**, *12*, 2441. (d) Dubes, A.; Udachin, K. A.; Shahgaldian, P.; Lazar, A. N.; Coleman, A. W.; Ripmeester, J. A. *New J. Chem.* **2005**, *29*, 1141. (e) Pojarova, M.; Ananchenko, G. S.; Udachin, K. A.; Perret, F.; Coleman, A. W.; Ripmeester, J. A. *New J. Chem.* **2007**, *31*, 871. (f) Ananchenko, G. S.; Udachin, K. A.; Pojarova, M.; Dubes, A.; Ripmeester, J. A.; Jebors, S.; Coleman, A. W. *Cryst. Growth Des.* **2006**, *6*, 2141.

(12) (a) Gutsche, C. D. *Acc. Chem. Res.* **1983**, *16*, 161. (b) Gutsche, C. D.; Dhawan, B.; Levine, J. A.; No, K. H.; Bauer, L. J. *Tetrahedron* **1983**, *39*, 409.

(13) (a) Oueslati, I.; Abidi, R.; Amri, H.; Thuery, P.; Nierlich, M.; Asfari, Z.; Harrowfield, J.; Vicens, J. *Tetrahedron Lett.* **2000**, *41*, 8439. (b) Shinkai, S.; Fujimoto, K.; Otsuka, T.; Ammon, H. L. *J. Org. Chem.* **1992**, *57*, 1516. (c) Beer, P. D.; Drew, M. G. B.; Gale, P. A.; Leeson, P, B.; Ogden, M. I. *J. Chem. Soc., Dalton Trans.* **1994**, 3479. (d) Dijkstra, P. J.; Brunink, J. A. J.; Bugge, K.-E.; Reinhoudt, D. N.; Harkema, S.; Ungaro, R.; Ugozzoli, F.; Ghidini, E. *J. Am. Chem. Soc.* **1989**, *111*, 7567.

(14) Vicens, J.; Bohmer, V. *Calixarenes, a Versatile Class of Macrocyclic Compounds*; Kluwer Academic Publishers: Dordrecht, The Netherlands, 1991.

(15) (a) Iwamoto, K.; Shinkai, S. *J. Org. Chem.* **1992**, *57*, 7066. (b) Sharma, S. K.; Gutsche, C. D. *Tetrahedron* **1994**, *50*, 4087.

(16) Bohmer, V.; Ferguson, G.; Gallagher, J. F.; Lough, A. J.; McKervey, A.; Madigan, E.; Moran, M. B.; Phillips, J.; Williams, G. *J. Chem. Soc., Perkin Trans. 1* **1993**, 1521.

(17) Collins, E. M.; McKervey, M. A.; Madigan, E.; Moran, M. B.; Owens, M.; Ferguson, G.; Harris, S. J. *J. Chem. Soc., Perkin Trans. 1* **1991**, 3137.

(18) Kim, J. S.; Quang, D. T. *Chem. Rev.* **2007**, *107*, 3780.

(19) Creaven, B. S.; Donlon, D. F.; McGinley, J. *Coord. Chem. Rev.* **2009**, *253*, 893.

(20) Gutsche, C. D. In *Calixarenes Revisited, Monographs in Supramolecular Chemistry*; Stoddart, J. F., Ed.; Royal Society of Chemistry: Cambridge, UK, 1998; Vol. 1.

(21) Dondoni, A.; Marra, A. *Chem. Rev.* **2010**, *110*, 4949.

(22) Bohmer, V. *Angew. Chem., Int. Ed. Engl.* **1995**, *34*, 713.

(23) Rao, C. P.; Dey, M. *Encycl. Nanosci. Nanotechnol.* **2004**, *1*, 475.

(24) Leray, I.; Valeur, B. *Eur. J. Inorg. Chem.* **2009**, 3525.

(25) Valeur, B.; Leray, I. *Coord. Chem. Rev.* **2000**, *205*, 3.

(26) Valeur, B.; Leray, I. *Inorg. Chim. Acta* **2007**, *360*, 765.

(27) Perret, F.; Lazar, A. N.; Coleman, A. W. *Chem. Commun.* **2006**, 2425.

(28) Sliwa, W. *J. Inclusion Phenom. Macrocyclic Chem.* **2005**, *52*, 13.

(29) Beer, P. D. *Acc. Chem. Res.* **1998**, *31*, 71.

(30) Homden, D. M.; Redshaw, C. *Chem. Rev.* **2008**, *108*, 5086.

(31) Molenveld, P.; Engbersen, J. F. J.; Reinhoudt, D. N. *Chem. Soc. Rev.* **2000**, *29*, 75.

(32) Casnati, A.; Sansone, F.; Ungaro, R. *Acc. Chem. Res.* **2003**, *36*, 246.

(33) Baldini, L.; Casnati, A.; Sansone, F.; Ungaro, R. *Chem. Soc. Rev.* **2007**, *36*, 254.

(34) (a) Luo, H.; Dai, S.; Bonnesen, P. V.; Buchanan, A. C.; Holbrey, J. D.; Bridges, N. J.; Rogers, R. D. *Anal. Chem.* **2004**, *76*, 3078. (b) Casnati, A.; Barboso, S.; Rouquette, H.; Schwing-Weill, M.-J.; Arnaud-Neu, F.; Dozol, J.-F.; Ungaro, R. *J. Am. Chem. Soc.* **2001**, *123*, 12182.

(35) Iqbal, K. S. J.; Cragg, P. J. *Dalton Trans.* **2007**, 26.

(36) Sameni, S.; Jeunesse, C.; Matt, D.; Harrowfield, J. *Chem. Soc. Rev.* **2009**, *38*, 2117.

(37) de Silva, A. P.; Gunaratne, H. Q. N.; Gunnlaugsson, T.; Huxley, A. J. M.; McCoy, C. P.; Rademacher, J. T.; Rice, T. E. *Chem. Rev.* **1997**, *97*, 1515.

(38) Maes, W.; Dehaen, W. *Chem. Soc. Rev.* **2008**, *37*, 2393.

(39) Ibach, S.; Prautzsch, V.; Vogtle, F. *Acc. Chem. Res.* **1999**, *32*, 729.

(40) Harvey, P. D. *Coord. Chem. Rev.* **2002**, *233*, 289.

(41) Redshaw, C. *Coord. Chem. Rev.* **2003**, *244*, 45.

(42) Atwood, J. L.; Barbour, L. J.; Hardie, M. J.; Raston, C. L. *Coord. Chem. Rev.* **2001**, *222*, 3.

(43) Danil de Namor, A. F. *Coord. Chem. Rev.* **1999**, *190*, 283.

(44) Wieser, C.; Dieleman, C. B.; Matt, D. *Coord. Chem. Rev.* **1997**, *165*, 93.

(45) (a) Hansch, R.; Mendel, R. R. *Curr. Opin. Plant Biol.* **2009**, *12*, 259. (b) Finney, L. A.; O'Halloran, T. V. *Science* **2003**, *300*, 931. (c) Feinberg, H.; Greenblatt, H. M.; Shoham, G. *J. Chem. Inf. Comput. Sci.* **1993**, *33*, 501. (d) Linder, M. C.; Hazegh-Azam, M. *Am. J. Clin. Nutr.* **1996**, *63*, 797S. (e) Holm, R. H.; Kennepohl, P.; Solomon, E. I. *Chem. Rev.* **1996**, *96*, 2239.(f) Lippard, S. J.; Berg, J. M. *Principles of Bioinorganic Chemistry*; University Science Books: Mill Valley, CA, 1994. (g) Thiele, D. J. *J. Nutr.* **2003**, *133*, 1579S. (h) Bott, A. W. *Curr. Sep.* **1999**, *18*, 47.

(46) (a) Chakrabarti, P. *J. Mol. Biol.* **1993**, *234*, 463. (b) Miller, C. *Nature* **2006**, *440*, 484. (c) Burkhard, P.; Tai, C.-H.; Jansonius, J. N.; Cook, P. F. *J. Mol. Biol.* **2000**, *303*, 279. (d) Kubik, S.; Reyheller, C.; Stuwe, S. *J. Inclusion Phenom. Macrocyclic Chem.* **2005**, *52*, 137. (e) Burlingham, B. T.; Widlanski, T. S. *J. Org. Chem.* **2001**, *66*, 7561. (f) Gettins, P.; Coleman, J. E. *J. Biol. Chem.* **1984**, *259*, 11036.

(47) (a) Nelson, D.; Cox, M. M. *Principles of Biochemistry*, 4th ed.; W. H. Freeman: New York, 2004. (b) Voet, D.; Voet, J. *Biochemistry*, 3rd ed.; John Wiley & Sons: New York, 2004.

(48) (a) Mercer, J. F. B. *Trends Mol. Med.* **2001**, *7*, 64. (b) Hambidge, M. *J. Nutr.* **2000**, *130*, 1344S. (c) Krupanidhi, S.; Sreekumar, A.; Sanjeevi, C. B. *Indian J. Med. Res.* **2008**, *128*, 448. (d) Scheinberg, I. H.; Sternlieb, I. *Am. J. Clin. Nutr.* **1996**, *63*, 842S. (e) Siah, C. W.; Trinder, D.; Olynyk, J. K. *Clin. Chim. Acta* **2005**, *358*, 24. (f) Gao, X.; Campian, J. L.; Qian, M.; Sun, X.-F.; Eaton, J. W. *J. Biol. Chem.* **2009**, *284*, 4767.

(49) (a) Jones, C. M.; Worthington, H. *J. Dent.* **2000**, *28*, 389. (b) Zimmermann, M. B. *J. Trace Elem. Med. Biol.* **2008**, *22*, 81.

(50) (a) Heafield, M. T.; Fearn, S.; Steventon, G. B.; Waring, R. H.; Williams, A. C.; Sturman, S. G. *Neurosci. Lett.* **1990**, *110*, 216. (b) Puka-Sundvall, M.; Eriksson, P.; Nilsson, M.; Sandberg, M.; Lehmann, A. *Brain Res.* **1995**, *705*, 65.

(51) (a) Nolan, E. M.; Lippard, S. J. *Chem. Rev.* **2008**, *108*, 3443. (b) Mushtakova, V. M.; Fomina, V. A.; Rogovin, V. V. *Biol Bull.* **2005**, *32*, 276.

(52) (a) Dietrich, B. *Pure Appl. Chem.* **1993**, *65*, 1457.(b) Sessler, J. L.; Gale, P. A.; Cho, W.-S. *Anion Receptor Chemistry*; Royal Society of Chemistry: Cambridge, 2006.

(53) (a) Sessler, J. L.; Camiolo, S.; Gale, P. A. *Coord. Chem. Rev.* **2003**, *240*, 17. (b) Atwood, J. L.; Holman, K. T.; Steed, J. W. *Chem. Commun.* **1996**, 1401. (c) Llinares, J. M.; Powell, D.; Bowman-James, K. *Coord. Chem. Rev.* **2003**, *240*, 57. (d) Best, M. D.; Tobey, S. L.; Anslyn, E. V. *Coord. Chem. Rev.* **2003**, *240*, 3. (e) Gale, P. A.; Quesada, R. *Coord. Chem. Rev.* **2006**, *250*, 3219.

(54) (a) Saelensminde, G.; Halskau, O.; Jonassen, I. *Extremophiles* **2009**, *13*, 11. (b) Mitchell, J. B. O.; Nandi, C. L.; McDonald, I. K.; Thornton, J. M. *J. Mol. Biol.* **1994**, *239*, 315. (c) Kruppa, M.; Konig, B. *Chem. Rev.* **2006**, *106*, 3520.

(55) (a) Duke, R. M.; Veale, E. B.; Pfeffer, F. M.; Kruger, P. E.; Gunnlaugsson, T. *Chem. Soc. Rev.* **2010**, *39*, 3936. (b) Martinez-Manez, R.; Sancenon, F. *Chem. Rev.* **2003**, *103*, 4419. (c) Gale, P. A. *Coord. Chem. Rev.* **2003**, *240*, 191. (d) Hembury, G. A.; Borovkov, V. V.; Inoue, Y. *Chem. Rev.* **2008**, *108*, 1. (e) Zhang, X. X.; Bradshaw, J. S.; Izatt, R. M. *Chem. Rev.* **1997**, *97*, 3313. (f) Pu, L. *Chem. Rev.* **2004**, *104*, 1687.

(56) (a) Beer, P. D.; Gale, P. A.; Chen, Z.; Drew, M. G. B.; Heath, J. A.; Ogden, M. I.; Powell, H. R. *Inorg. Chem.* **1997**, *36*, 5880. (b) Gbidini, E.; Ugozzoli, F.; Ungaro, R.; Harkema, S.; El-Fadl, A. A.; Reinhoudt, D. N. *J. Am. Chem. Soc.* **1900**, *112*, 6979. (c) Casnati, A.; Pochini, A.; Ungaro, R.; Ugozzoli, F.; Arnaud, F.; Fanni, S.; Schwing, M.-J.; Egberink, R. J. M.; de Jong, F.; Reinhoud, D. N. *J. Am. Chem. Soc.* **1995**, *117*, 2767.

(57) (a) Mahon, M. F.; McGinley, J.; Rooney, A. D.; Walsh, J. M. D. *Tetrahedron* **2008**, *64*, 11058. (b) Sun, J.; Liu, D. M.; Wang, J. X.; Yan, C. G. *J. Inclusion Phenom. Macrocyclic Chem.* **2009**, *64*, 317.

(58) Arnaud-Neu, F.; Collins, E. M.; Deasy, M.; Ferguson, G.; Harris, S. J.; Kaitner, B.; Lough, A. J.; McKervey, M. A.; Marques, E.; Ruhl, B. L.; Schwing-Weill, M. J.; Seward, E. M. *J. Am. Chem. Soc.* **1989**, *111*, 8681.

(59) Zhang, W.-C.; Huang, Z.-T. *Synthesis* **1997**, 1073.

(60) (a) Al-Saraierh, H.; Miller, D. O.; Georghiou, P. E. *J. Org. Chem.* **2005**, *70*, 8273. (b) Bukhaltsev, E.; Goldberg, I.; Cohen, R.; Vigalok, A. *Organometallics* **2007**, *26*, 4015. (c) Tzadka, E.; Goldberg, I.; Vigalok, A. *Chem. Commun.* **2009**, 2041.

(61) Chowdhury, S.; Georghiou, P. E. *J. Org. Chem.* **2001**, *66*, 6257.

(62) Ohseto, F.; Murakami, H.; Araki, K.; Shinkai, S. *Tetrahedron Lett.* **1992**, *33*, 1217.

(63) Bitter, I.; Grun, A.; Toth, G.; Balazs, B.; Toke, L. *Tetrahedron* **1997**, *53*, 9799.

(64) (a) Tomapatanaget, B.; Pulpoka, B.; Tuntulani, T. *Chem. Lett.* **1998**, 1037. (b) Kraft, D.; van Loon, J.-D.; Owens, M.; Ver-boom, W.; Vogt, W.; McKervey, M. A.; Bohmer, V.; Reinhoudt, D. N. *Tetrahedron Lett.* **1990**, *31*, 4941.

(65) Calvo-Flores, F. G.; Isac-Garcia, J.; Hernandez-Mateo, F.; Perez-Balderas, F.; Calvo-Asin, J. A.; Sanchez-Vaquero, E.; Santoyo-Gonzalez, F. *Org. Lett.* **2000**, *2*, 2499.

(66) Kumar, A.; Ali, A.; Rao, C. P. *J. Photochem. Photobiol., A* **2006**, *177*, 164.

(67) Dessingou, J.; Joseph, R.; Rao, C. P. *Tetrahedron Lett.* **2005**, *46*, 7967.

(68) Dey, M.; Rao, C. P.; Guionneau, P. *Inorg. Chem. Commun.* **2005**, *8*, 998.

(69) Dey, M.; Chinta, J. P.; Long, G. J.; Rao, C. P. *Indian J. Chem., Sect. A* **2009**, *48A*, 1484.

(70) Joseph, R.; Chinta, J. P.; Rao, C. P. *J. Org. Chem.* **2010**, *75*, 3387.

(71) Pathak, R. K.; Ibrahim, S. M.; Rao, C. P. *Tetrahedron Lett.* **2009**, *50*, 2730.

(72) Park, S. Y.; Yoon, J. H.; Hong, C. S.; Souane, R.; Kim, J. S.; Matthews, S. E.; Vicens, J. *J. Org. Chem.* **2008**, *73*, 8212.

(73) Dey, M.; Rao, C. P.; Saarenketo, P.; Rissanen, K.; Kolehmainen, E. *Eur. J. Inorg. Chem.* **2002**, 2207.

(74) Pathak, R. K.; Dikundwar, A. G.; Row, T. N. G.; Rao, C. P. *Chem. Commun.* **2010**, *46*, 4345.

(75) Bagatin, I. A.; de Souza, E. S.; Ito, A. S.; Toma, H. E. *Inorg. Chem. Commun.* **2003**, *6*, 288.

(76) Zhang, J. F.; Bhuniya, S.; Lee, Y. H.; Bae, C.; Lee, J. H.; Kim, J. S. *Tetrahedron Lett.* **2010**, *51*, 3719.

(77) Joseph, R.; Ramanujam, B.; Pal, H.; Rao, C. P. *Tetrahedron Lett.* **2008**, *49*, 6257.

(78) Unob, F.; Asfari, Z.; Vicens, J. *Tetrahedron Lett.* **1998**, *39*, 2951.

(79) Kim, H. J.; Kim, S. H.; Kim, J. H.; Anh, L. N.; Lee, J. H.; Lee, C.-H.; Kim, J. S. *Tetrahedron Lett.* **2009**, *50*, 2782.

(80) Banthia, S.; Samanta, A. *Org. Biomol. Chem.* **2005**, *3*, 1428.

(81) Oueslati, I.; Thuery, P.; Shkurenko, O.; Suwinska, K.; Harrowfield, J. M.; Abidi, R.; Vicens, J. *Tetrahedron* **2007**, *63*, 62.

(82) Xu, Z.; Kim, S.; Kim, H. N.; Han, S. J.; Lee, C.; Kim, J. S.; Qian, X.; Yoon, J. *Tetrahedron Lett.* **2007**, *48*, 9151.

(83) Ashram, M. *J. Chem. Soc., Perkin Trans. 2* **2002**, 1662.

(84) Chang, K.-C.; Luo, L.-Y.; Diau, E. W.-G.; Chung, W.-S. *Tetrahedron Lett.* **2008**, *49*, 5013.

(85) Senthilvelan, A.; Ho, I.-T.; Chang, K.-C.; Lee, G.-H.; Liu, Y.-H.; Chung, W.-S. *Chem.-Eur. J.* **2009**, *15*, 6152.

(86) Psychogios, N.; Regnouf-de-Vains, J.-B. *Tetrahedron Lett.* **2001**, *42*, 2799.

(87) Psychogios, N.; Regnouf-de-Vains, J.-B.; Stoeckli-Evans, H. M. *Eur. J. Inorg. Chem.* **2004**, 2514.

(88) Liu, J.-M.; Zheng, Q.-Y.; Yang, J.-L.; Chen, C.-F.; Huang, Z.-T. *Tetrahedron Lett.* **2002**, *43*, 9209.

(89) Joseph, R.; Chinta, J. P.; Rao, C. P. *Inorg. Chim. Acta* **2010**, *363*, 2833.

(90) Joseph, R.; Ramanujam, B.; Acharya, A.; Rao, C. P. *Tetrahedron Lett.* **2009**, *50*, 2735.

(91) Joseph, R.; Ramanujam, B.; Acharya, A.; Rao, C. P. *J. Org. Chem.* **2009**, *74*, 8181.

(92) Bodenant, B.; Weil, T.; Businelli-Pourcel, M.; Fages, F.; Barbe, B.; Pianet, I.; Laguerre, M. *J. Org. Chem.* **1999**, *64*, 7034.

(93) Gruber, T.; Fischer, C.; Felsmann, M.; Seichter, W.; Weber, E. *Org. Biomol. Chem.* **2009**, *7*, 4904.

(94) Kim, H. J.; Quang, D. T.; Hong, J.; Kang, G.; Ham, S.; Kim, J. S. *Tetrahedron* **2007**, *63*, 10788.

(95) Choi, M. J.; Kim, M. Y.; Chang, S.-K. *Chem. Commun.* **2001**, 1664.

(96) Chawla, H. M.; Singh, S. P.; Upreti, S. *Tetrahedron* **2006**, *62*, 9758.
(97) Chen, Q.-Y.; Chen, C.-F. *Tetrahedron Lett.* **2005**, *46*, 165.
(98) Kim, J. H.; Hwang, A.-R.; Chang, S.-K. *Tetrahedron Lett.* **2004**, *45*, 7557.
(99) Cha, N. R.; Kim, M. Y.; Kim, Y. H.; Choe, J.-I.; Chang, S.-K. *J. Chem. Soc., Perkin Trans. 2* **2002**, 1193.
(100) Joseph, R.; Ramanujam, B.; Acharya, A.; Khutia, A.; Rao, C. P. *J. Org. Chem.* **2008**, *73*, 5745.
(101) Colleran, J. J.; Creaven, B. S.; Donlon, D. F.; McGinley, J. *Dalton Trans.* **2010**, *39*, 10928.
(102) Talanova, G. G.; Elkarim, N. S. A.; Talanov, V. S.; Bartsch, R. A. *Anal. Chem.* **1999**, *71*, 3106.
(103) Métivier, R.; Leray, I.; Valeur, B. *Chem.-Eur. J.* **2004**, *10*, 4480.
(104) Métivier, R.; Leray, I.; Valeur, B. M. *Photochem. Photobiol. Sci.* **2004**, *3*, 374.
(105) Ocak, U.; Ocak, M.; Surowiec, K.; Bartsch, R. A.; Gorbunova, M. G.; Tu, C.; Surowiec, M. A. *J. Inclusion Phenom. Macrocyclic Chem.* **2009**, *63*, 131.
(106) Metivier, R.; Leray, I.; Lebeau, B.; Valeur, B. *J. Mater. Chem.* **2005**, *15*, 2965.
(107) Danil de Namor, A. F.; Chahine, S.; Castellano, E. E.; Piro, O. E. *J. Phys. Chem. A* **2005**, *109*, 6743.
(108) Danil de Namor, A. F.; Chahine, S.; Castellano, E. E.; Piroc, O. E.; Brooke, H. D. J. *Chem. Commun.* **2005**, 3844.
(109) Li, H.; Zhang, Y.; Wang, X.; Xiong, D.; Bai, Y. *Mater. Lett.* **2007**, *61*, 1474.
(110) Lu, J.; He, X.; Zeng, X.; Wan, Q.; Zhang, Z. *Talanta* **2003**, *59*, 553.
(111) Liu, Y.; Zhao, B.-T.; Chen, L.-X.; He, X.-W. *Microchem. J.* **2000**, *65*, 75.
(112) Tian, D.; Yan, H.; Li, H. *Supramol. Chem.* **2010**, *22*, 249.
(113) Joseph, R.; Gupta, A.; Rao, C. P. *J. Photochem. Photobiol., A* **2007**, *188*, 325.
(114) Othman, A. B.; Lee, J. W.; Wu, J.-S.; Kim, J. S.; Abidi, R.; Thuery, P.; Strub, J. M.; Van Dorsselaer, A.; Vicens, J. *J. Org. Chem.* **2007**, *72*, 7634.
(115) Zhan, J.; Tian, D.; Li, H. *New J. Chem.* **2009**, *33*, 725.
(116) Halouani, H.; Dumazet-Bonnamour, I.; Perrin, M.; Lamartine, R. *J. Org. Chem.* **2004**, *69*, 6521.
(117) Liu, Y.; Zhao, B.-T.; Zhang, H.-Y.; Ju, H.-F.; Chen, L.-X.; He, X.-W. *Helv. Chim. Acta* **2001**, *84*, 1969.
(118) Chen, L.; Zhang, J.; Zhao, W.; He, X.; Liu, Y. *J. Electroanal. Chem.* **2006**, *589*, 106.
(119) Kim, S. K.; Kim, S. H.; Kim, H. J.; Lee, S. H.; Lee, S. W.; Ko, J.; Bartsch, R. A.; Kim, J. S. *Inorg. Chem.* **2005**, *44*, 7866.
(120) Singh, N.; Kumar, M.; Hundal, G. *Tetrahedron* **2004**, *60*, 5393.
(121) Regnouf-de-Vains, J.-B.; Dalbavie, J.-O.; Lamartine, R.; Fenet, B. *Tetrahedron Lett.* **2001**, *42*, 2681.
(122) Zeng, X.; Weng, L.; Chen, L.; Leng, X.; Zhang, Z.; He, X. *Tetrahedron Lett.* **2000**, *41*, 4917.
(123) Zeng, X.; Weng, L.; Chem, L.; Xu, F.; Li, Q.; Leng, X.; He, X.; Zhang, Z.-Z. *Tetrahedron* **2002**, *58*, 2647.
(124) Zeng, X.; Sun, H.; Chen, L.; Leng, X.; Xu, F.; Li, Q.; He, X.; Zhang, W.; Zhang, Z.-Z. *Org. Biomol. Chem.* **2003**, *1*, 1073.
(125) Zeng, X.; Weng, L.; Chen, L.; Leng, X.; Ju, H.; He, X.; Zhang, Z.-Z. *J. Chem. Soc., Perkin Trans. 2* **2001**, 545.
(126) Lu, J.-Q.; Pang, D.-W.; Zeng, X.-S.; He, X.-W. *J. Electroanal. Chem.* **2004**, *568*, 37.
(127) Xie, J.; Zheng, Q.-Y.; Zheng, Y.-S.; Chen, C.-F.; Huang, Z.-T. *J. Inclusion Phenom. Macrocyclic Chem.* **2001**, *40*, 125.
(128) Creaven, B. S.; Deasy, M.; Flood, P. M.; McGinley, J.; Murray, B. A. *Inorg. Chem. Commun.* **2008**, *11*, 1215.
(129) Kumar, M.; Mahajan, R. K.; Sharma, V.; Singh, H.; Sharma, N.; Kaur, I. *Tetrahedron Lett.* **2001**, *42*, 5315.
(130) Othman, A. B.; Lee, J. W.; Huh, Y.-D.; Abidi, R.; Kim, J. S.; Vicens, J. *Tetrahedron* **2007**, *63*, 10793.
(131) Sirit, A.; Kocabas, E.; Memon, S.; Karakucuk, A.; Yilmaz, M. *Supramol. Chem.* **2005**, *17*, 251.
(132) Rojanathanes, R.; Pipoosananakaton, B.; Tuntulani, T.; Bhanthumnavin, W.; Orton, J. B.; Cole, S. J.; Hursthouse, M. B.; Grossel, M. C.; Sukwattanasinitt, M. *Tetrahedron* **2005**, *61*, 1317.
(133) Marchand, A. P.; Chong, H.-S.; Kumar, T. P.; Huang, Z.; Alihodzic, S.; Watson, W. H.; Ejsmont, K. *Tetrahedron* **2002**, *58*, 10205.
(134) Ji, H.-F.; Dabestani, R.; Brown, G. M. *J. Am. Chem. Soc.* **2000**, *122*, 9306.
(135) Kerdpaiboon, N.; Tomapatanaget, B.; Chailapakul, O.; Tuntulani, T. *J. Org. Chem.* **2005**, *70*, 4797.
(136) Tantrakarn, K.; Ratanatawanate, C.; Pinsuk, T.; Chailapakul, O.; Tuntulani, T. *Tetrahedron Lett.* **2003**, *44*, 33.
(137) Webber, P. R. A.; Cowley, A.; Beer, P. D. *Dalton Trans.* **2003**, 3922.
(138) Webber, P. R. A.; Chen, G. Z.; Drew, M. G. B.; Beer, P. D. *Angew. Chem., Int. Ed.* **2001**, *40*, 2265.
(139) Webber, P. R. A.; Beer, P. D.; Chen, G. Z.; Felix, V.; Drew, M. G. B. *J. Am. Chem. Soc.* **2003**, *125*, 5774.
(140) Marchand, A. P.; Chong, H.-S.; Takhi, M.; Power, T. D. *Tetrahedron* **2000**, *56*, 3121.
(141) Liu, Y.; Wang, H.; Wang, L.-H.; Li, Z.; Zhang, H.-Y.; Zhang, Q. *Tetrahedron* **2003**, *59*, 7967.
(142) He, X.; Lam, W. H.; Zhu, N.; Yam, V. W.-W. *Chem.-Eur. J.* **2009**, *15*, 8842.
(143) Tabakci, M.; Memon, S.; Yilmaz, M.; Roundhill, D. M. *J. Inclusion Phenom. Macrocyclic Chem.* **2003**, *45*, 265.
(144) Li, H.; Zhan, J.; Chen, M.; Tian, D.; Zou, Z. *J. Inclusion Phenom. Macrocyclic Chem.* **2010**, *66*, 43.
(145) Danil de Namor, A. F.; Chaaban, J. K.; Abbas, I. *J. Phys. Chem. A* **2006**, *110*, 9575.
(146) De Namor, A. F. D.; Aparicio-Aragon, W. B.; Goitia, M. T.; Casal, A. R. *Supramol. Chem.* **2004**, *16*, 423.
(147) Chen, Y.-J.; Chung, W.-S. *Eur. J. Org. Chem.* **2009**, 4770.
(148) Chang, K.-C.; Su, I.-H.; Lee, G.-H.; Chung, W.-S. *Tetrahedron Lett.* **2007**, *48*, 7274.
(149) Chang, K.-C.; Su, I.-H.; Wang, Y.-Y.; Chung, W.-S. *Eur. J. Org. Chem.* **2010**, 4700.
(150) Chung, T. D.; Park, J.; Kim, J.; Lim, H.; Choi, M.-J.; Kim, J. R.; Chang, S.-K.; Kim, H. *Anal. Chem.* **2001**, *73*, 3975.
(151) Liu, Z.; Jiang, L.; Liang, Z.; Gao, Y. *Tetrahedron Lett.* **2005**, *46*, 885.
(152) Liu, Y.; Zhao, B.-T.; Zhang, H.-Y.; Wada, T.; Inoue, Y. *J. Chem. Soc., Perkin Trans. 2* **2001**, 1219.
(153) Bagatin, I. A.; Toma, H. E. *New J. Chem.* **2000**, *24*, 841.
(154) Hao, W.; Heng-Yi, Z.; Yu, L. *Chin. J. Chem.* **2005**, *23*, 740.
(155) Jurecka, P.; Vojtísek, P.; Novotný, K.; Rohovec, J.; Lukes, I. *J. Chem. Soc., Perkin Trans. 2* **2002**, 1370.
(156) Leydier, A.; Lecercle, D.; Pellet-Rostaing, S.; Favre-Reguillon, A.; Taran, F.; Lemaire, M. *Tetrahedron* **2008**, *64*, 11319.
(157) Beer, P. D.; Brindley, G. D.; Fox, O. D.; Grieve, A.; Ogden, M. I.; Szemes, F.; Drew, M. G. B. *J. Chem. Soc., Dalton Trans.* **2002**, 3101.
(158) Brindley, G. D.; Fox, O. D.; Beer, P. D. *J. Chem. Soc., Dalton Trans.* **2000**, 4354.
(159) Evans, C. J.; Nicholson, G. P. *Sens. Actuators, B* **2005**, *105*, 204.
(160) Beer, P. D.; Szemes, F.; Passaniti, P.; Maestri, M. *Inorg. Chem.* **2004**, *43*, 3965.
(161) Lin, Y.; Leydier, A.; Metay, E.; Favre-Reguillon, A.; Bouchu, D.; Pellet-Rostaing, S.; Lemaire, M. *J. Inclusion Phenom. Macrocyclic Chem.* **2008**, *61*, 187.
(162) Fischer, C.; Sarti, G.; Casnati, A.; Carrettoni, B.; Manet, I.; Schuurman, R.; Guardigli, M.; Sabbatini, N.; Ungaro, R. *Chem.-Eur. J.* **2000**, *6*, 1026.
(163) Jung, H. S.; Kim, H. J.; Vicens, J.; Kim, J. S. *Tetrahedron Lett.* **2009**, *50*, 983.
(164) Lee, S. H.; Kim, H. J.; Lee, Y. O.; Vicens, J.; Kim, J. S. *Tetrahedron Lett.* **2006**, *47*, 4373.

(165) Kim, H. J.; Kim, S. K.; Lee, J. Y.; Kim, J. S. *J. Org. Chem.* **2006**, *71*, 6611.
(166) Chawla, H. M.; Shrivastava, R.; Sahu, S. N. *New J. Chem.* **2008**, *32*, 1999.
(167) Nam, K. C.; Kang, S. O.; Ko, S. W. *Bull. Korean Chem. Soc.* **1999**, *20*, 953.
(168) Lee, H. K.; Yeo, H.; Park, D. H.; Jeon, S. *Bull. Korean Chem. Soc.* **2003**, *24*, 1737.
(169) McConnell, A. J.; Serpell, C. J.; Thompson, A. L.; Allan, D. R.; Beer, P. D. *Chem.-Eur. J.* **2010**, *16*, 1256.
(170) Lankshear, M. D.; Dudley, I. M.; Chan, K.-M.; Cowley, A. R.; Santos, S. M.; Felix, V.; Beer, P. D. *Chem.-Eur. J.* **2008**, *14*, 2248.
(171) Lankshear, M. D.; Cowley, A. R.; Beer, P. D. *Chem. Commun.* **2006**, 612.
(172) Morales-Sanfrutos, J.; Ortega-Munoz, M.; Lopez-Jaramillo, J.; Hernandez-Mateo, F.; Santoyo-Gonzalez, F. *J. Org. Chem.* **2008**, *73*, 7768.
(173) Joseph, R.; Gupta, A.; Rao, C. P. *Indian J. Chem., Sect. A* **2007**, *46*, 1095.
(174) Bozkurt, S.; Karakucuk, A.; Sirit, A.; Yilmaz, M. *Tetrahedron* **2005**, *61*, 10443.
(175) Yilmaz, A.; Tabakci, B.; Akceylan, E.; Yilmaz, M. *Tetrahedron* **2007**, *63*, 5000.
(176) Jeong, H.; Choi, E. M.; Kang, S. O.; Nam, K. C.; Jeon, S. *J. Electroanal. Chem.* **2000**, *485*, 154.
(177) Nam, K. C.; Kang, S. O.; Jeong, H. S.; Jeon, S. *Tetrahedron Lett.* **1999**, *40*, 7343.
(178) Kang, S. O.; Oh, J. M.; Yang, Y. S.; Chun, J. C.; Jeon, S.; Nam, K. C. *Bull. Korean Chem. Soc.* **2002**, *23*, 145.
(179) Chawla, H. M.; Sahu, S. N.; Shrivastava, R. *Tetrahedron Lett.* **2007**, *48*, 6054.
(180) Sdira, S. B.; Felix, C.; Giudicelli, M.-B.; Vocanson, F.; Perrin, M.; Lamartine, R. *Tetrahedron Lett.* **2005**, *46*, 5659.
(181) Metay, E.; Duclos, M. C.; Pellet-Rostaing, S.; Lemaire, M.; Schulz, J.; Kannappan, R.; Bucher, C.; Saint-Aman, E.; Chaix, C. *Supramol. Chem.* **2009**, *21*, 68.
(182) Beer, P. D.; Drew, M. G. B.; Gradwell, K. *J. Chem. Soc., Perkin Trans. 2* **2000**, 511.
(183) Oh, J. M.; Cho, E. J.; Ryu, B. J.; Lee, Y. J.; Nam, K. C. *Bull. Korean Chem. Soc.* **2003**, *24*, 1538.
(184) Hamdi, A.; Nam, K. C.; Ryu, B. J.; Kim, J. S.; Vicens, J. *Tetrahedron Lett.* **2004**, *45*, 4689.
(185) Chen, Q.-Y.; Chen, C.-F. *Eur. J. Org. Chem.* **2005**, 2468.
(186) Hu, X.; Chan, A. S. C.; Han, X.; He, J.; Cheng, J.-P. *Tetrahedron Lett.* **1999**, *40*, 7115.
(187) Watchasit, S.; Kaowliew, A.; Suksai, C.; Tuntulani, T.; Ngeontae, W.; Pakawatchai, C. *Tetrahedron Lett.* **2010**, *51*, 3398.
(188) Yang, Y. S.; Ko, S. W.; Song, I. H.; Ryu, B. J.; Nam, K. C. *Bull. Korean Chem. Soc.* **2003**, *24*, 681.
(189) Beer, P. D.; Timoshenko, V.; Maestri, M.; Passaniti, P.; Balzani, V. *Chem. Commun.* **1999**, 1755.
(190) Cho, E. J.; Ryu, B. J.; Yeo, H. M.; Lee, Y. J.; Nam, K. C. *Bull. Korean Chem. Soc.* **2005**, *26*, 470.
(191) Quinlan, E.; Matthews, S. E.; Gunnlaugsson, T. *Tetrahedron Lett.* **2006**, *47*, 9333.
(192) Liu, S.-Y.; He, Y.-B.; Wu, J.-L.; Wei, L.-H.; Qin, H.-J.; Meng, L.-Z.; Hu, L. *Org. Biomol. Chem.* **2004**, *2*, 1582.
(193) Singh, N.; Lee, G. W.; Jang, D. O. *Tetrahedron* **2008**, *64*, 1482.
(194) Stoikov, I. I.; Gafiullina, L. I.; Ibragimova, D. S.; Antipin, I. S.; Konovalov, A. I. *Russ. Chem. Bull. Int. Ed.* **2004**, *53*, 1172.
(195) Demirtas, H. N.; Bozkurt, S.; Durmaz, M.; Yilmaz, M.; Sirit, A. *Tetrahedron* **2009**, *65*, 3014.
(196) Liu, X.-X.; Zheng, Y.-S. *Tetrahedron Lett.* **2006**, *47*, 6357.
(197) He, Y.; Xiao, Y.; Meng, L.; Zeng, Z.; Wu, X.; Wu, C.-T. *Tetrahedron Lett.* **2002**, *43*, 6249.
(198) Karakucuk, A.; Durmaz, M.; Sirit, A.; Yilmaz, M.; Demir, A. S. *Tetrahedron: Asymmetry* **2006**, *17*, 1963.
(199) Sdira, S. B.; Felix, C. P.; Giudicelli, M.-B. A.; Seigle-Ferrand, P. F.; Perrin, M.; Lamartine, R. J. *J. Org. Chem.* **2003**, *68*, 6632.
(200) Qing, G.-Y.; He, Y.-B.; Wang, F.; Qin, H.-J.; Hu, C.-G.; Yang, X. *Eur. J. Org. Chem.* **2007**, 1768.
(201) Qing, G.-Y.; He, Y.-B.; Zhao, Y.; Hu, C.-G.; Liu, S.-Y.; Yang, X. *Eur. J. Org. Chem.* **2006**, 1574.
(202) Qing, G.-Y.; He, Y.-B.; Chen, Z.-H.; Wu, X.-J.; Meng, L.-Z. *Tetrahedron: Asymmetry* **2006**, *17*, 3144.
(203) Liu, S.-Y.; He, Y.-B.; Qing, G.-Y.; Xu, K.-X.; Qin, H.-J. *Tetrahedron: Asymmetry* **2005**, *16*, 1527.
(204) Yakovenko, A. V.; Boyko, V. I.; Kalchenko, V. I.; Baldini, L.; Casnati, A.; Sansone, F.; Ungaro, R. *J. Org. Chem.* **2007**, *72*, 3223.
(205) Guang-Yan, Q.; Zhi-Hong, C.; Feng, W.; Xi, Y.; Ling-Zhi, M.; Yong Bing, H. *Chin. J. Chem.* **2008**, *26*, 721.
(206) Qing, G.-Y.; Qin, H.-J.; He, Y.-B.; Hu, C.-G.; Wang, F.; Hu, L. *Supramol. Chem.* **2008**, *20*, 265.
(207) Kocabas, E.; Karakucuk, A.; Sirit, A.; Yilmaz, M. *Tetrahedron: Asymmetry* **2006**, *17*, 1514.
(208) Guo, W.; Wang, J.; Wang, C.; He, J.-Q.; He, X.-W.; Cheng, J.-P. *Tetrahedron Lett.* **2002**, *43*, 5665.
(209) Zheng, Y.-S.; Zhang, C. *Org. Lett.* **2004**, *6*, 1189.
(210) Lambert, A.; Regnouf-de-Vains, J.-B.; Rinaldi, D.; Ruiz-Lopez, M. F. *J. Phys. Org. Chem.* **2006**, *19*, 157.
(211) Budka, J.; Tkadlecova, M.; Lhotak, P.; Stibor, I. *Tetrahedron* **2000**, *56*, 1883.
(212) Yang, F.; Ji, Y.; Guo, H.; Lin, J.; Peng, Q. *Synth. Commun.* **2007**, *37*, 79.
(213) Lu, J. Q.; Zhang, L.; Sun, T. Q.; Wang, G. X.; Wu, L. Y. *Chin. J. Chem.* **2006**, *17*, 575.
(214) Acharya, A.; Ramanujam, B.; Chinta, J. P.; Rao, C. P. *J. Org. Chem.* **2011**, *76*, 127.
(215) Lazar, A. N.; Danylyuk, O.; Suwinska, K.; Coleman, A. W. *J. Mol. Struct.* **2006**, *825*, 20.
(216) Chinta, J. P.; Acharya, A.; Kumar, A.; Rao, C. P. *J. Phys. Chem. B* **2009**, *113*, 12075.
(217) Perret, F.; Morel-Desrosiers, N.; Coleman., A. W. *J. Supramol. Chem.* **2002**, *2*, 533.
(218) Liu, F.; Lu, G.-Y.; He, W.-J.; Liu, M.-H.; Zhu, L.-G.; Wu, H.-M. *New J. Chem.* **2002**, *26*, 601.
(219) Danylyuk, O.; Lazar, A. N.; Coleman, A. W.; Suwinsk, K. *J. Mol. Struct.* **2008**, *891*, 404.
(220) Lazar, A. N.; Navaza, A.; Coleman, A. W. *Chem. Commun.* **2004**, 1052.
(221) Lazar, A. N.; Danylyuk, O.; Suwinska, K.; Coleman, A. W. *New J. Chem.* **2006**, *30*, 59.
(222) Coleman, A. W.; Silva, E. D.; Nouar, F.; Nierlich, M.; Navaza, A. *Chem. Commun.* **2003**, 826.